EROSION AND TRANSPORT OF BED-LOAD SEDIMENT

EROSION AND TRANSPORT
OF
BED-LOAD SEDIMENT

PROEFSCHRIFT

door
RAFAEL FERNANDEZ LUQUE
DRS. WIS- EN NATUURKUNDE
geboren te Murcia

Dit proefschrift is goedgekeurd door de promotor:

PROF. IR. J.O. HINZE

STELLINGEN

1. In afwijking van de gangbare mening kan worden aangetoond dat bij uitschuring van een zandbed door vloeistofstroming, zolang er geen bulkerosie optreedt, de turbulente vloeistofschuifspanning aan het bedoppervlak een kritische waarde niet zal overschrijden.

   Dit proefschrift, hoofdstuk 6.

2. Grote vloeistofdrukgradiënten boven een korrelbed, die instantaan in een sterk turbulente grenslaag kunnen ontstaan, zullen aanleiding geven tot bulkerosie, waarbij verschillende korrellagen van het bed tegelijkertijd kunnen worden geërodeerd.

   Dit proefschrift, hoofdstuk 8.

3. De veronderstelling van Williams en Kemp, dat bij het begin van zandtransport door vloeistofstroming ribbels ontstaan zodra de stroming sterk genoeg is om het bed uit te schuren, is niet algemeen juist.

   P.B. Williams & P.H. Kemp (1971)
   Proc. ASCE J. Hydr. Div., 97, No. HY4, 505.

4. Mits professioneel gehanteerd, biedt het filmmedium meer mogelijkheden bij de studie van sediment-transport dan door onderzoekers op dit vakgebied vaak wordt gerealiseerd.

5. Bagnold's voorwaarde voor het zichzelf voortdurend in stand houden van suspensiestromen, namelijk dat het arbeidsvermogen van de suspensie voldoende moet zijn om de deeltjes in suspensie te houden en de stromingsweerstand te overwinnen, is op fysische gronden niet haalbaar.

   R.A. Bagnold (1962)
   Proc. Roy. Soc., 265 A, No. 1322, 315.

6. Ondiepe funderingen in de zeebodem kunnen geleidelijk wegzakken binnen een plastische zone die door golven onstaat en tijdens de golfwerking in stand wordt gehouden.

   R. Fernández Luque & R. van Beek
   Soc. Pet. Eng. J., 14, No. 4, 330.
   (1974)

7. Instabiliteit van verplaatsbare boorplatforms, ten gevolge van erosie om de poten, kan het meest doeltreffend worden bestreden door de poten als een open vakwerk met dragende, in het midden opengewerkte, voet uit te voeren, en ze bij het plaatsen van het platform op gekontroleerde wijze tot een bepaalde diepte de zeebodem in te spuiten.

8. Het bezwijken van een holte, door afschuiving, in een belaste zandsteen-formatie, wordt bepaald door een eindige limietwaarde voor de plastische vervorming van de zandsteen om die holte.

9. Voor een praktische poriënvolume-analyse van laagporeuze materialen, door middel van de lage-temperatuur-desorptie-methode, lijkt ethaan het meest geschikte adsorbaat.

10. Het aantal ideeën dat gegenereerd wordt in een industrieel laboratorium, en resulteert in de ontwikkeling van nieuwe produkten en/of technologieën, neemt eerder toe dan af als een beperkt en zorgvuldig omschreven programma aan het werk ten grondslag wordt gelegd.

R. Fernández Luque,
"Erosion and transport of bed-load sediment",
Delft, 11 december 1974

De wetenschap bestaat uit ideeën of
begrippen; de ideeën zijn echter slechts
middel, want het gaat er in de weten-
schap niet om feiten door wetten te
vervangen, doch om feiten door middel
van wetten te leren kennen. Feiten zijn
het einddoel van de wetenschap, daar is
ze op gericht.

De ideas consta la ciencia, sí,
de conceptos; pero no son ellas,
las ideas, más que medio, porque
no es ciencia conocer las leyes
por los hechos, sino los hechos
por las leyes; en el hecho termina
la ciencia, a el se dirige.

Miguel de Unamuno
(Ensayos)

CONTENTS   <u>Page</u>

EROSION AND TRANSPORT OF BED-LOAD SEDIMENT

INTRODUCTION

Today the mechanism of bed-load transport is not yet completely understood. The existing bed-load transport formulae are either purely empirical, such as SHIELDS' formula (1936) or the well-known MEYER-PETER & MULLER equation (1948), or have an underlying theory, for instance the theory of KALINSKE (1947), EINSTEIN (1950), BAGNOLD (1956), or YALIN (1963). These theories are, however, based on assumptions some of which are not fully justified. The theoretical and experimental work reported in this thesis is intended to clarify a number of fundamental aspects of the mechanism of bed-load transport.

A basic understanding of the mass- and momentum-exchange processes that occur in the zone of transition between the flow region and the bed during bed-load transport is essential in order to derive generalised sediment-transport equations. Spatial averages are necessary to obtain a measure of the 'macro'-stresses induced by an erosive flow in that zone. VAN DEEMTER & VAN DER LAAN (1961) formally obtained equations for the momentum and mechanical-energy balance of a dispersed two-phase flow system, taking into account the effect of differences in velocity between the fluid and the particles. HINZE (1962) worked out these equations for a Newtonian fluid containing solid particles, taking also the effect of turbulence into account by applying the well-known Reynolds' procedure. In this thesis we shall consider the mass- and linear-momentum-balance equation for a Newtonian fluid containing solid particles, rigorously defining average quantities, such as the average fluid and solid velocity or stress components, along 'smooth' statistical surface elements in the mixture. HEINRICH & DESOYER (1956) pointed out that a statistical surface intersects the fluid and the solid at random and therefore cannot be used to calculate the fluid drag on particles in a porous medium. For this purpose he defined 'wavy' surfaces intersecting the solid at intergranular contacts only. We shall use such 'wavy' surfaces to express the balance of forces acting on the particles of a fluid-solid mixture in turbulent bulk motion, introducing an apparent viscosity for the fluid component. We shall also indicate the limitations of this procedure. These equations will be applied to calculate the attenuation of viscous-momentum transfer from the boundary towards the interior of a granular bed subject to a surface flow, the average drag and lift

forces exerted by a turbulent shear flow on particles of the bed surface, and the balance of forces acting on a bed load under uniform-flow conditions.

Stability conditions will be formulated for a loose granular bed subject to erosive flow, at SHIELDS' grain-movement condition (1936), and during bed-load transport. This will lead us to the conclusion that the bed load must reduce the maximum turbulent fluid shear at the bed surface, at sufficiently high bed shear stress, to the critical threshold drag that would lead to the initiation of non-ceasing scour.

In order to verify our conclusion that the bed load reduces the maximum turbulent fluid shear at the bed surface to a critical value, and to study the mechanism of bed-load transport in general, we carried out a series of experiments in which we measured the mean bed shear stress at SHIELDS' grain-movement condition and at the initiation of non-ceasing scour. We also measured the rate of bed-load transport, the average particle velocity, the rate of deposition and the average length of individual steps of saltating bed-load particles, in water, as a function of the time-mean bed shear stress and the slope of the bed surface, using different bed materials. These experiments will prove that certain assumptions in the theories of KALINSKE, EINSTEIN, BAGNOLD and YALIN are unjustified.

KALINSKE (1947) expressed the rate of bed-load transport as a product of the number of particles participating in the motion, the average velocity of the bed-load particles, and the particle volume. He assumed that the areal bed-load concentration, defined as the total projected area of particles in motion, has a constant value of 0.35. We found experimentally that this assumption is incorrect. The areal bed-load concentration increases almost linearly with the difference between the average bed-shear stress and the critical bed-shear stress at the threshold of continuous sediment motion.

EINSTEIN (1950) expressed the rate of bed-load transport as the number of particles eroded from the bed surface per unit area and time (equal to the number of particles deposited on the bed surface per unit area and time, under uniform-flow conditions), the particle volume and the average distance covered by the bed-load particles from the moment they are eroded until the moment they are deposited on the bed. EINSTEIN related this distance to the probability of a saltating particle being deposited when striking the bed surface. He assumed that this probability is equal to one minus the probability that a particle of the bed surface is eroded at any time, and concluded that the total average distance covered by the bed-load particles must increase with increasing bed-shear stress. We found experimentally that the total average distance

covered by the bed-load particles is independent of the time-mean bed shear stress and that therefore these two probabilities are not related to each other.

BAGNOLD (1956) proposed a theory for bed-load transport based on the work done by the fluid to transport the sediment. He considered the stress equilibrium in steady flow, introducing the concept of a 'dispersive' grain pressure on the bed surface, and assumed that at low bed-load concentrations the fluid component of the turbulent bed-shear stress equals the critical bed-shear stress at the threshold of sediment motion, while at high bed-load concentrations the fluid component of the turbulent bed-shear stress may be neglected. We found experimentally that at low bed-load concentrations the fluid component of the turbulent bed-shear stress is practically equal to the total bed-shear stress, and we concluded on a theoretical basis that at high bed-load concentrations, during erosion with or without simultaneous deposition, the fluid component of the turbulent bed-shear stress must be practically equal to the critical bed-shear stress at the initiation of non-ceasing scour in the absence of a bed load.

YALIN (1963) derived an expression for the rate of bed-load transport based on dimensional analysis and the dynamics of the average saltating motion of the grain. He assumed that the saltation of a grain is analogous to the ballistics of a missile, in the sense that the grain gains its maximum level during a saltation owing to its initial velocity when it is lifted from the bed surface, and not to the continuous action of a driving force. We found experimentally that this assumption is not valid for saltation in water. Close examination of the motion of saltating particles in water showed that these particles were transported nearly in suspension for the greater part of their trajectory. Both the vertical and horizontal accelerations of the particles were then very low in comparison with the acceleration that they would experience owing to a drag force equal to their submerged weight. This implies that the saltating particles experience a lift force by the shear flow for the greater part of their trajectory, which is approximately equal to their submerged weight, and a drag force that is much smaller.

In a recent paper BAGNOLD (1973) discussed the nature of saltation and bed-load transport in water and concluded that the fluid thrust necessary to maintain the motion of bed-load particles in water is exerted by virtue of a 'slip' velocity between the fluid and the particles. We measured the average transport velocity of suspended bed-load particles in water and found that it was equal to the average fluid velocity calculated for a turbulent flow without a bed load, at about three particle diameters above the bed surface, minus a

constant. The constant was proportional to the critical shear velocity at SHIELDS' grain-movement condition. Since those particles were practically not accelerated, on an average, we did not interpret this velocity defect as an average 'slip' velocity between the fluid and the suspended bed-load particles, but concluded that the average fluid velocity at the particle level (about three diameters above the bed surface) was reduced by a constant value owing to the presence of the bed load. This constant value can be explained by considering that the turbulent shear flow must exert a lift force on the suspended particles that is practically equal to their submerged weight. Our conclusion seems to be confirmed by FRANCIS' experiments (1973). FRANCIS studied experimentally the mechanism of saltation and describes in his paper an experiment where one marked grain was observed while moving in the company of many other grains of a bed load. Its velocity was reduced to below the level it would have as a solitary grain in the same water stream, thus indicating, according to FRANCIS, how the friction of the grain load reacts to the stream to give lower speeds close to the bed.

We can conclude that a loose granular bed must be severely eroded instantaneously where the momentum of the surface flow changes radically and the bed load cannot reduce the maximum turbulent fluid shear at the bed surface to the critical threshold drag that leads to the initiation of non-ceasing scour, i.e. where the bed load cannot protect the bed surface against scour.

Severe scour generally occurs in areas of highly turbulent flow where the fluid instantaneously induces large pressure gradients in a transition zone between the bed and the bed load. We shall present a method that permits determination of the extent of the zone of 'instantaneous instability' or 'bulk erosion' under a two-dimensional jet of rapidly increasing energy, and we shall compare the results of our calculation with those of a simple experiment.

2. MASS AND LINEAR-MOMENTUM BALANCE EQUATIONS FOR A FLUID CONTAINING SOLID PARTICLES

2.1. Balance of mass and momentum in integral form

Consider a volume V of an incompressible Newtonian fluid containing solid particles, bounded by a closed surface S intersecting the fluid and the particles at random (Fig. 1 shows an element ΔS of such a 'smooth' surface). The integral mass and linear-momentum balance equations for the fluid and the solid components of the mixture inside that volume read (according to the summation convention for repeated indices):

Mass-balance equation for the fluid:

$$\oint_{S^f} \rho_f v_i^f \, n_i \, d \, S^f + \frac{\partial}{\partial t} \iiint_{V^f} \rho_f \, d \, V^f = 0 \tag{1a}$$

Mass-balance equation for the solid:

$$\oint_{S^s} \rho_s v_i^s \, n_i \, d \, S^s + \frac{\partial}{\partial t} \iiint_{V^s} \rho_s \, d \, V^s = 0 \tag{1b}$$

Momentum-balance equation for the fluid:

$$\frac{\partial}{\partial t} \iiint_{V^f} \rho_f v_i^f \, d \, V^f + \oint_{S^f} \rho_f v_i^f v_j^f \, n_j \, d \, S^f =$$

$$= \oint_{S^f} \sigma_{ij}^f \, n_j \, d \, S^f + \iint_{S^b} \sigma_{ij}^f \, n_j \, d \, S^b + \iiint_{V^f} \rho_f g_i \, d \, V^f \tag{2a}$$

Momentum-balance equation for the solid:

$$\frac{\partial}{\partial t} \iiint_{V^s} \rho_s v_i^s \, d \, V^s + \oint_{S^s} \rho_s v_i^s v_j^s \, n_j \, d \, S^s =$$

$$= \oint_{S^s} \sigma_{ij}^s n_j \, d \, S^s - \iint_{S^b} \sigma_{ij}^f \, n_j \, d \, S^b + \iiint_{V^s} \rho_s g_i \, d \, V^s \tag{2b}$$

where

$$\sigma_{ij}^f = - p^f \delta_{ij} + \mu \, (\frac{\partial v_i^f}{\partial x_j} + \frac{\partial v_j^f}{\partial x_i}) \tag{3}$$

is the fluid stress tensor.

The index f on these equations indicates that the integration is restricted to the fluid part S^f of the boundary surface S or to the fluid part V^f of the volume V, whilst the index s refers to the solid part of S of V. The index b indicates that the integration is carried out over the total fluid solid boundary surface S^b inside the volume V. The expression n_i represents the projection along the i-axis of a fixed cartesian frame, of the unit vector $\vec{n}$ along the outward normal of (a) an element dS^f or dS^S of the closed surface S around the volume V, (b) an element dS^b of the fluid/solid boundary surface of the fluid volume V^f (see Fig. 1a). The other symbols have their usual meaning [ρ is the density and $\vec{v}$ the velocity of the fluid (f) or solid (s) phase, σ_{ij}^S the solid-stress tensor, p^f the fluid pressure, μ the fluid viscosity and $\vec{g}$ the acceleration due to gravity].

2.2. Averaging procedure

To derive bulk differential expressions for the mass and linear-momentum balance equations (1) and (2), we have to define average quantities for the fluid and solid components of the mixture, for small but finite dimensions.

Consider a plane statistical surface element ΔS around a given point in the mixture (see Fig. 1). We define for any relevant quantity ξ surface averages $\bar{\xi}^f$ and $\bar{\xi}^S$ along the fluid and the solid parts of ΔS, respectively:

$$\bar{\xi}^f = \frac{1}{\Delta S^f} \iint_{\Delta S^f} \xi \, d \, S^f \tag{4a}$$

$$\bar{\xi}^S = \frac{1}{\Delta S^S} \iint_{\Delta S^S} \xi \, d \, S^S \tag{4b}$$

The average definitions are, of course, only meaningful if the surface elements ΔS are chosen large enough in comparison with the dimensions of the grains and of the intergranular spaces to ensure smoothing out of all fluctuations of the micro-quantities and, on the other hand, small enough with respect to the gross dimensions of the flow region considered to avoid measurable smoothing out of the macro-field itself. The latter implies that the size of ΔS can be chosen such that, within a certain range, a change in size of ΔS does not affect the average value.

When, in addition, the surface averages, averaged over the fluid and solid parts of a statistical surface element ΔS, vary 'slowly', e.g. linearly, over a statistical length element ΔL_n in the direction x_n perpendicular to ΔS,

they may be interpreted as volumetric mean values, obtained by averaging over a statistical volume element ΔV chosen symmetrically around ΔS with lateral surface area ΔS and thickness ΔL_n; they are thus independent of the orientation of ΔS in the mixture.

$$\bar{\xi}^f = \frac{1}{\Delta L_n} \int_{\Delta L_n} \bar{\xi}^f \, d\, x_n = \frac{1}{\Delta V^f} \iiint_{\Delta V^f} \xi \, d\, V^f \tag{5a}$$

$$\bar{\xi}^s = \frac{1}{\Delta L_n} \int_{\Delta L_n} \bar{\xi}^s \, d\, x_n = \frac{1}{\Delta V^s} \iiint_{\Delta V^s} \xi \, d\, V^s \tag{5b}$$

For special purposes, e.g. to describe the shearing filter flow along the surface of a porous medium, volume averages can also be defined by averaging any relevant quantity ξ over the fluid or solid part of a flat volume element δV of very small (but finite) thickness δL_n, provided the projected area ΔS_n of the volume element is sufficiently large. For a statistically disordered medium, the local average concentration of the solid component, represented by the symbol C, is by definition the same for a statistical cut ΔS and a statistical volume element ΔV.

$$C = \frac{\Delta S^s}{\Delta S} = \frac{\Delta V^s}{\Delta V} \tag{6}$$

We define surface averages along the fluid/solid boundary surface inside a statistical volume element ΔV of the mixture, as follows:

$$\bar{\xi}^b = \frac{1}{\Delta V} \iint_{\Delta S^b} \xi \, d\, S^b \tag{7}$$

where ΔS^b is the total surface area of the solid component inside the statistical volume element ΔV. We define the specific surface area of the solid inside ΔV, as:

$$A = \frac{\Delta S^b}{\Delta V^s} = \frac{1}{C} \frac{\Delta S^b}{\Delta V} \tag{8}$$

Using the surface averages defined by equations (4), we can define tensor components $(\bar{\sigma}_{ij}^f, \bar{\sigma}_{ij}^s)$ for the average stresses $(\bar{f}_i^f, \bar{f}_i^s)$ transmitted to the fluid and solid parts of ΔS, by considering mutually perpendicular macro-surface elements:

$$\bar{f}_i^f = \bar{\sigma}_{ij}^f \, n_j, \quad \bar{f}_i^s = \bar{\sigma}_{ij}^s \, n_j$$

Here n_j is the projection along the j-axis of a fixed Cartesian frame of the unit vector $\vec{n}$ along the outward-drawn normal of ΔS. We can thus express the total average stress $\tilde{f}_i$ acting along ΔS as follows:

$$\tilde{f}_i = (1 - C) \, \bar{\sigma}_{ij}^f \, n_j + C \, \bar{\sigma}_{ij}^s \, n_j \tag{9}$$

In soil mechanics and in the mechanics of sediment transport one is interested in the stresses acting at intergranular contacts rather than in the stresses that act across an arbitrary cross-section of the particles. Evidently, intergranular stresses cannot be averaged with respect to smooth statistical surfaces, but rather with respect to 'wavy' non-statistical surfaces, as proposed by HEINRICH & DESOYER (1956) and more extensively by MANDL (1964). Such a surface fluctuates around a corresponding smooth surface S and thereby intersects the solid component of the mixture at intergranular contacts only. Hence, we allow the fluid part of $\tilde{S}$ to partly coincide with the total fluid/fluid contact area of S (S^f), and to partly follow (as closely as possible to S) the smallest solid fluid contact area around S ($\tilde{S}^b$). The solid part of $\tilde{S}$ ($\tilde{S}^s$) will then automatically coincide with the total intergranular contact area along the shortest path around S through the fluid component of the mixture (see Fig. 1).

Next, we define surface averages along the total fluid/fluid + fluid/solid contact area $\Delta \tilde{S}^f \equiv \Delta S^f + \Delta \tilde{S}^b$ and along the solid/solid contact area $\Delta \tilde{S}^s$ of the finite surface element $\Delta \tilde{S}$:

$$\tilde{\xi}^f = \frac{1}{\Delta S} \iint\limits_{\Delta \tilde{S}^f} \xi \, d \tilde{S}^f \tag{10a}$$

$$\tilde{\xi}^s = \frac{1}{\Delta S} \iint\limits_{\Delta \tilde{S}^s} \xi \, d \tilde{S}^s \tag{10b}$$

Here ΔS is the total fluid + solid area of the corresponding smooth, flat surface element.

Let us now apply this averaging procedure to the stresses

$$f_i = \sigma_{ij} n_j \tag{11}$$

transmitted to $\Delta \tilde{S}$. We can define tensor components for the average stresses

transmitted to the f and s parts of $\widetilde{\Delta S}$ by considering mutually perpendicular 'wavy' elements:

$$\widetilde{f}_i^f = \widetilde{\sigma}_{ij}^f n_j; \quad \widetilde{f}_i^s = \widetilde{\sigma}_{ij}^s n_j$$

Here n_j is the projection along the j-axis of a fixed cartesian frame of the unit vector $\vec{n}$ along the outward-drawn normal of the corresponding smooth surface element ΔS. We can thus express the total average stress acting on $\widetilde{\Delta S}$ as follows:

$$\frac{1}{\Delta S} \left[\iint\limits_{\Delta \widetilde{S}^s} f_i \, d\widetilde{S}^s + \iint\limits_{\Delta \widetilde{S}^f} f_i \, d\widetilde{S}^f \right] = \widetilde{\sigma}_{ij}^s n_j + \widetilde{\sigma}_{ij}^f n_j$$

It can easily be shown that the total average stresses acting on $\widetilde{\Delta S}$ equal the total average stresses acting on the corresponding ΔS if inertial forces associated with the rotation of the individual particles may be neglected:

$$\widetilde{f}_i = \widetilde{\sigma}_{ij}^s n_j + \widetilde{\sigma}_{ij}^f n_j = C \, \overline{\sigma}_{ij}^s n_j + (1-C) \, \overline{\sigma}_{ij}^f n_j \tag{12}$$

$$\widetilde{\sigma}_{ij}^s + \widetilde{\sigma}_{ij}^f = C \, \overline{\sigma}_{ij}^s + (1-C) \, \overline{\sigma}_{ij}^f \tag{12a}$$

The 'macro'-stresses $\widetilde{f}_i^f = \widetilde{\sigma}_{ij}^f n_j$ and $\widetilde{f}_i^s = \widetilde{\sigma}_{ij}^s n_j$ are defined as the bulk average stresses acting along the fluid part and the intergranular contacts (as a sum of intergranular contact forces), respectively, of a 'wavy' macroscopic surface element with unit (outward) normal vector $\vec{n}$, per unit bulk (fluid + solid) area of the corresponding smooth macroscopic surface element. We can define as follows the average pressure acting across the fluid and solid parts, respectively of a closed 'wavy' surface on a 'macro'-volume element of a fluid containing solid particles:

$$\widetilde{p} = \widetilde{p}^f + \widetilde{p}^s \tag{13}$$

$$\widetilde{p}^f = -\frac{1}{3} \widetilde{\sigma}_{ii}^f \tag{13a}$$

$$\widetilde{p}^s = -\frac{1}{3} \widetilde{\sigma}_{ii}^s \tag{13b}$$

2.3. Balance of mass and momentum in differential form

Applying the averaging procedure described in the preceding Section (2.2), we may write the mass and linear-momentum balance equations for the fluid and the solid components of a statistical volume element of the mixture, bounded by a smooth surface, in terms of bulk-surface and bulk-volume integrals:

Mass balance

$$\oiint_S \rho_f \, (1-C) \, \bar{v}_i^f \, n_i \, dS + \frac{\partial}{\partial t} \iiint_V \rho_f \, (1-C) \, dV = 0 \qquad \underline{\text{fluid}} \qquad (14a)$$

$$\oiint_S \rho_s \, C \, \bar{v}_i^s \, n_i \, dS + \frac{\partial}{\partial t} \iiint_V \rho_s \, C \, dV = 0 \qquad \underline{\text{solid}} \qquad (14b)$$

Momentum balance

$$\frac{\partial}{\partial t} \iiint_V \rho_f \, (1-C) \, \bar{v}_i^f \, dV + \oiint_S \rho_f \, (1-C) \, \overline{v_i v_j}^f \, n_j \, dS$$

$$= \oiint_S (1-C) \left[-\bar{p}^f \, \delta_{ij} + \mu \left(\frac{\partial \bar{v}_i^f}{\partial x_j} + \frac{\partial \bar{v}_i^f}{\partial x_i} \right) \right] n_j \, dS +$$

$$+ \iiint_V [\rho_f \, (1-C) \, g_i + R_i] \, dV \qquad \underline{\text{fluid}} \qquad (15a)$$

$$\frac{\partial}{\partial t} \iiint_V \rho_s \, C \, \bar{v}_i^s \, dV + \oiint_S \rho_s \, C \, \overline{v_i v_j}^s \, n_j \, dS =$$

$$= \oiint_S C \, \bar{\sigma}_{ij}^s \, n_j \, dS +$$

$$+ \iiint_V [\rho_s \, C \, g_i - R_i] \, dV \qquad \underline{\text{solid}} \qquad (15b)$$

Here R_i is defined as the average reaction force per unit bulk volume exerted by the solid upon the fluid inside a statistical volume element ΔV [averaged according to equation (7)]:

$$R_i = \frac{1}{\Delta V} \iint\limits_{\Delta S^b} \left[-p^f \delta_{ij} + \mu \left(\frac{\partial v_i^f}{\partial x_j} + \frac{\partial v_j^f}{\partial x_i} \right) \right] n_j \, dS^b \tag{16}$$

It should be noted that these 'macro'-equations pertain to the instantaneous balance of mass and linear momentum in the fluid-solid mixture.

If the condition of 'slow' spatial variation of the surface means is satisfied, the surface averages $\overline{\partial v_i / \partial x_j}^f$ in equation (15a) will be equal to the corresponding volume averages, and we may apply Gauss' theorem to these averages:

$$\overline{\frac{\partial v_i}{\partial x_j}}^f + \overline{\frac{\partial v_j}{\partial x_i}}^f = \frac{1}{\Delta V^f} \iiint\limits_{\Delta V^f} \left(\frac{\partial v_i^f}{\partial x_j} + \frac{\partial v_j^f}{\partial x_i} \right) \, dV^f$$

$$= \frac{1}{\Delta V^f} \oiint\limits_{S^f} (v_i^f n_j + v_j^f n_i) \, dS^f + \frac{1}{\Delta V^f} \iint\limits_{\Delta S^b} (v_i^f n_j + v_j^f n_i) \, dS^b \tag{17}$$

The first integral on the right-hand side of this equation extends over the fluid part S^f of the boundary surface S around the statistical volume element ΔV and is equal to:

$$\oiint\limits_{S^f} (v_i^f n_j + v_j^f n_i) \, dS^f = \oiint\limits_{S} (1-C) (\bar{v}_i^f n_j + \bar{v}_j^f n_i) \, dS \tag{18}$$

or, applying Gauss' theorem in the inverse sense:

$$\oiint\limits_{S^f} (v_i^f n_j + v_j^f n_i) \, dS^f = \left\{ \frac{\partial}{\partial x_j} \left[(1-C) \bar{v}_i^f \right] + \frac{\partial}{\partial x_i} \left[(1-C) \bar{v}_j^f \right] \right\} \Delta V \tag{18a}$$

In order to evaluate the second integral on the right-hand side of equation (17) we apply Gauss' theorem to the volume-averaged strain-rate tensor in the solid part of the same statistical volume element; this of course is equal to zero if the particles are undeformable:

$$\overline{\frac{\partial v_i}{\partial x_j}}^s + \overline{\frac{\partial v_i}{\partial x_i}}^s = \frac{1}{\Delta V^s} \iiint_{\Delta V^s} (\frac{\partial v_i^s}{\partial x_j} + \frac{\partial v_j^s}{\partial x_i}) \, d\,V^s$$

$$= \frac{1}{\Delta V^s} \oint_{S^s} (v_i^s n_j + v_j^s n_i) \, d\,S^s - \frac{1}{\Delta V^s} \iint_{\Delta S^b} (v_i^s n_j + v_j^s n_i) \, d\,S^b$$

$$= 0 \tag{19}$$

Since $v_i^f = v_i^s$ on the boundary surface inside ΔV:

$$\iint_{\Delta S^b} (v_i^f n_j + v_j^f n_i) \, d\,S^b = \iint_{\Delta S^b} (v_i^s n_j + v_j^s n_i) \, d\,S^b$$

$$= \oint_{S^s} (v_i^s n_j + v_j^s n_i) \, d\,S^s$$

$$= \oint_S C \, (\bar{v}_i^s n_j + \bar{v}_j^s n_i) \, d\,S \tag{20}$$

or, applying Gauss' theorem again in the inverse sense:

$$\iint_{\Delta S^b} (v_i^f n_j + v_j^f n_i) \, d\,S^b = \{\frac{\partial}{\partial x_j} [C \, \bar{v}_i^s] + \frac{\partial}{\partial x_i} [C \, \bar{v}_j^s]\} \, \Delta V \tag{20a}$$

The average stresses $\mu \, (\overline{\partial v_i/\partial x_j}^f + \overline{\partial v_j/\partial x_i}^f)$ in equation (15a) can thus be written [see equations (3), (6), (17), (18a) and (20a)]:

$$\overline{\sigma}_{ij}^f + \bar{p}^f \delta_{ij} = \mu \, (\overline{\frac{\partial v_i}{\partial x_j}}^f + \overline{\frac{\partial v_j}{\partial x_i}}^f) = \frac{\mu}{1-C} \{\frac{\partial}{\partial x_j} [(1-C) \, \bar{v}_i^f + C \, \bar{v}_i^s] +$$

$$+ \frac{\partial}{\partial x_i} [(1-C) \, \bar{v}_j^f + C \, \bar{v}_j^s]\} \tag{21}$$

If the condition of 'slow' spatial variation of the surface means is satisfied, we can apply Gauss' theorem to the surface integrals in equations (14) and (15) and transform them into volume integrals. Since the region of integration is arbitrarily chosen and time-independent, the balances of mass and linear momentum are then obtained in differential form.

The mass-balance equations are:

$$\frac{\partial}{\partial x_i} [\rho_f (1-C) \bar{v}_i^f] + \frac{\partial}{\partial t} [\rho_f (1-C)] = 0 \qquad \text{\underline{fluid}} \qquad (22a)$$

$$\frac{\partial}{\partial x_i} [\rho_s C \bar{v}_i^s] + \frac{\partial}{\partial t} [\rho_s C] = 0 \qquad \text{\underline{solid}} \qquad (22b)$$

Summation of equations (22a) and (22b) gives:

$$\frac{\partial}{\partial x_i} [\rho_f (1-C) \bar{v}_i^f + \rho_s C \bar{v}_i^s] = -(\rho_s - \rho_f) \frac{\partial C}{\partial t} \qquad \text{\underline{mixture}} \qquad (23a)$$

$$\frac{\partial}{\partial x_i} [(1-C) \bar{v}_i^f + C \bar{v}_i^s] = 0 \qquad \text{\underline{mixture}} \qquad (23b)$$

The linear-momentum balance equations in differential form reads as follows [using the average expression (21) and equation (23b)]:

$$\frac{\partial}{\partial t} [\rho_f (1-C) \bar{v}_i^f] + \frac{\partial}{\partial x_j} [\rho_f (1-C) \overline{v_i v_j}^f] =$$

$$-\frac{\partial}{\partial x_i} [(1-C) \bar{p}^f] + \mu \frac{\partial^2}{\partial x_j \partial x_j} [(1-C) \bar{v}_i^f + C \bar{v}_i^s] + \rho_f (1-C) g_i + R_i$$

$$\text{\underline{fluid}} \qquad (24a)$$

$$\frac{\partial}{\partial t} [\rho_s C \bar{v}_i^s] + \frac{\partial}{\partial x_j} [\rho_s C \overline{v_i v_j}^s] =$$

$$= \frac{\partial}{\partial x_j} [C \bar{\sigma}_{ij}^s] + \rho_s C g_i - R_i \qquad \text{\underline{solid}} \qquad (24b)$$

Summation of equations (24a) and (24b) gives:

$$\frac{\partial}{\partial t} [\rho_f (1-C) \bar{v}_i^f + \rho_s C \bar{v}_i^s] + \frac{\partial}{\partial x_j} [\rho_f (1-C) \overline{v_i v_j}^f + \rho_s C \overline{v_i v_j}^s] =$$

$$\frac{\partial}{\partial x_j} [C \bar{\sigma}_{ij}^s] - \frac{\partial}{\partial x_i} [(1-C) \bar{p}^f] + \mu \frac{\partial^2}{\partial x_j \partial x_j} [(1-C) \bar{v}_i^f + C \bar{v}_i^s] +$$

$$[\rho_f (1-C) + \rho_s C] g_i \qquad \text{\underline{mixture}} \qquad (25)$$

3. BALANCE OF FORCES ACTING ON THE PARTICLES OF A FLUID-SOLID MIXTURE IN TURBULENT BULK MOTION

Using the areal averages described in the preceding Section (2.3) we cannot calculate the balance of forces acting on the particles of a fluid-solid mixture, because the smooth surface S enclosing an arbitrary bulk volume of the mixture intersects the particles at random. We therefore now consider the forces acting across a finite element $\Delta \widetilde{S}$ of a 'wavy' surface $\widetilde{S}$, as defined in Section 2.2. Substitution of equations (12) and (13) in equation (25) gives the following differential equation for the fluid-solid mixture, using expression (21) for $\bar{\sigma}_{ij}^{f}$:

$$\frac{\partial}{\partial t} [\rho_f (1-C) \bar{v}_i^f + \rho_s C \bar{v}_i^s] + \frac{\partial}{\partial x_j} [\rho_f(1-C) \overline{v_i v_j}^f + \rho_s C \overline{v_i v_j}^s] = - \frac{\partial}{\partial x_i} (\widetilde{p}^f + \widetilde{p}^s) +$$

$$+ \frac{\partial}{\partial x_j} (\widetilde{\sigma}_{ij}^s + \widetilde{p}^s \delta_{ij}) + \frac{\partial}{\partial x_j} (\widetilde{\sigma}_{ij}^f + \widetilde{p}^f \delta_{ij}) + [\rho_f (1-C) + \rho_s C] g_i \qquad (26)$$

Let ΔV be a finite volume element bounded by a closed 'wavy' surface, and $\widetilde{F}_i$ the average force per unit bulk volume exerted by the fluid upon the particles enclosed by $\Delta \widetilde{V}$. $\widetilde{F}_i$ is related to the average reaction force R_i exerted by the solid upon the fluid inside a statistical volume element V bounded by the corresponding smooth surface, by

$$\widetilde{F}_i = - R_i + \frac{1}{\Delta V} \left[\oiint\limits_{\widetilde{S}^f} f_i \, d \widetilde{S}^f - \oiint\limits_{\bar{S}^f} f_i \, d \bar{S}^f \right] \qquad (27)$$

Using the averaging formulae (4a) and (10a) and the expressions (6), (11) and (12), we find:

$$\widetilde{F}_i = - R_i + \frac{1}{\Delta V} \oiint\limits_{S} \left[\widetilde{\sigma}_{ij}^f - (1-C) \bar{\sigma}_{ij}^f \right] n_j \, d S$$

$$= - R_i + \frac{\partial}{\partial x_j} \left[\widetilde{\sigma}_{ij}^f - (1-C) \bar{\sigma}_{ij}^f \right] \qquad (27a)$$

The drag force exerted by the fluid upon the solid enclosed by $\Delta \widetilde{V}$ is thus not the same as the drag force of the fluid upon the solid enclosed by ΔV, due to a difference in solid/fluid contact area at the boundary.

Substitution of (12a) and (27a) in equations (24) gives the following differential equations for the linear-momentum balance in the fluid and solid components of the mixture, using expressions (13) and (21):

$$\frac{\partial}{\partial t} \left[\rho_f (1-C) \; \bar{v}_i^f \right] + \frac{\partial}{\partial x_j} \left[\rho_f (1-C) \; \overline{v_i v_j}^f \right] =$$

$$= - \frac{\partial \tilde{p}^f}{\partial x_i} + \frac{\partial}{\partial x_j} \; (\tilde{\sigma}_{ij}^f + \tilde{p}^f \, \delta_{ij}) + \rho_f (1-C) \; g_i - \tilde{F}_i \qquad \underline{\text{fluid}} \qquad (28a)$$

$$\frac{\partial}{\partial t} \left[\rho_s \, C \; \bar{v}_i^s \right] + \frac{\partial}{\partial x_j} \left[\rho_s \, C \; \overline{v_i v_j}^s \right] =$$

$$- \frac{\partial \tilde{p}^s}{\partial x_i} + \frac{\partial}{\partial x_j} \; (\tilde{\sigma}_{ij}^s + \tilde{p}^s \, \delta_{ij}) + \rho_s \, C \, g_i + \tilde{F}_i \qquad \underline{\text{solid}} \qquad (28b)$$

EINSTEIN (1906, 1911) has shown theoretically that the viscous 'macro'-stresses transmitted through a dilute suspension ($C \leq 0.1$) of naturally buoyant spherical particles ($\bar{v}_i^s = \bar{v}_i^f = \tilde{v}_i$) under steady 'slow' flow conditions can be expressed as follows:

$$\tilde{\sigma}_{ij}^f + \tilde{p}^f \, \delta_{ij} = \mu^* \; (\frac{\partial \tilde{v}_i}{\partial x_j} + \frac{\partial \tilde{v}_j}{\partial x_i}) \qquad (29)$$

where

$$\mu^* = \mu \, (1 + \frac{5}{2} \, C) \qquad (30a)$$

is the apparent viscosity of the suspension.

EILERS (1941) carried out careful experiments on suspensions of almost rigid bitumen particles ($D_s = 1.6 - 9.7 \, \mu m$) in water. He suggested the following empirical expression for the apparent viscosity of concentrated suspensions:

$$\mu^* = \mu \, \left(1 + \frac{0.975}{(C_o / C) - 1} \right)^2 \qquad (30b)$$

where $C_o = 0.78$ is a limit value for the solid concentration. BAGNOLD (1954) measured the total shear stress $\tilde{\tau}$ and normal dispersive grain pressure $\tilde{p}^s$ (defined as the normal force per unit bulk area due to intergranular contact forces) in sheared suspensions of spherical particles ($d_s = 1.32$ mm) in water. He suggested the following empirical expressions for $\tilde{\tau}$ and $\tilde{p}^s$ within the C-limits $0.1 < C < 0.6$, in the viscous regime:

$$\tilde{\tau} = \tilde{\sigma}^s_{xy} + \tilde{\sigma}^f_{xy} = 2.25 \, \lambda^{\frac{3}{2}} \, \mu \, \frac{d\tilde{u}}{dy} = \mu^* \, \frac{d\tilde{u}}{dy} \tag{31a}$$

$$\tilde{p}^s = -\tilde{\sigma}^s_{yy} = 1.3 \, \tilde{\sigma}_{xy} \tag{31b}$$

Here
$$\lambda = \left[\left(\frac{C_o}{C} \right)^{\frac{1}{3}} - 1 \right]^{-1} \tag{32}$$

is defined as the 'linear grain concentration' and $C_o = 0.74$.

The viscous regime is defined according to BAGNOLD by $N < 40$, where

$$N = \frac{\lambda^{\frac{1}{2}} \, \rho_s D^2_s}{\mu} \, \frac{d\tilde{u}}{dy} \tag{33}$$

is a measure of the ratio between inertial and viscous stresses in the suspension.

VAN DER POEL (1958) calculated the apparent viscosity of concentrated suspensions by extending a method developed by FRÖHLICH & SACK (1946) for dilute suspensions. The results of his calculations are in fair agreement with EILERS' experiments up to a concentration of $C = 0.6$, as shown in the table below, although his theory does not take intergranular contact forces into account.

BAGNOLD's equation (31a) predicts a much higher apparent viscosity than Eilers' equation (30b), as it is shown in the table below. This is due primarily to the fact that BAGNOLD performed his experiments at much higher shear rates ($\frac{d\tilde{u}}{dy} > 10^4 s^{-1}$, $N > 6$) than EILERS ($\frac{d\tilde{u}}{dy} < 100 \, s^{-1}$, $N < 10^{-6}$). CLARKE (1967) found a marked increase in the apparent viscosity of dense settling suspensions of glass spheres ($D_s = 53 - 76 \mu$ m) in water with the shear rate at shear rates ranging between 100 and 300 s^{-1} ($N = 1-3$), caused by intergranular contact forces. At very low shear rates, these interactions may be neglected and VAN DER POEL's theory is valid for $C \leq 0.6$. At shear rates $N > 1$ and concentrations $C > 0.1$ intergranular contact forces contribute substantially to the apparent viscosity, but still the contribution of viscous shear $\tilde{\sigma}^f_{xy}$ should be at least equal to the value predicted by VAN DER POEL's theory for $C \leq 0.6$.

Volume concentration C	μ^*/μ		
	Eilers' experiments	Van der Poel's theory ($\mu^* = \mu^{*f}$)	Bagnold's equation (31a)
0.10	1.25	1.29	2.44
0.20	1.84	1.73	5.57
0.30	2.55	2.50	10.8
0.40	4.0	4.08	20.7
0.50	7.6	8.10	43.1
0.60	18.0	21.4	115

From the above it follows that the viscous 'macro'-stresses $(\tilde{\sigma}_{ij}^f + \tilde{p}^f \delta_{ij})$ acting along 'wavy' surfaces in a concentrated suspension are proportional, within a limited range of shear rates, to the viscous 'macro'-stresses $(1-C)(\bar{\sigma}_{ij}^f + \bar{p}^f \delta_{ij})$ acting along the corresponding smooth surfaces:

$$\tilde{\sigma}_{ij}^f + \tilde{p}^f \delta_{ij} = \frac{\mu^{*f}}{\mu} (1-C)(\bar{\sigma}_{ij}^f + \bar{p}^f \delta_{ij}) \tag{34}$$

Here μ^{*f} is the apparent viscosity of the fluid component of the mixture.

At high shear rates, we must also take turbulent momentum transfer by the fluid and by the solid into account. The terms $\rho_f(1-C) \overline{v_i v_j}^f$ and $\rho_s C \overline{v_i v_j}^s$ in equations (24) represent an instantaneous momentum flux through the boundary surface S. The average products of the velocity components may be written as the sum of the products of the individual averages and the average products of the local deviations v_i' of the velocity components from their average value:

$$\overline{v_i v_j}^f = \bar{v}_i^f \bar{v}_j^f + \overline{v_i' v_j'}^f \tag{35a}$$

$$\overline{v_i v_j}^s = \bar{v}_i^s \bar{v}_j^s + \overline{v_i' v_j'}^s \tag{35b}$$

The terms $\rho_f(1-C) \overline{v_i' v_j'}^f$ and $\rho_s C \overline{v_i' v_j'}^s$ can be interpreted as stresses, in addition to the fluid pressure, the viscous fluid stresses and the solid stresses.

The linear-momentum balance equations (28) reduce by substitution of expressions (21) and (34) for the viscous 'macro'-stresses and expressions (35) for the turbulent fluid and solid velocity components, for a fluid-solid mixture in turbulent motion, to:

$$\frac{\partial}{\partial t} \left[\rho_f (1-C) \, \bar{v}_i^f \right] + \frac{\partial}{\partial x_j} \left[\rho_f (1-C) \, \bar{v}_i^f \, \bar{v}_j^f \right] =$$

$$= - \frac{\partial \tilde{p}^f}{\partial x_i} + \mu^{*f} \frac{\partial^2 \tilde{v}_i}{\partial x_j \partial x_j} - \frac{\partial}{\partial x_j} \left[\rho_f (1-C) \, \overline{v_i' v_j'}^f \right] + \rho_f (1-C) \, g_i - \tilde{F}_i \qquad (36a)$$

$$\frac{\partial}{\partial t} \left[\rho_s C \, \bar{v}_i^s \right] + \frac{\partial}{\partial x_j} \left[\rho_s C \, \bar{v}_i^s \, \bar{v}_j^s \right] =$$

$$= - \frac{\partial \tilde{p}^s}{\partial x_i} + \frac{\partial}{\partial x_j} (\tilde{\sigma}_{ij}^s + \tilde{p}^s \delta_{ij}) - \frac{\partial}{\partial x_j} \left[\rho_s C \, \overline{v_i' v_j'}^s \right] + \rho_s C \, g_i + \tilde{F}_i \qquad (36b)$$

where

$$\tilde{v}_i = (1-C) \, \bar{v}_i^f + C \, \bar{v}_i^s \qquad (37)$$

The apparent viscosity μ^{*f}, defined by equation (34), is a function of the solid concentration and may only be considered constant within a limited range of shear rates. It may be useful to stress that in the above equations terms with an overscore represent surface averages and not time averages. The above equations thus describe the instantaneous situation in the turbulent condition. If, in addition, we want to consider the time-mean situation, also fluctuations in time of the solid concentration have to be taken into account.

4. HYDRODYNAMIC FORCES ON A GRANULAR BED

4.1. Attenuation of viscous-momentum transfer to the interior of the bed

Let us consider the hydrodynamic forces acting under the surface of a granular bed subject to a surface flow. Under the bed surface we may generally neglect inertial forces in the fluid flow. Under these conditions the fluid velocity v_i^f and the fluid pressure p^f have to satisfy the continuity equation

$$\frac{\partial v_i^f}{\partial x_i} = 0 \qquad (38)$$

and the equation of motion:

$$- \frac{\partial p^f}{\partial x_i} + \mu \frac{\partial^2}{\partial x_j \partial x_j} v_i^f + \rho_f g_i = 0 \qquad (39)$$

These micro-equations and the microscopic boundary conditions have to be averaged correctly if a macroscopic flow equation and macroscopic boundary conditions are to be obtained.

At first sight, this problem looks very similar to the spatial 'smoothing' of a homogeneous turbulent flow. Many authors have been misled by this analogy and have assumed that the commutability of averaging and differentiation procedures holds not only in the theory of homogeneous turbulence, but also in the case of porous media. Proper averaging of the terms of equation (39) according to the method described in Section 2.2 over the fluid part δV^f of a finite volume element bounded by a smooth statistical surface in a porous medium with a constant solid concentration shows, however, that this is not the case:

$$\overline{\frac{\partial p}{\partial x_i}}^f = \frac{\partial}{\partial x_i} \bar{p}^f + \frac{1}{\delta V^f} \iint_{\Delta S^b} p^f n_i \, dS^b \tag{40a}$$

$$\overline{\frac{\partial^2 v_i}{\partial x_j \partial x_j}}^f = \frac{\partial}{\partial x_j} \overline{\frac{\partial v_i}{\partial x_j}}^f + \frac{1}{\delta V^f} \iint_{\Delta S^b} \overline{\frac{\partial v_i}{\partial x_j}}^f n_j \, dS^b \tag{40b}$$

$$\overline{\frac{\partial v_i}{\partial x_j}}^f = \frac{\partial}{\partial x_j} \bar{v}_i^f \tag{40c}$$

Properly averaging the terms of equation (39), SAFFMAN (1971) derived the following expression for the reaction force per unit bulk volume exerted by the solid on the pore fluid in a porous medium, apart from the hydrostatic buoyancy force

$$R_i' = -\frac{\partial}{\partial x_i} (1-C) (\bar{p}^f - p_H) + \mu \frac{\partial^2 \tilde{v}_i^f}{\partial x_j \partial x_j} \tag{41}$$

where $\bar{p}^f$ is the areal mean pore pressure, $\tilde{v}_i^f = (1-C) \bar{v}_i^f$ the superficial fluid velocity, and

$$p_H = p_{Ho} + \rho_f g_j x_j \tag{42}$$

is the hydrostatic pressure.

According to MANDL (1963), DARCY's law (1856) for filter flow through a statistically homogeneous porous medium follows from these equations using similarity arguments [see also FERNANDEZ LUQUE & MANDL (197.)] . This means that if $[(p^f-p_H), v_i^f]$ is a solution of (38) and (39) and $v_i^f = 0$ on solid walls, the fields $[\lambda (p^f-p_H), \lambda v_i^f]$ (λ = constant) are also solutions that satisfy the boundary condition $\lambda v_i^f = 0$ on solid walls. Consequently, the transition to a similar solution of the micro-equations does not influence the ratio $R_i'/\tilde{v}_i^f$, and hence the average reaction force of the flow R_i' is proportional to $\tilde{v}_i^f$. Moreover, it follows from equations (38), (39), (41) and (42) that the reaction force R_i' is proportional to the fluid viscosity μ. Hence, the proportionality between R_i' and $\tilde{v}_i^f$ may be expressed as follows:

$$R_i' = - \frac{\mu}{K} (1-C) \tilde{v}_i \tag{43}$$

in accordance with DARCY's law (1856) for a filter flow driven by a pressure gradient in a statistically homogeneous porous medium

$$- \frac{\partial}{\partial x_i} (\bar{p}^f - p_H) = \frac{\mu}{K} \tilde{v}_i \tag{44}$$

Here K is a structural constant of the porous medium, i.e. the permeability. This does not mean, according to MANDL, that K is an absolute structural constant, as is usually assumed, but rather that K is a structural constant only with respect to a class of mathematically similar micro-flow fields. We must therefore expect the reaction force R_i' for a filter flow driven by shearing along the boundary of a porous medium to be different from that for a filter flow driven by a pressure gradient, even if $\tilde{v}_i^f$ is the same.

Let us consider a filter flow driven solely by shearing along the boundary of a 'smooth' bed of granular sediment. We choose a local frame [x, y] with the x-coordinate parallel to the bed surface in the average flow direction and the y-coordinate normal to the bed surface, pointing upwards. We define the bed surface y = 0 as a flat statistical surface element $\Delta S[0]$ intersecting the particles of the bed surface at random and assume that the bed has a constant porosity for $y \leq 0$ (see Fig. 2). The average drag force per unit bulk volume R_x' exerted by the shearing filter flow on the total solid/fluid boundary surface enclosed by a finite volume element $\delta V[y]$, bounded by two sufficient large statistical surface elements $\Delta S[y - \frac{1}{2} \delta y]$ and $\Delta S[y + \frac{1}{2} \delta y]$ a small but finite distance δy apart $((y \pm \frac{1}{2} \delta y) \leq 0)$, can be expressed as follows according to equations (41) and (43) (see Fig. 2).

$$- R_x' = \mu \frac{\partial^2}{\partial y^2} \widetilde{u}^f = \frac{\mu}{K_v} (1-C) \widetilde{u}^f \tag{45}$$

where K_v is the 'shear' permeability of the porous medium. Since the micro-flow behaviour is similar for different values of y, K_v is independent of y and equation (45) yields the following exponential velocity profile and fluid-shear stress distribution:

$$\widetilde{u}^f[y] = \widetilde{u}_o^f \, e^{y \sqrt{\frac{1-C}{K_v}}} \tag{46}$$

$$\overline{\sigma}_{xy}^f = \frac{\mu}{1-C} \frac{\partial \widetilde{u}^f}{\partial y} = (\overline{\sigma}_{xy}^f)_o \, e^{y \sqrt{\frac{1-C}{K_v}}} \tag{47}$$

The attenuation constant

$$\sqrt{\frac{1-C}{K_v}} = \frac{1}{\widetilde{u}^f} \frac{\partial \widetilde{u}^f}{\partial y} = \frac{1}{\overline{\sigma}_{xy}^f} \frac{\partial \overline{\sigma}_{xy}^f}{\partial y} \tag{48}$$

represents the hindrance of the viscous-momentum transfer by the solid material. Obviously, the latter depends on the surface area of porous medium per unit pore volume. Assuming linear dependence, we obtain

$$\sqrt{\frac{1-C}{K_v}} \sim \frac{CA}{1-C}$$

This relationship is the same as the KOZENY formula (1927) for the 'pressure' permeability K

$$\sqrt{\frac{1-C}{K}} = 2.23 \frac{CA}{1-C} \tag{49}$$

For a uniform bed of spherical grains $A = 6 \, D_s$, where A is the specific surface area of the solid and D_s the grain diameter.

MANDL (1963, 197.) found the following filter-flow equation by super-position of a filter flow driven by a pore-pressure gradient [equation (44)] and a filter flow driven by shearing along the boundary of a porous medium (equation 46).

$$\widetilde{u}^f[y] = - \frac{K}{\mu} \frac{\partial}{\partial x} (\overline{p}^f - p_H) + (\widetilde{u}_o^f + \frac{K}{\mu} \frac{\partial}{\partial x} (\overline{p}^f - p_H)) \, e^{y \sqrt{\frac{1-C}{K_v}}} \tag{50}$$

Beavers & Joseph (1967) measured the boundary velocity of a Poiseuille flow over a horizontal fluid-saturated porous block. They related the slip velocity $\tilde{u}_o^f$ at the boundary $y = 0$ of the permeable block to the average shear stress $\tilde{\sigma}_o$ exerted by the Poiseuille flow on the block surface by the ad-hoc boundary condition

$$(\tilde{\sigma}_{xy})_o = \frac{a}{\sqrt{K}} \; (\mu \; \tilde{u}_o^f + K \; \frac{\partial \overline{p}^f}{\partial x}) \tag{51}$$

and, using the results of their experiments, calculated the factor a, defined in our terminology (see equations (47), (50) and (51) as

$$a = \sqrt{\frac{K/K_v}{(1-C)}} \quad \left(\frac{\tilde{\sigma}_{xy}}{\overline{\sigma}_{xy}^f}\right)_{y=0} \tag{52}$$

assuming that the boundary y=0 intersects the roughness elements of the bed surface at random (see Fig. 2). They used aloxite as a porous material with a granular structure, and foametal as a material with a cellular structure. For the aloxite $(K=10^{-6} \; in^2$, average pore size = 0.013 in), they found a = 0.1. Sine $(\tilde{\sigma}_{xy}) > (\overline{\sigma}_{xy}^f)_o$ because the crests of the upper roughness elements absorb a significant part of the total bed shear stress, these results indicate that the 'shear' permeability K_v of a porous material with a granular structure is much higher than its pressure permeability K (it should be noted here that Beavers & Joseph measured K_v near the surface and K inside the porous block). Assuming $(\tilde{\sigma}_{xy})_o = 1.5 \; (\overline{\sigma}_{xy}^f)_o$ and C = 0.6 at y = 0 (near the block surface), we find for the aloxite specimen with a granular structure (a = 0.1, $K = 10^{-6} in^2$, av. pore size = 0.013 in) that $K_v = 560 \, K$, or, using the Kozeny formula (1927) for the pressure permeability K (equation 49).

$$\sqrt{\frac{1-C}{K_v}} \quad \approx \quad 0.1 \; \frac{CA}{1-C} \tag{53}$$

Since the micro-flow behaviour of a steady 'slow' viscous shear flow in a statistically disordered porous medium is similar for different values of y, the ratio $\tilde{\sigma}_{xy}^f / \overline{\sigma}_{xy}^f$ is a structural constant of the porous medium independent of y. Thus, the attenuation of viscous-momentum transfer from the boundary to the interior of the porous medium is related in the same way to (sufficiently large) statistical surface elements chosen parallel to the bed surface as it is to the corresponding 'wavy' surface elements [see equation (48) and (53)]

$$\frac{1}{\widetilde{\sigma}^f_{xy}} \frac{\partial \widetilde{\sigma}^f_{xy}}{\partial y} = \frac{1}{\bar{\sigma}^f_{xy}} \frac{\partial \bar{\sigma}^f_{xy}}{\partial y} = \sqrt{\frac{1-C}{K_v}} \approx 0.1 \left(\frac{CA}{1-C}\right)_{y=0} \tag{54}$$

These equations show that the viscous-momentum transfer from the boundary to the interior of a granular bed is absorbed entirely by the solid skeleton within a boundary layer of two or three particle diameters. From here, any drag force on the solid is exerted by a pore-pressure gradient.

The linear-momentum balance equations (28a) reduce for the viscous boundary layer in a stationary sediment bed with respect to the Cartesian frame shown in Fig. 2, whilst only retaining terms of the highest magnitude, to

$$\frac{\partial \widetilde{\sigma}^f_{xy}}{\partial y} - \frac{\partial \widetilde{p}^f}{\partial x} + \rho_f g_x = \widetilde{F}'_x \tag{55a}$$

$$-\frac{\partial \widetilde{p}^f}{\partial y} + \rho_f g_y = \widetilde{F}'_y \tag{55b}$$

where
$$\widetilde{F}'_i = \widetilde{F}_i + \rho_f C g_i \tag{56}$$

is the drag force per unit bulk volume exerted by the fluid flow upon the solid particles (excluding the hydrostatic buoyancy force).

4.2. Drag and lift forces on particles of the bed surface

4.2.1. At low Reynolds' numbers

Let us now consider the average drag and lift forces acting on the individual particles at the surface of a loose granular bed of uniform particle size D_s, subject to turbulent flow. We choose a local frame of reference (x, y) with the x-axis along the bed surface in the main flow direction, and the y-axis normal to the bed surface, pointing upwards. The plane $y = 0$ intersects the particles (topmost grains) of the bed surface at random. We allow the macro-element $\Delta S(0)$ of the bed surface to have a slope in the flow direction.

At low particle Reynolds' numbers ($Re_D < 0.5$), where we define

$$Re_D = \frac{\rho_f D_s \bar{u}^f}{\mu} \tag{57}$$

we may express the average drag (F'_x) and lift (F'_y) forces exerted by the fluid flow (apart from the hydrostatic buoyancy force $- \alpha_3 D_s^3 \rho_f \vec{g}$) upon the particles of sieve diameter D_s, bounded by two sufficiently large 'wavy' surface elements $\Delta \widetilde{S} [y - \frac{1}{2} \delta y]$ and $\Delta \widetilde{S} [y + \frac{1}{2} \delta y]$, chosen parallel to the bed surface (y=0) a short distance $\delta y \ll D_s$ apart (see Fig. 2)

$$F'_x = \frac{\alpha_3 D_s^3}{C} \left(\frac{\partial \widetilde{\sigma}_{xy}^f}{\partial y} - \frac{\partial}{\partial x} (\widetilde{p} - p_H) \right) \tag{58a}$$

$$F'_y = - \frac{\alpha_3 D_s^3}{C} \frac{\partial}{\partial y} (\widetilde{p}^f - p_H) \tag{58b}$$

Here $\widetilde{\sigma}_{xy}^f$ is areal-average fluid shear stress and $\widetilde{p}^f$ the average fluid pressure transmitted across $\Delta \widetilde{S}^f [y]$ per unit area of the corresponding smooth surface element $\Delta S [y]$. C is defined as the areal solid concentration along $\Delta S [y]$ and is also equal to the volume concentration of solid enclosed between $\Delta S [y - \frac{1}{2} \delta y]$ and $\Delta S [y + \frac{1}{2} \delta y]$. The ratio $C/(\alpha_3 D_s^3)$ represents the number of particles with an average volume $\alpha_3 D_s^3$ enclosed per unit bulk volume between $\Delta \widetilde{S} [y - \frac{1}{2} \delta y]$ and $\Delta \widetilde{S} [y + \frac{1}{2} \delta y]$.

According to SHIELDS (1936), we can also express F'_x as

$$F'_x = C_d \tfrac{1}{4} \rho_f \bar{u}^{f^2} \alpha_1 D_s^2 \tag{59}$$

where C_d is a drag coefficient and $\bar{u}^f$ the average fluid velocity at the particle level. At low particle Reynolds' numbers, $C_d \sim \mu/(\rho_f D_s \bar{u}^f)$ and

$$\bar{u}^f = \bar{u}_0^f + \frac{y}{\mu} (\widetilde{\sigma}_{xy})_0 \qquad (y \geq 0) \tag{60}$$

Equations (58) should thus be modified as follows for a granular bed with a non-uniform particle-size distribution:

$$F'_x = \frac{\alpha_{11} D_s}{CA^2} \left(\frac{\partial \widetilde{\sigma}_{xy}^f}{\partial y} - \frac{\partial}{\partial x} (\widetilde{p} - p_H) \right) \tag{61a}$$

$$F'_y = - \frac{\alpha_{12} D_s}{CA^2} \frac{\partial}{\partial y} (\widetilde{p} - p_H) \tag{61b}$$

where α_{11} and α_{12} are particle-shape factors (For a bed of uniform spherical grains $\alpha_{11} = \alpha_{12} = 6\pi$).

The attenuation of viscous-momentum transfer by particles of the bed surface may be expressed as follows in accordance with equations (58a), (59) [with $C_d \sim \mu/(\rho_f D_s \bar{u}^f)$], (60) and (61), and by analogy with equation (54):

$$\frac{1}{\overset{\sim}{\sigma}{}^f_{xy}} \ \frac{\partial \overset{\sim}{\sigma}{}^f_{xy}}{\partial y} = a_1 \ CA \tag{62}$$

Here a_1 is an attenuation factor, depending on $(A.y)$ and on the shape of the particles.

A sufficiently slow viscous shear flow $(\tilde{v}{}^f_y = 0)$ does not exert an average lift force on the solid in a statistically disordered porous medium. As shown below, this follows from the symmetry of the micro-streamline pattern around (spherical) particles in a shear flow.

An inspection of the micro-streamline pattern around a rigid particle in a 'slow' viscous shear flow does not tell us the direction in which the fluid streams. From the symmetry of the streamline pattern around a spherical particle, it follows that the normal component (normal to the bed surface) of the viscous force on any microscopic surface element in the upstream region of the particle is equal in magnitude but opposite in direction to the corresponding component on the downstream side of the particle.

Similarly, from the symmetry of the streamline pattern it follows that the component normal to the bed surface of the fluctuation pressure $p^{f'} = p^f - \tilde{p}{}^f$ on any microscopic element of the particle surface in the upstream region is balanced by a corresponding component in the downstream region. The resulting force exerted by shear flow on a spherical particle is thus in the average flow direction. [This is no longer true when inertial forces start to play a role in the flow - see SAFFMAN (1964)].

4.2.2. At high Reynolds' numbers

At high particle Reynolds' numbers, the flow is generally driven by shearing along the boundary and we can express as follows the average drag and lift forces on particles of the bed surface, (F'_x, F'_y), for a bed of uniform particle size, under turbulent flow conditions, neglecting unsteady-flow terms:

$$F'_x = \frac{\alpha_3 D_s^3}{C} \ \frac{\partial \overset{\sim}{\tau}{}^f_{xy}}{\partial y} \tag{63a}$$

$$F'_y = - \frac{\alpha_3 D_s^3}{C} \ \frac{\partial}{\partial y} \ (\tilde{p}{}^f + \rho_f(1-C) \ \overline{v'v'}{}^f - p_H) \tag{63b}$$

Here

$$\tilde{\tau}_{xy}^{f} = \tilde{\sigma}_{xy}^{f} - \rho_{f}(1-C) \overline{u'v'}^{f} \tag{64}$$

is the surface average total fluid shear and $\{\tilde{p} + \rho_{f}(1-C) \overline{v'v'}^{f}\}$ the total fluid pressure transmitted across a 'wavy' 'macro'-surface element $\Delta\tilde{S}(y)$ chosen parallel to the bed surface $y = 0$. (u', v') are the (x,y)-components of the turbulent fluid velocity fluctuations.

According to SHIELDS (1936), we can also express F_x' by means of equation (59), where C_D is only a weak function of Re_D for $Re_D \gg 1$. The time-average fluid velocity $\bar{u}$ is given for $Re_D \gg 1$, as a function of y, by [NIKURADSE (1933)]

$$\frac{\bar{u}^{f}}{u^{*}} = 5.75 \log \frac{y}{k_s} + 8.5 \qquad (y \geq 0) \tag{65}$$

For turbulent boundary layers with suction or injection, the logarithmic velocity scale is according to TENNEKES (1964) proportional to $(u^{*} + 9 \ \overline{v}_{o}^{f})$, at low suction rates and not too high injection rates $(-0.04 \leq \overline{v}_{o}^{f}/u^{*} \leq 0.2)$:

$$\frac{\bar{u}^{f}}{(u^{*} + 9 \ \overline{v}_{o}^{f})} = 5.75 \log \frac{y}{k_s} + 8.5 \tag{65a}$$

Here $u^{*} = (\tilde{\tau}_{o}^{f}/\rho_{f})^{\frac{1}{2}}$ is the mean shear velocity, and k_s the surface roughness (approximately equal to the particle diameter D_s). Equations (63) should thus be modified as follows for a granular bed with a non-uniform particle-size distribution:

$$F_x' = \frac{\alpha_{21} D_s^2}{CA} \ \frac{\partial \tilde{\tau}_{xy}^{f}}{\partial y} \tag{66a}$$

$$F_y' = - \frac{\alpha_{22} D_s^2}{CA} \ \frac{\partial}{\partial y} \ (\tilde{p}^{f} + \rho_{f}(1-C) \overline{v'v'}^{f} - p_H) \tag{66b}$$

where α_{21} and α_{22} are particle-shape factors. (For a bed of uniform spherical grains $\alpha_{21} = \alpha_{22} = \pi$).

The attenuation of turbulent momentum transfer by particles of the bed surface obviously depends on the total surface area of particles obstructing the flow and can be expressed as follows in accordance with equations (59), (65) and (66a) for $\bar{u}^{f} = \bar{u}$, and by analogy with equation (62)

$$\frac{1}{\tilde{\tau}_{xy}^{f}} \ \frac{\partial \tilde{\tau}_{xy}^{f}}{\partial y} = a_1 \ CA \tag{67}$$

Here a_1 depends on A.y or y/k_s, Re_D and the shape of the particles. According to equations (66a) and (67), the attenuation factor can also be considered as

$$a_1 = \frac{\alpha_2}{\alpha_{21}} \left(\frac{F'_x}{\alpha_2 D_s^2 \widetilde{\tau}^f_{xy}} \right)_{y=0} \tag{68}$$

where $F'_x/(\alpha_2 D_s^2 \widetilde{\tau}^f_{xy})_{y=o}$ is the apparent shear stress exerted by the flow on that portion of the bed surface occupied by a grain $(\alpha_2 D_s^2)$ divided by the areal average turbulent fluid shear stress at the bed surface, $\widetilde{\tau}^f_o$. For a uniform bed of spherical grains $A = 6/D_s$, $\alpha_2 = \pi/4$, $\alpha_3 = \pi/6$ and $F'_x = a_1 \pi D_s^2 \widetilde{\tau}^f_o$.

A shearing flow also exerts a lift force on the grains at high shear particle Reynolds' numbers.

$$F'_y = \xi_o F'_x \tag{69}$$

The lift factor ξ_o must depend on A.y, Re_D and the shape of the particles. CHEPIL (1959) found from experiment that for large values ($\gg 1$) of Re_D the lift coefficient on prominent particles in an air stream has a constant value of $\xi_o = 0.85$. For turbulent boundary layers with suction or injection, ξ_o will also be a function of $\overline{v}^f_o/u^*$.

5. BALANCE OF FORCES ON THE BED LOAD

In the main turbulent flow above a granular bed, particles are transported in suspension. These particles constitute the 'suspended load'. In a thin turbulent boundary layer between the bed and the main flow, particles are transported rolling and saltating over the bed. Turbulent momentum is transferred by the fluid to these particles that constitute the 'bed load', and is then transmitted as a shear stress and a 'dispersive' grain pressure, to the bed.

Let us consider the balance of forces acting on the bed load under uniform-flow conditions. We choose for that purpose a local frame of reference x,y with the x-coordinate parallel to the bed surface in the average flow direction and the y-coordinate perpendicular to the bed surface, pointing upwards. We locate the origin of the frame on the flat 'wavy' macro-surface element $\Delta\widetilde{S}[0]$ separating the particles of the bed load from those of the bed. We separate the bed load from the main flow by means of a smooth macro-surface element $\Delta S[\delta_B]$ at a small distance δ_B above the bed, assuming that no

particles are transported in suspension.

The linear-momentum balance equations (36) reduce with respect to this frame for $0 \leq y \leq \delta_B$, only retaining terms of the highest magnitude, to:

$$\frac{\partial}{\partial t}\left[\rho_f(1-C)\,\bar{u}^f\right] + \frac{\partial}{\partial x}\left[\rho_f(1-C)\bar{u}^f\bar{u}^f\right] + \frac{\partial}{\partial y}\left[\rho_f(1-C)\,\bar{u}^f\bar{v}^f\right] =$$

$$= -\frac{\partial}{\partial x}\left[\tilde{p}^f + \rho_f(1-C)\,\overline{u'u'}^f - p_H\right] + \frac{\partial\tilde{\tau}_{xy}^f}{\partial y} - \widetilde{F}_x' \tag{70a}$$

$$0 = -\frac{\partial}{\partial y}\left[\tilde{p}^f + \rho_f(1-C)\,\overline{v'v'}^f - p_H\right] - \widetilde{F}_y' \tag{70b}$$

$$\frac{\partial}{\partial t}\left[\rho_s C\,\bar{u}^s\right] + \frac{\partial}{\partial x}\left[\rho_s C\,\bar{u}^s\bar{u}^s\right] + \frac{\partial}{\partial y}\left[\rho_s C\,\bar{u}^s\bar{v}^s\right] =$$

$$= -\frac{\partial}{\partial x}\left[\tilde{p}^s + \rho_s C\,\overline{u'u'}^s\right] + \frac{\partial\tilde{\tau}_{xy}^s}{\partial y} + (\rho_s - \rho_f)\,C\,g_x + \widetilde{F}_x' \tag{70c}$$

$$0 = -\frac{\partial}{\partial y}\left[\tilde{p}^s + \rho_s C\,\overline{v'v'}^s\right] + (\rho_s - \rho_f)\,C\,g_y + \widetilde{F}_y' \tag{70d}$$

Here (u, v) are the (x, y)-components of the fluid (f) or solid (s) velocities, (u', v') are the corresponding turbulent velocity fluctuations, and (F_x', F_y') are the average drag and lift forces exerted per unit bulk volume by the flow upon the bed-load particles [equation (56)],

$$\tilde{\tau}_{xy}^s = \tilde{\sigma}_{xy}^s - \rho_s\,C\,\overline{u'v'}^s \tag{71}$$

is the surface-average total solid shear stress and $\tilde{\tau}_{xy}^f$ the average total fluid shear stress [equation (64)] in the saltation layer.

Under uniform-flow conditions, these surface averages may also be considered time averages (denoted by the suffix ‾) if the bed surface $\Delta\widetilde{S}[0]$ is chosen sufficiently large. Equations (70) then reduce to

$$\frac{\partial\overline{\tilde{\tau}_{xy}^f}}{\partial y} - \overline{\widetilde{F}_x'} = 0 \tag{72a}$$

$$-\frac{\partial}{\partial y}\left\{\overline{\tilde{p}^f} + \rho_f(1-\bar{C})\,\overline{v'v'}^f - p_H\right\} - \overline{\widetilde{F}_y'} = 0 \tag{72b}$$

$$\frac{\partial\overline{\tilde{\tau}_{xy}^s}}{\partial y} + (\rho_s - \rho_f)\,\bar{C}\,g_x + \overline{\widetilde{F}_x'} = 0 \tag{72c}$$

$$-\frac{\partial}{\partial y}\left\{\overline{\widetilde{p}^{\,s}} + \rho_s\,\overline{C}\,\overline{v'v'}^{\,s}\right\} + (\rho_s - \rho_f)\,\overline{C}\,g_y + \overline{\widetilde{F}'_y} = 0 \tag{72d}$$

Integration of equations (72) over the entire thickness δ_B of the saltation layer gives

$$\overline{\widetilde{\tau}}_0 - \overline{\widetilde{\tau}^{\,f}_0} = \overline{\widetilde{\tau}^{\,s}_0} = \int_0^{\delta_B} \overline{\widetilde{F}'_x}\,dy \tag{73a}$$

$$\left\{\overline{\widetilde{p}^{\,f}} + \rho_f(1-\overline{C})\,\overline{v'v'}^{\,f} - p_H\right\}_{y=\delta_B} - \left\{\overline{\widetilde{p}^{\,f}} + \rho_f(1-\overline{C})\,\overline{v'v'}^{\,f} - p_H\right\}_{y=0} = -\int_0^{\delta_B}\overline{\widetilde{F}'_y}\,dy \tag{73b}$$

$$\overline{\widetilde{\tau}^{\,s}_0} = \int_0^{\delta_B}\overline{\widetilde{F}'_x}\,dy + \int_0^{\delta_B}(\rho_s - \rho_f)\,\overline{C}\,g_x\,dy \tag{73c}$$

$$\overline{\widetilde{p}^{\,s}_0} = -\int_0^{\delta_B}\overline{\widetilde{F}'_y}\,dy - \int_0^{\delta_B}(\rho_s - \rho_f)\,\overline{C}\,g_y\,dy \tag{73d}$$

where $\overline{\tau}_0$ is the total average bed shear stress (at $y = \delta_B$) and $(\overline{\widetilde{\tau}^{\,f}_0}, \overline{\widetilde{\tau}^{\,s}_0})$ the corresponding fluid and solid components (at $y = 0$).

Let $\overline{n}_B$ be the average number of bed-load particles rolling and saltating per unit area above the bed surface and let $(\overline{F}'_x, \overline{F}'_y)$ be the average drag and lift forces exerted by the flow on these particles (excluding the hydrostatic buoyancy force). Then

$$\int_0^{\delta_B}\overline{\widetilde{F}'_i}\,dy = \overline{n}_B\,\overline{F}'_i \tag{74a}$$

Let further $\alpha_3 D_s^3$ be the average volume of the bed-load particles and D_s the corresponding sieve diameter. Then

$$\int_0^{\delta_B}(\rho_s - \rho_f)\,\overline{C}\,g_i\,dy = \alpha_3 D_s^3\,(\rho_s - \rho_f)\,g_i\,\overline{n}_B \tag{74b}$$

The integral linear momentum balance equations (73) can thus be simplified as follows for a bed-load of uniform particle size:

$$\overline{\tau}_0 - \overline{\widetilde{\tau}^{\,f}_0} = \overline{\widetilde{\tau}^{\,s}_0} = \overline{n}_B\,\overline{F}'_x \tag{75a}$$

$$\left\{ \overline{\widetilde{p}^f} + \rho_f(1-\overline{C}) \ \overline{v'v'}^f - p_H \right\}_{y=\delta_B} - \left\{ \overline{\widetilde{p}^f} + \rho_f(1-\overline{C}) \ \overline{v'v'}^f - p_H \right\}_{y=0} = - \overline{n}_B \ \overline{F}'_y \quad (75b)$$

$$\overline{\widetilde{\tau}^s_o} = \overline{n}_B \ \{ \overline{F}'_x + \alpha_3 D^3_s \ (\rho_s - \rho_f) \ g_x \} \quad (75c)$$

$$\overline{\widetilde{p}^s_o} = - \ \overline{n}_B \ \{ \overline{F}'_y - \alpha_3 D^3_s \ (\rho_s - \rho_f) \ g_y \} \quad (75d)$$

According to these equations, an average drag force of the fluid on the bed-load particles results in a reduction of turbulent fluid shear at the bed surface, while an average 'dispersive grain pressure' on the bed results in a turbulent fluid pressure drop across the surface.

6. STABILITY CONDITIONS FOR BED SURFACE

6.1. SHIELDS' grain-movement condition

The upper layer of particles on a loose granular bed will start rolling if the moment of the surface forces exerted by the fluid on the particles at points of contact with underlying particles is greater than the moment of the resisting force of gravity (see Fig. 3). According to CHEPIL (1959), we can express the average threshold drag acting on grains of sieve diameter D_s at the surface $y = 0$ of a horizontal sediment bed, bounded by two 'wavy' surfaces $\Delta \widetilde{S} (\pm \frac{1}{2} \delta y)$, located a short distance $\delta y \ll D_s$ apart, as

$$\left(\frac{F'_x}{\alpha_3 \ D^3_s \ (\rho_s - \rho_f) \ g - F'_y} \right)_{y=0} = \tan \alpha \quad (76)$$

where α should be approximately equal to the angle of repose (32° for a loose sand bed). CHEPIL (1959) found from experiments that for the topmost grains on a loose granular bed $\alpha = 24^o$. This small value is due to the fact that the drag force on those grains acts above the centre of the particles (see Fig. 2).

Substitution of (63a), (67) and (69) in (76) gives the following equation for the turbulent bed shear stress at the threshold of sediment motion

$$\frac{\widetilde{\tau}^f_o}{(\rho_s - \rho_f) \ g \ D_s} = \frac{\alpha_3 \tan \alpha}{\alpha_{21} \ a_1 \ (1 + \xi_o \tan \alpha)} \quad (77)$$

GRASS (1970) has shown that for any given area of a flat bed there will be a random distribution of critical shear stresses corresponding to those shear stresses that will move individual grains. This randomness is caused by (a) a variation in drag force for a given bed shear stress (this variation is primarily a function of y/D_s), and (b) a variation in the critical drag angle α. We may define α in equation (76) as the average drag angle for the topmost grains that form part of the bed at one moment during incipient sediment motion. We can define the bed surface $y = 0$ at any given moment by the wavy surface $\Delta\widetilde{S}(0)$ separating the particles of the bed (at rest) from those of the bed load (in motion).

SHIELDS (1936) plotted the temporal mean bed shear stress $\bar{\tau}_0$ in dimensionless form

$$\frac{1}{\psi} = \frac{\bar{\tau}_0}{(\rho_s - \rho_f)\, g\, D_s} \tag{78}$$

at the threshold of continuous sediment motion ($\bar{\tau}_0 = \bar{\tau}_c$) versus the shear REYNOLDS' number

$$Re_D^* = \frac{D_s}{\mu}\sqrt{\rho_f\,\bar{\tau}_0} = \frac{\rho_f D_s u^*}{\mu} \tag{79}$$

and found that $1/\psi_c$ has values ranging from 0.035 for $Re_D^* \approx 10$ to 0.06 for $Re_D^* \approx 2$ and $Re_D^* \approx 400$ (see Fig. 5).

We can also define a critical shear stress τ_c as the areal-average turbulent fluid shear, $\widetilde{\tau}_c^f(0)$, that will just move the topmost grains forming part of the bed at any given moment at the threshold of continuous sediment motion. GRASS (1970) has shown that at SHIELDS' grain-movement condition the topmost grains are just moved by the temporal mean bed shear stress $\bar{\tau}_c$. Using SHIELDS' $\bar{\tau}_c$ for $\widetilde{\tau}_0^f$, we find by comparing expressions (77) and (78) that the attenuation of turbulent momentum transfer from the surface to the interior of the bed is correctly expressed by equation (67), the attenuation factor a_1 being a weak function of Re_D^*. For $\alpha = 24^\circ$ and $\xi_0 = 0.85$, as found by CHEPIL (1959), $\alpha_3 = \frac{\pi}{6}$ and $\alpha_{21} = \pi$, valid for a bed of uniform spherical particles), a_1 has according to equation (77) values ranging from 1.54 for $1/\psi_c = 0.035$ to 0.90 for $1/\psi_c = 0.06$. According to equation (68), this means that for $Re_D^* \geq 10$ the topmost grains 'absorb' 3.6 - 6 times the areal average bed shear stress.

Substitution of expressions (61a) and (62) for F'_x, neglecting the longitudinal fluid-pressure gradient at the bed surface, and of $F'_y = 0$, in (76), gives the following equation for the areal-average viscous fluid shear at the threshold of sediment motion, at low shear Reynolds' numbers $(Re^*_D < 0.5)$

$$\frac{\tilde{\tau}^f_o}{(\rho_s - \rho_f)\, g\, D_s} = \frac{\alpha_3 A\, D_s \tan \alpha}{\alpha_{11} a_1\, A\, D_s} \tag{80}$$

Vanoni (1964) found empirically $1/\psi_c = 0.22$ for $Re^*_D = 0.4$. This value should also be valid for $Re_D < 0.4$, as long as there is no cohesion between the particles (It should be noted here that this is not predicted by Shields' diagram). For $1/\psi_c = 0.22$ as found by Vanoni for $Re^*_D = 0.4$, $\alpha = 24^o$ as predicted by Chepil for high shear Reynolds' number, $\alpha_3 = \frac{\pi}{6}$, $\alpha_{11} = 6\pi$ and $A = 6/D_s$ (valid for a bed of uniform spherical particles), the attenuation factor a_1 has according to equation (80) a value of 0.337.

If the bed surface has a downward slope β in the flow direction, $1/\psi_c$ is reduced by a factor

$$\frac{1}{\psi_c} = \left(\frac{1}{\psi_c}\right)_{\beta=0} \frac{\sin (\alpha - \beta)}{\sin \alpha} \tag{81}$$

This follows from the balance of moments acting at points of contact with underlying particles on the topmost grains, assuming that the average hydrodynamic drag and lift forces on those grains act at fixed particle points that are independent of the slope β (see Fig. 3). This assumption is justified for either sufficiently small (< 0.5) or very large (>>1) shear Reynolds' numbers (when the flow pattern is similar for different flow velocities).

6.2. During bed-load transport

Let us consider during bed-load transport the conditions for stability of the upper layer of particles that at a given moment form part of a small area $\Delta\tilde{S}(0)$ of a loose granular bed. Experiments have shown that the number of bed-load particles colliding with or rolling over a certain portion of the bed's surface at a particular moment during bed-load transport is very small compared with the number of particles that form part of that surface at that moment. As a result, the particles of the bed load that exert contact forces at relatively few and constantly changing points on the bed's surface cannot stabilise the far greater number of other surface particles. Consequently, the various forces that continuously act together on the upper layer of particles

forming part of the bed at any given moment during bed-load transport, i.e. gravity, surface forces of the fluid and intergranular forces from underlying particles, must be in equilibrium.

During bed-load transport there will be 'locally' (above the area $\Delta \widetilde{S}(0)$) and instantaneously, in arbitrary succession:

a. simultaneous erosion and deposition,

b. erosion but no deposition,

c. deposition but no erosion.

During erosion, in cases a. and b., the topmost grains forming part of the bed at one particular moment (at rest, by definition) must be at the threshold of motion. The fluid part $\widetilde{\tau}_o^f$ of the turbulent bed shear stress $\widetilde{\tau}_o$ must then be equal to the critical fluid-shear stress τ_c that will just move the topmost grains that form part of the bed at that particular moment. In case c., during deposition without simultaneous erosion, $\widetilde{\tau}_o^f$ will be smaller than τ_c.

According to this concept, the bed load, consisting of particles rolling and saltating over the bed, reduces the maximum fluid-shear stress $\widetilde{\tau}_{o,max}^f$ at the bed surface to the critical value τ_c by exerting an average reaction force on the surrounding fluid. This concept is in agreement with BAGNOLD's theory (1956) for low bed-load concentrations. However, BAGNOLD assumed this value, and also the temporal mean value of $\widetilde{\tau}_o^f$, $\overline{\tau}_o^f$, to be constant as long as the bed-load concentration is so low that it does not seriously affect the turbulence structure at the bed surface. GRASS (1970) and WILLIAMS & KEMP (1971), on the other hand, have pointed out that for any given area of a flat bed there will be a random distribution of critical drag forces that will move individual grains. At incipient particle motion only the topmost grains will be eroded, τ_c will thus increase as $\widetilde{\tau}_o$ increases and the bed load will not effectively reduce the fluid part of the turbulent bed shear stress. This can also hardly be expected since at incipient motion the bed-load particles only cover a small portion of the bed surface. With increasing bed-load transport rate, however, τ_c must become a constant, τ_{sc}. This will occur once the bed is so smooth due to erosion of the most protruding particles and selective deposition that it will not become smoother just by removing the topmost grains that are at rest. This can be shown and τ_{sc} can be determined experimentally, as follows.

Consider a uniform flow over a 'smooth' granular bed of uniform particle size, of which one part is consolidated and one part is loose. The consolidated part of the bed is located upstream of the loose part. At the threshold of sediment motion only the topmost grains of the loose bed will be eroded and these grains will be carried away downstream by the flow or will be selectively deposited in local depressions of the bed surface. The bed-load transport will thus cease after a short while. With increasing flow velocity, more particles will be eroded from the bed surface but the bed-load transport will soon cease again as long as the maximum turbulent bed shear stress $\tilde{\tau}_{o,max}$ is less than the critical value τ_{sc}. The bed-load transport will not cease, however, once $\tilde{\tau}_{o,max}$ exceeds τ_{sc}. This will lead to non-ceasing scour of the loose bed. The critical shear stress τ_{sc} can thus be determined by measuring the maximum turbulent bed shear stress at the initiation of non-ceasing scour.

We may conclude that at a sufficiently high bed shear stress, the bed load, consisting of particles rolling and saltating over the bed, will reduce the maximum turbulent fluid shear at the bed surface to the critical value τ_{sc}. This conclusion is inevitable, since, if $\tilde{\tau}_o^f$ were to exceed τ_{sc}, the topmost grains under the 'wavy' bed surface $\tilde{S}(0)$ would not be at rest and would thus, by definition, form part of the bed load. The bed load thus forms a protective 'shield' at high bed-load concentrations, which controls the erosion rate.

At high concentrations, the bed load will seriously affect the turbulence structure at the bed surface. This may have an influence on the ratio between fluid shear stress and distribution of drag forces on the particles of the bed surface, and therefore on the value of τ_{sc}. BAGNOLD (1954, 1956) concluded from the results of experiments he performed with concentrated suspensions sheared in the annular space between two concentric drums, that $\tilde{\tau}_o^f$ must approach zero for high bed-load concentrations. In our opinion, this is not true because during bed-load transport particles are almost continuously eroded from the bed surface by the turbulent flow, also at high concentrations.

7. BED-LOAD TRANSPORT EXPERIMENTS

7.1. Description of experiments

In order to verify our conclusion that the bed load reduces the maximum turbulent fluid shear at the bed surface to a critical value, τ_{sc}, and to study the mechanism of bed-load transport in general, we carried out a series of experiments in which we measured the mean rate of bed-load transport $(\bar{q}_s)$, the average particle velocity $(\bar{u}_s)$, the average number of particles deposited per unit area per second $(\bar{n}_D)$ and the average length of individual particle steps $(\bar{\lambda}_B D_s)$, in water, as a function of temporal mean bed shear stress $(\bar{\tau}_o)$. Use was made of five different bed materials, and the measurements were taken at a horizontal position and three different downward slopes $(12^o, 18^o$ and $22^o)$ of the flow channel.

Figures 4a and 4b show the 8 m long, 0.20 m high and 0.10 m wide closed rectangular flow channel with transparent sides used for this purpose, which was mounted on a 2.5 m high scaffolding thus permitting rotation about an axis perpendicular to the transparent sides. Water was withdrawn from a constant-level reservoir located at a height of 3.5 m above the centre of the channel and entered the flow channel through a diffuser designed to give the flow at the entrance approximately the same velocity distribution as at the centre of the flow channel. The degree of turbulence, however, was higher at the entrance. A 1 m long consolidated bed with a slope of 1 : 30 was buried under the loose bed right behind the diffuser to prevent scour at the entrance of the channel. During bed-load transport, the length of the flat portion of the loose bed ranged between 7 m at the beginning and 5 - 5.5 m at the end of each experiment (see Fig. 4a). The maximum scour depth behind the consolidated slope was in none of the cases more than 10 mm.

In order to measure the critical bed shear stress at the initiation of scour, we placed a 4 m long consolidated bed of the original grain size between the diffuser and the consolidated slope, and we observed the non-ceasing scour at a distance of 6 m from the diffuser.

Water flowing out of the channel was discharged via a second constant-level tank 5 m below the reservoir.

We used two sands as bed material (density ρ_s = 2640 kg/m^3) with mean (by weight) sieve diameters of D_s = 0.9 mm and D_s = 1.8 mm, gravel $(\rho_s$ = 2640 kg/m$^3)$ of D_s = 3.3 mm, walnut grains $(\rho_s$ = 1340 kg/m$^3)$ of D_s = 1.5 mm and magnetite $(\rho_s$ = 4580 kg/m$^3)$ of D_s = 1.8 mm. All fractions had upper and lower sieve limits of 1.33 D_s and 0.67 D_s, respectively, a standard deviation

of $0.17 D_s$, and $D_{90} = 1.25 D_s$ (D_{90} is the diameter for which 90% of the material by weight is finer). The water depth ranged from 0.08 m for the gravel and the magnetite to 0.12 m for the other bed materials.

The average flow velocity was measured during bed-load transport with a small Pitot tube through the entire cross-section of the channel at different locations and was found to be practically two-dimensional above the (5 cm wide) centre part of the bed. Figure 4b shows a contour plot of the average flow velocity distribution in the channel. We computed the temporal mean bed shear stress $\bar{\tau}_o$ at the centre part of the bed using the Moody diagram for pipe friction with the hydraulic radius corresponding to the 0.05 m wide centre part of the bed region. We also measured the hydraulic gradient (with an electrical pressure transducer), and $\bar{\tau}_o$ values derived from this gradient showed good agreement with values derived from the Moody diagram. Finally, we also measured the turbulent fluid-velocity fluctuations during bed-load transport at a distance of 4.5 or 9 mm above the centre part of the bed, using a laser-Doppler velocity meter. For that purpose a He-Ne laser beam with a diameter of 1 mm was split into two parallel beams, 34 mm apart, and the beams were focussed by means of a lens with a focal distance of 190 mm, crossing at the centre of the flow channel. The distance between two adjacent maxima (intensity) in water was 4.72×10^{-6} m and the volume of water enclosed by the crossing beams was approx. 10^{-2} mm^3. Milk particles were added to the water of the flow channel (1 litre per 25 m^3 of water) in order to scatter the diffracted light. The resulting Doppler frequency was measured by means of a photo-electric cell and an electronic frequency follower connected to a tape recorder and a high-speed ultra-violet chart recorder (see Fig. 4b). The probability density $P(u)$ of the longitudinal velocity was obtained by sampling the U.V.-recordings.

We measured the mean rate of bed-load transport ($\bar{q}_s$) by photographing at regular intervals the foreset bedding formed by the sediment transported above the centre part of the channel in a 0.04 m deep and 0.4 m long transparent container at the end of the channel (see Fig. 4a). We only measured the bed-load transport as long as the bed was flat. Through the transparent side walls of the channel, a 16 mm colour film (speed 32 - 45 frames/s) was taken of a small portion (0.25 x 0.10 m) of the bed during bed-load transport. The film was taken at a distance of 6 m from the entrance of the channel, in a plane perpendicular to the axis of the channel. It was taken at an angle of 63° to the plane of the bed surface in cases where the water depth was 0.12 m, and at an angle of 43° in cases where the water depth was 0.08 m. These angles were reduced in the flow channel to 42° and 31°, respectively, owing to

refraction of the light (see Fig. 4b). The average particle velocity ($\bar{u}_s$), the mean number of particles deposited per unit area per second ($\bar{n}_D$) and the average length of individual particle steps ($\bar{\lambda}_B D_s$) were measured visually above the 5 cm wide centre part of the bed by projecting the film repeatedly at a speed of 16 frames/s and averaging the observed $\bar{u}_s$, $\bar{n}_D$ and $\bar{\lambda} D_s$ values. Each value reported in this paper represents an average of at least 20 measurements. The average particle velocity $\bar{u}_s$ was measured visually by following, with a pencil in one hand and a stopwatch in the other, small groups of particles moving together to establish the time required by the particles to cover a fixed distance on the screen. A ruler and a stopwatch shown in the film allowed us to calculate the original time and distance. The number of particles $\bar{n}_D$ deposited per unit area per second were counted visually on a small rectangular portion of 20 x 20 to 50 x 50 mm^2 of the bed surface shown on the projection screen, which was further covered with black paper. The average length $\bar{\lambda}_B D_s$ of individual particle steps was drawn with a pencil on the screen while the film was projected. Individual frames of the colour film were also projected in a sequence to study the motion of individual bed-load particles more closely.

7.2. Results of experiments

Tables 1-6 and Figs. 5-14 show the results of the experiments. We only measured the bed-load transport at low shear stress ($1.1 < \bar{\tau}_o/\bar{\tau}_c \leq 2.7$), without ripples, and the turbulence intensity was relatively low in our closed flow channel. During our experiments the flow Reynolds' number as defined by the Moody diagram ranged from 3.10^4 to 12.10^4. The shear Reynolds' number, however, as defined by equation (11) was sufficiently large ($15 \leq Re_D^* \leq 165$) to ensure fully developed turbulent flow near the bed surface, particularly for the heavy sediments gravel and magnetite.

Figure 5 shows the temporal mean bed shear stress at the threshold of continuous sediment motion [$\bar{\tau}_c = (\rho_s - \rho_f) g D_s/\psi_c$] as a function of the shear Reynolds' number (Re_D^*). We found that at SHIELDS' grain-movement condition the bed-load concentration C_B, defined as the total projected area of bed-load particles above a unit bulk area of the bed, had a temporal mean value of $\bar{C}_B = 0.001$ (this corresponds to an average distance between two adjacent bed-load particles of approx. 25 D_s). We used this value of $\bar{C}_{Bc}$ to define $\bar{\tau}_c$ for all bed materials and slopes.

Figure 6a shows the probability density P[u] of the turbulent fluid velocity distribution P(u) derived by sampling the longitudinal velocity fluctuations measured at a distance of y = 4.5 mm above the bed of magnetite (below the threshold of bed-load transport: $1/\psi$ = 0.0275). This function has an almost normal distribution with a standard deviation of 0.19 $\bar{u}$, a skewness factor of 0.017 and a flatness factor (kurtosis) of 2.99.

Figure 6b shows the probability density P(u) measured during bed-load transport at a distance of 4.5 mm above the finest-sand bed (D_s = 0.9 mm).

We also measured the turbulent fluid-velocity fluctuations at a distance of 9 mm above the bed of magnetite (Fig. 6c) and found for the standard deviation of the longitudinal velocity distribution divided by the mean fluid velocity at y = 9 mm a value (0.18) that was 5% lower than at y = 4.5 mm (Fig. 6a). Figures 6d, 6e and 6f show P(u) for the other bed materials measured during bed-load transport at y = 9 mm. These velocity distributions have a standard deviation ranging from 0.14 $\bar{u}$ for the bed of walnut grains to 0.21 $\bar{u}$ for the gravel bed.

Figure 7 shows the maximum time interval Δt_{max} during which the instantaneous bed shear stress $\tilde{\tau}_0$ exceeded a given value $(\tilde{\tau}_0/\bar{\tau}_0)$ without interruption, derived from the longitudinal fluid-velocity distribution measured for 10 s at a distance of y = 4.5 mm above the bed of magnetite (D_s = 1.8 mm) and above the finest-sand bed (D_s = 0.9 mm).

Figure 8 shows the temporal mean bed-shear stress at the initiation of scour $[\bar{\tau}_{sc} = (\rho_s - \rho_f)g\,D_s/\psi_{sc}]$ versus the shear REYNOLDS' number (Re_D^*) for a horizontal bed of different materials (see also Tables 1-5). The value of $1/\psi_{sc}$ varies between 0.050 for the finest-sand bed (D_s = 0.9 mm) and 0.058 for the gravel bed (D_s = 3.3 mm).

Figure 9 and Tables 1-5 show the rate of bed-load transport as a function of the time mean bed-shear stress for the different bed materials at different slopes of the bed surface, using the dimensionless expressions $1/\psi$ (equation 78), the $1/\psi_c$-values shown in Fig. 5 and EINSTEIN's dimenionless expression for the intensity of bed-load transport

$$\Phi = \frac{\bar{q}_s}{D_s \sqrt{\left(\frac{\rho_s}{\rho_f} - 1\right)g D_s}} \tag{82}$$

The line in Fig. 10 satisfies the equation

$$\Phi = 5.7 \left(\frac{1}{\psi} - \frac{1}{\psi_c} \right)^{3/2} \tag{83}$$

Figure 10 and Tables 1-5 show the average number of particles deposited on the bed surface per unit area per second, $\bar{n}_D$, in a dimensionless form

$$N_D = \frac{\bar{n}_D D_s^3}{\sqrt{\left(\frac{\rho_s}{\rho_f} - 1 \right) g D_s}} \tag{84}$$

as a function of $(1/\psi - 1/\psi_c)$, for the different bed materials at different slopes of the bed surface. The line satisfies the equation

$$N_D = 0.038 \left(\frac{1}{\psi} - \frac{1}{\psi_c} \right)^{3/2} \tag{85}$$

Figure 11 and Tables 1-5 show the average particle velocity (denoted by $\bar{u}_s$) as a function of the shear velocity

$$u^* = (\bar{\tau}_o/\rho_f)^{\frac{1}{2}} \tag{86}$$

and the critical shear velocity u_c^*, corresponding to SHIELDS' grain-movement condition for the different bed materials at different slopes of the bed surface. The line satisfies the equation

$$\bar{u}_s = 11.5 \, (u^* - 0.7 \, u_c^*) \tag{87}$$

We plotted $\bar{u}_s$ directly versus $(u^* - 0.7 \, u_c^*)$ and not simply versus u^* because u_c^* had different values for different bed materials and different slopes of the bed surface (see Tables 1-5). The scatter of the data points about a single line would have been distinctly larger than shown in Fig. 11 if we had simply plotted $\bar{u}_s$ versus u^*.

We also measured the average velocity of bed-load particles by projecting a sequence of individual frames of the film (see Fig. 12). We did this for a horizontal bed of sand ($D_s = 1.8$ mm) at four different shear velocities. Table 6 shows the results. We found that this average velocity, denoted by $\bar{u}_B$, was less than $\bar{u}_s$. For saltating particles we found $\bar{u}_B = 0.8 \, \bar{u}_s$. Close examination of the motion of saltating particles showed that these particles were transported almost in suspension for the greater part of their trajectory at the average velocity $\bar{u}_s$. They struck the bed surface at this average

velocity, and then their longitudinal velocity was reduced to a fraction of $\bar{u}_s$. By following small groups of particles that moved together on the projection screen we obviously followed those particles that were carried in suspension at almost the same velocity and not those particles that were just being eroded and had a much lower transport velocity.

We measured the instantaneous velocity reduction of the sand particles due to collisions with the bed surface, at various transport rates, and found that for $(1/\psi - 1/\psi_c) \leq 0.04$ the longitudinal velocity reduction was $0.85\ \bar{u}_s$, as an average. At the highest transport rates (for $\frac{1}{\psi} - \frac{1}{\psi_c} > 0.04$) we could no longer measure the velocity reduction because it was difficult to distinguish the motion of individual particles on the projection screen.

Figure 13 shows a cumulative frequency curve of the length $\lambda_B D_s$ of individual steps of saltating bed-load particles, measured over a horizontal bed of walnut grains, sand and magnetite. Within the experimental range, the average step length was proportional to the particle size, the proportionality factor $\bar{\lambda}_B$ being independent of the solid density and of the mean bed-shear stress.

7.3. Evaluation of experimental results and discussion

Figure 5 shows that the measured $\frac{1}{\psi_c}$ values fit the SHIELDS' curve well for $\beta = 0^o$, especially for the heavy sediments gravel, magnetite and sand of $D_s = 1.8$ mm. The $\frac{1}{\psi_c}$- values for these bed materials at downward slopes of $\beta = 12^o$, 18° and 22° satisfy equation (81) for $\alpha = 47^o$. The $\frac{1}{\psi_c}$ -values for the lighter sediments walnut grains and sand of $D_s = 0.9$ mm also satisfy equation (81) for $\alpha = 47^o$ and $\beta = 12^o$, but give somewhat larger values of α, according to this equation, for $\beta = 18^o$ and 22°. Since equation (81) is valid for sufficiently large shear REYNOLDS' numbers $(Re_D^* \gg 1)$ we may conclude that at SHIELDS' grain-movement condition $\alpha = 47^o$ for $Re_D^* \gg 1$. This value is much larger than the value of $\alpha = 24^o$, which CHEPIL (1959) found for the topmost grains on a loose granular bed (even larger than the angle of repose), while according to GRASS (1979) the topmost grains are just moved by the temporal mean bed shear stress $\bar{\tau}_c$. Apparently, at the grain-movement condition we use, comparing $\frac{1}{\psi_c}$ at different slopes of the bed surface for $\overline{C}_B = 0.001$, particles with an α-value of 47° are at the threshold of motion owing to a large instantaneous bed shear stress. If we assume that the topmost grains have an α-value of 24° and are just moved by the time mean shear, grains with an α-value of 47° are moved, according to equation (77), by an instantaneous bed shear stress equal to 1.74 times the temporal mean shear (for $\xi_o = 0.85$).

We can obtain an estimate of the probability density of the turbulent bed shear-stress, $P(\tilde{\tau}_o)$, by assuming that the instantaneous bed shear stress $\tilde{\tau}_o$ is proportional to the square of the instantaneous fluid velocity u at a short distance of 4.5 mm above the bed (see Figs. 6 and 14). This assumption is only valid as an approximation because for this purpose a distance of 4.5 mm is not sufficiently close to the bed surface. According to GRASS (1970), the standard deviation of $P(\tilde{\tau}_o)$ should be equal to $0.4\,\bar{\tau}_o$, while we found a value $0.36\,\bar{\tau}_o$ for a sand bed (see Fig. 14). Our value is apparently 7.5% too low. For $\tilde{\tau}_{o,max}$ we found a value of $2.57\,\tilde{\tau}_o$, which according to GRASS's results should have been $2.8\,\bar{\tau}_o$. For $\tilde{\tau}_{o,min}$ we found a value of $0.25\,\bar{\tau}_o$, which should have been $0.18\,\bar{\tau}_o$.

For a particle of the bed surface that becomes unstable at a critical bed shear stress τ_c, to be eroded at a higher instantaneous bed shear stress, this shear stress must prevail at the bed surface for a sufficiently long period of time for the particle to be lifted from the bed. Let us try to estimate how long this period must be. We assume that the particle starts rolling at $t = 0$ in a direction that makes an angle $\alpha = 47^o$ with the plane of the bed surface, and must cover a distance of at least $0.1\,D_s$ in this direction before it can be eroded. We further assume that the bed shear stress increases from $\tilde{\tau}_o$ at $t = 0$ ($u_s = \dot{u}_s = 0$) to $\tilde{\tau}_{o,max}$ at $t = \frac{1}{2}\,\Delta\,t_{max}(\tilde{\tau}_o)$, and then decreases again, according to the maximum time versus shear distribution represented by Fig.7, until the particle stops again. At the critical shear stress τ_c, the drag force in the direction of incipient motion is equal to the resisting force of gravity:

$$\alpha_3 D_s^3\,(\rho_s - \rho_f) g\,\cos\,\alpha$$

At $\tilde{\tau}_o > \tau_c$, the excess drag force in the average flow direction is for $u_s \ll u_f$

$$\left(\frac{\tilde{\tau}_o}{\tau_c} - 1\right)\alpha_3 D_s^3\,(\rho_s - \rho_f)g\,\sin\,\alpha\,\cos\,\alpha + C_M \alpha_3 D_s^3\,\rho_f(\dot{u}_f\,\sin^2\alpha - \dot{u}_s) =$$

$$= \alpha_3 D_s^3\,\rho_s \dot{u}_s \qquad\qquad (88)$$

Here $C_M \rho_f \alpha_3 D_s^3$ is the virtual mass of fluid accelerated with the particle, u_o the areal-average fluid velocity at the particle level and u_s the longitudinal particle velocity. For $u_f = 6\,(\tilde{\tau}_o/\rho_f)^{\frac{1}{2}}$ (see equation 65), $C_M = 0.5$ (this is the theoretical value for spherical particles in a dilute suspension), $\alpha = 47^o$ and $\tau_c = 2\,\bar{\tau}_o$, a sand particle ($\rho_s/\rho_f = 2.64$) subject to this acceleration scheme

travels a maximum distance of 0.062 mm in the direction of incipient motion, while a magnetite particle ($\rho_s/\rho_f = 4.58$) travels 0.092 mm. If $\tau_c = 2.05\,\bar{\tau}_o$, the sand particle only travels 0.033 mm and the magnetite particle 0.045 mm. From the foregoing we must conclude that the critical bed shear stress τ_c cannot exceed approximately $2\,\bar{\tau}_o$ for sand particles of $D_s \geq 0.33$ mm, or magnetite particles of $D_s \geq 0.045$ mm. This maximum value of τ_c should rather be $2.2\,\bar{\tau}_o$, assuming that we underestimated σ_{τ_o} by 7.5%. The critical bed shear stress at the initiation of scour varies according to Fig. 8, between $0.11 \leq \tau_{sc}/[(\rho_s - \rho_f)g\,D_s] \leq 0.13$, assuming that $\tau_{sc} = 2.2\,\bar{\tau}_{sc}$.

WILLIAMS & KEMP (1971) measured the threshold drag at the initiation of non-ceasing scour by assuming that this condition corresponds to the initiation of ripples on an initially flat bed. They found similar values for $\bar{\tau}_{sc}$ as we did for similar shear REYNOLDS' numbers. In our closed flow channel, however, ripples only started to develop at much larger values of the mean bed shear stress, as shown in Tables 1-5. Ripples started to develop slowly, outside the measuring section, at the values of $1/\psi$ marked by a single asterisk. At the values marked with a double asterisk, a regular ripple pattern developed very quickly along the whole length of the channel and the experiment had to be stopped. It is interesting to note here that if these ripples were small (in height) and the value of $1/\psi$ was reduced to a smaller value, but still larger than $1/\psi_{sc}$ (say $1/\psi = 1.6/\psi_c$), they would disappear and the bed would be flat again. We therefore gained the impression that, although the condition $\bar{\tau}_o > \bar{\tau}_{sc}$ is required for the initiation of ripples, this condition is not sufficient.

Expression (83) for the rate of bed-load transport is in agreement with the MEYER-PETER & MÜLLER formula (1948) for bed-load transport, apart from the small value of the coefficient (5.7). MEYER-PETER & MÜLLER found a value of 8 for this coefficient, while WILSON (1966) found a best-fit value of 12 when measuring the bed-load transport at high shear stress. The smallness of the coefficient we obtained can be explained by the fact that we only measured bed-load transport at low shear stress ($1.1 \leq \bar{\tau}_o/\bar{\tau}_c \leq 2.7$), that our $1/\psi_c$-values were on an average, smaller than $1/\psi_c = 0.047$ used in MEYER-PETER & MÜLLER's equation (see Tables 1-5), that the turbulence intensity was relatively low in our closed flow channel, and, finally, that we defined D_s as the average sieve diameter of a fraction, while each fraction had upper and lower sieve limits of $1.33\,D_s$ and $0.67\,D_s$, respectively, and $D_{90} = 1.25\,D_s$.

According to EINSTEIN (1950), bed-load particles are transported along the bed in a series of steps, the length of which is proportional to the particle size, and deposited on the bed after passing through one or more of these steps.

The rate of deposition per unit area then depends on the transport rate past a given section and on the probability that the dynamic forces are such that a particle may be deposited. The rate of erosion from this area, on the other hand, depends on the number and properties of particles in the unit area and on the probability that the hydrodynamic force on each particle is sufficiently large to move it. For the bed to be stable, the average rate of deposition must be equal to the average rate of erosion. The mean transport rate $\bar{q}_s$, expressed as solid volume of particles of diameter D_s moving through a cross-section per unit width, can then be expressed, according to EINSTEIN's theory (see list of symbols), as:

$$\bar{q}_s = \alpha_3 D_s^3 A_L D_s \bar{n}_D \tag{89}$$

where $A_L D_s$ is the average distance covered by the bed-load particles from the moment they are eroded until the moment they are deposited on the bed. According to EINSTEIN's theory, this distance is related to the average length of the individual particle steps, $\bar{\lambda}_B D_s$, by

$$A_L = \bar{\lambda}_B / P_D \tag{90}$$

where P_D is the probability of a bed-load particle being deposited as it strikes the bed.

Substitution of equations (82), (83), (84) and (85) in (89) shows that A_L was a constant during all our experiments, equal to 288 for $\alpha_3 = 0.52$. We also found a constant average value for $\bar{\lambda}_B$, independent of D_s, ρ_s, β and $1/\psi$. This value was equal to $\bar{\lambda}_B = 16$.

Figure 13 shows a cumulative frequency curve of the λ_B-distribution for horizontal beds of walnut grains, sand and magnetite. The probability P_D of a bed load particle being deposited as it struck the bed was, according to equation (90) a constant:

$$P_D = 0.0555 \text{ (for } 1.1 \leq \bar{\tau}_o / \tau_o \leq 2.7)$$

This proves that P_D mainly depends on the probability that a particle strikes the bed at a local depression of its surface where $\tilde{\tau}_o < \tau_c$. Once eroded, the bed-load particles performed an average of $A_L / \bar{\lambda}_B = 18$ steps before being deposited again. This result contradicts EINSTEIN's theory (1950). [According to EINSTEIN's theory: $P_D = 1 - P_E = 1/(1 + A_* \Phi)$, where P_E is the probability that a particle of the bed surface is eroded at any time, and where A_* is an empirical factor with a value of 43.5].

For the greater part of their trajectory, both the vertical and the horizontal accelerations of saltating bed-load particles were very small in comparison with the acceleration that they would experience owing to a drag force equal to their submerged weight (see Fig. 12). This implies that the saltating particles experience a lift force by the shear flow, for the greater part of their trajectory, which is approximately equal to their submerged weight, and that the average fluid velocity at the bed-load particle level is reduced by the presence of the bed load. This result contradicts YALIN's theory (1963). [According to YALIN, the saltation of a grain is analogous to the ballistics of a missile]. The average lift force can be expressed as follows for suspended bed-load particles transported at the terminal velocity $\bar{u}_s$, according to equation (87)

$$C_L \tfrac{1}{2} \rho_f (11.5\, u^* - \bar{u}_s)^2\, \alpha_2 D_s^2 = 32.4\, C_L\, \frac{\alpha_2}{\alpha_3}\, \frac{1}{\psi_c}\, \alpha_3 D_s^3\, (\rho_s - \rho_f) g \tag{91}$$

where $11.5\, u^*$ is the average fluid velocity at a short distance above the suspended particles (not at the particle level since the particles are not accelerated in suspension). This average fluid velocity would prevail at a distance of $y = 3.3\, k_s$ above the bed surface, in the absence of a bed load, according to equation (65). For $C_L = 0.514$, $\alpha_2/\alpha_3 = 3/2$ and $1/\psi_c = 0.04$, the lift force is equal to the submerged particle weight.

If the bed surface is inclined in the flow direction, the component of the submerged particle weight perpendicular to the bed surface is only $\alpha_3 D_s^3 (\rho_s - \rho_f) g \cos \beta$, where β is the slope angle. For values of β smaller than 25°, $\cos \beta$ is larger than 0.9, and this will hardly affect the longitudinal velocity of suspended bed-load particles.

We can now estimate the average drag force on saltating bed-load particles as follows. For this purpose we consider a particle that has just been lifted from a horizontal bed and is accelerated, at a distance of the order of one particle diameter above the bed surface, by a flow that has a constant longitudinal velocity $\bar{u}_f$, while the longitudinal particle velocity starts at $u_s = 0.15\, \bar{u}_s$ for $t = 0$ and reaches the terminal value $\bar{u}_s = k\, \bar{u}_f$ for $t = t_s$, after covering a distance of $\bar{\lambda}_B D_s = 16\, D_s$. The particle will experience a drag force and an acceleration ($\dot{u}_s$)

$$\alpha_3 D_s^3 \rho_s \dot{u}_s = \tfrac{1}{2} C_D \alpha_2 D_s^2 \left(1 + C_M \frac{\rho_f}{\rho_s} \right)^{-1} \rho_f (\bar{u}_f - u_s)^2 \tag{92}$$

where C_D is a drag coefficient and C_M an inertial coefficient associated with the virtual mass of fluid $C_M \rho_f \alpha_3 D_s^3$ accelerated with the particle. It will reach the terminal velocity $\bar{u}_s$, assuming that C_D and C_M are constants, for

$$\frac{t_s \bar{u}_s}{D_s} = \frac{2}{C_D} \frac{\alpha_3}{\alpha_2} \left(\frac{\rho_s}{\rho_f} + C_M \right) \left(\frac{k^2}{1-k} - \frac{0.15\,k^2}{1-0.15k} \right) \qquad (93)$$

where k is given by

$$\bar{\lambda}_B = 16 = \frac{2}{C_D} \frac{\alpha_3}{\alpha_2} \left(\frac{\rho_s}{\rho_f} + C_M \right) \left(\frac{k}{1-k} - \frac{0.15\,k}{1-0.15k} + \ln \frac{1-k}{1-0.15\,k} \right) \qquad (94)$$

The average longitudinal particle velocity during a saltation, $\bar{u}_B$, is given by

$$\frac{\bar{u}_B}{\bar{u}_s} = \frac{\bar{\lambda}_B D_s}{t_s \bar{u}_s} = 8\,C_D \frac{\alpha_2}{\alpha_3} \frac{\rho_f}{(\rho_s + \rho_f C_M)} \cdot \left(\frac{k^2}{1-k} - \frac{0.15\,k^2}{1-0.15\,k} \right)^{-1} \qquad (95)$$

The drag coefficient C_D is a weak function of the particle Reynolds' number $Re_D = \rho_f (\bar{u}_f - u_s) D_s / \mu$ for $Re_D \gg 1$. The inertial coefficient C_M has a theoretical value of 0.5 for spherical particles accelerated in a dilute suspension. Substitution of the empirical value $\bar{u}_B / \bar{u}_s = 0.8$ that we found for the ratio of the average to the terminal velocity of saltating sand particles, $\rho_s / \rho_f = 2.64$ and $C_M = 0.5$, in equations (94) and (95), gives $k = 0.85$ and $C_D = 0.98$. According to equation (92), the acceleration of the particle at the terminal velocity $\bar{u}_s = 0.85\,\bar{u}_f$ is negligible. The particle reaches a velocity of $0.75\,\bar{u}_s$ after covering a distance of only $3.1\,D_s$. For the other bed materials - walnut grains and magnetite - we find, according to these equations, very similar results. For walnut grains $(\rho_s / \rho_f = 1.34$, $C_M = 0.5$, $C_D = 1)$ $k = 0.9$ and $\bar{u}_B / \bar{u}_s = 0.834$. For magnetite $(\rho_s / \rho_f = 4.58$, $C_M = 0.5$, $C_D = 1)$ $k = 0.8$ and $\bar{u}_B / \bar{u}_s = 0.768$. This result is not very sensitive to variations of C_M.

According to equations (65) and (87), the average fluid velocity $\bar{u}_f = \bar{u}_s / 0.85$ at the suspended particle level prevails at a height above the bed surface of only $y/k_s = 0.17$ for $\bar{\tau}_o = \bar{\tau}_c$, and $y/k_s = 0.84$ for $\bar{\tau}_o = 3\,\bar{\tau}_c$. This explains why the bed-load particles strike the bed surface at the terminal velocity $\bar{u}_s$ and are, on an average, not decelerated, prior to colliding.

The average drag force on a saltating bed-load particle, F'_x, from the moment it starts a saltation $(u_s = 0.15\,\bar{u}_s)$ until it strikes the bed surface at the terminal velocity $\bar{u}_s$ and its longitudinal velocity is hereby reduced again to $0.15\,\bar{u}_s$, after covering a distance of $\bar{\lambda}_B D_s = 16\,D_s$ in $t_s = \bar{\lambda}_B D_s / \bar{u}_B$, is equal

to the transfer of momentum by the particle to the bed surface

$$F'_x = 0.85 \, \alpha_3 D_s^3 \, (\rho_s + C_M \rho_f) \, \frac{\bar{u}_s \bar{u}_B}{\lambda_B D_s} = c_1 \, \alpha_2 D_s^2 \, \rho_f \, \bar{u}_s^2 \tag{96}$$

where, according to equation (95)

$$c_1 = 0.425 \, C_D \left(\frac{k^2}{1-k} - \frac{0.15 \, k^2}{1-0.15k} \right)^{-1} \tag{97}$$

We calculated F'_x as the average drag force on a saltating bed-load particle at the average fluid velocity corresponding to the temporal mean bed shear stress $\bar{\tau}_o$. The instantaneous bed shear stress at this fluid velocity, however, is $0.96 \, \bar{\tau}_o$, due to the skewness of the probability-distribution function $P(\tilde{\tau}_o)$ (see Fig. 7). We may thus express the average drag force on the bed-load particles as a function of the instantaneous bed shear stress $\tilde{\tau}_o$, according to equations (86), (87) and (96), for $\bar{\tau}_o = \tilde{\tau}_o / 0.96$ as

$$F'_x (\tilde{\tau}_o) = 132 \, c_1 \, \alpha_2 D_s^2 \, (1.02 \sqrt{\tilde{\tau}_o} - 0.7 \sqrt{\bar{\tau}_c})^2 \tag{98}$$

According to equation (97), the factor c_1 has a value of 0.090 for sand (k = 0.85), 0.054 for walnut grains (k = 0.9), and 0.14 for magnetite (k = 0.8), assuming that $C_D = 1$ and $C_M = 0.5$.

We can relate any function of the instantaneous bed shear stress , $f(\tilde{\tau}_o)$, to the time mean value of that function, $\bar{f}(\bar{\tau}_o)$, by

$$\bar{f}(\bar{\tau}_o) = \int_{\tilde{\tau}_{o,min}}^{\tilde{\tau}_{o,max}} f(\tilde{\tau}_o) \, P(\tilde{\tau}_o, \, \bar{\tau}_o) \, d\tilde{\tau}_o \tag{99}$$

According to equation (98), the average drag force on the bed-load particles as a function of the instantaneous bed shear stress, $F'_x(\tilde{\tau}_o)$, is almost linearly proportional to $\tilde{\tau}_o$ (plus a constant). The temporal mean value of F'_x may therefore be represented by the same equation

$$\overline{F'_x} (\bar{\tau}_o) = 132 \, c_1 \, \alpha_2 D_s^2 \, (1.02 \sqrt{\bar{\tau}_o} - 0.7 \sqrt{\bar{\tau}_c})^2 \tag{100}$$

as long as the minimum instantaneous bed shear stress $\tau_{o,min} \approx 0.2 \, \bar{\tau}_o$ (see Fig. 7), is higher than SHIELDS' critical bed shear stress $\bar{\tau}_c$.

According to KALINSKE (1947), we can express the mean rate of bed-load transport $\bar{q}_s$ as

$$\bar{q}_s = \alpha_3 D_s^3 \bar{u}_B \bar{n}_B = \frac{\alpha_3}{\alpha_2} D_s \bar{u}_B \overline{C}_B \tag{101}$$

[see EINSTEIN's expression (89) for comparison]. Here $\bar{u}_B$ is the average velocity of the bed-load particles in the mean flow direction, $\bar{n}_B$ the number of particles, on an average, rolling and saltating over a unit area of the bed, and $\overline{C}_B$ ($= \alpha_2 D_s^2 \bar{n}_B$) the temporal mean, areal concentration of the bed load. KALINSKE (1947) assumed a constant value for $\overline{C}_B$ of 0.35, and concluded that $\bar{u}_B$ must be proportional to $\bar{q}_s/D_s$.

Substitution of (78), (82), (83), (86), (87) and (95) in equation (101) gives the following expression for $\bar{n}_B$ and $\overline{C}_B$

$$\overline{C}_B = \alpha_2 D_s^2 \bar{n}_B = \frac{\alpha_2}{\alpha_3} \frac{\bar{q}_s}{D_s \bar{u}_B} = c_2 \frac{\left(\frac{1}{\psi} - \frac{1}{\psi_c}\right)^{3/2}}{\sqrt{\frac{1}{\psi}} - 0.7\sqrt{\frac{1}{\psi_c}}} \tag{102}$$

where

$$c_2 = \frac{0.062}{C_D} \left(\frac{\rho_s}{\rho_f} + C_M\right) \left(\frac{k^2}{1-k} - \frac{0.15\,k^2}{1-0.15k}\right) \tag{103}$$

According to this equation, the factor c_2 has a value of 0.914 for sand ($\rho_s/\rho_f = 2.64$, $C_M = 0.5$, $C_D \doteq 1$, $k = 0.85$), 0.908 for walnut grains ($\rho_s/\rho_f = 1.34$, $C_M = 0.5$, $C_D = 1$, $k = 0.9$), and 0.973 for magnetite ($\rho_s/\rho_f = 4.58$, $C_M = 0.5$, $C_D = 1$, $k = 0.8$). Figure 15 shows $\overline{C}_B$ versus $(1/\psi - 1/\psi_c)$ for sand ($c_2 = 0.914$), for $1/\psi_c = 0.04 \pm 0.015$. For $0.01 \le (1/\psi - 1/\psi_c) \le 0.1$, this function is almost linearly proportional to $(1/\psi - 1/\psi_c)$, the proportionality factor being equal to $1.37 = 1.5\,c_2$. This result clearly contradicts KALINSKE's assumption (1947) that $\overline{C}_B$ is a constant (see Fig. 15).

Since the time mean value of $n_B(\tilde{\tau}_0)$, $\bar{n}_B(\bar{\tau}_0)$, is almost linearly proportional to $\bar{\tau}_0$ (see Fig. 15), $n_B(\tilde{\tau}_0) \approx \bar{n}_B(\bar{\tau}_0)$, given by equation (102), for $\tilde{\tau}_0 > \bar{\tau}_c$

$$n_B(\tilde{\tau}_0) = \frac{c_2(\tilde{\tau}_0 - \bar{\tau}_c)^{3/2}}{\alpha_2 D_s^3 (\rho_s - \rho_f)g \,(\sqrt{\tilde{\tau}_0} - 0.7\sqrt{\bar{\tau}_c})} \tag{104}$$

The average reduction in fluid shear at the bed surface due to the bed-load, $\bar{n}_B \bar{F}'_x$, is given as a function of the temporal mean bed shear stress $\bar{\tau}_o$, according to equations (97), (100), (102) and (103), by

$$\bar{n}_B \bar{F}'_x = 3.48 \left(\frac{\rho_s}{\rho_f} + C_M\right) \frac{\left(\bar{\tau}_o - \bar{\tau}_c\right)^{3/2} \left(1.02 \sqrt{\bar{\tau}_o} - 0.7 \sqrt{\bar{\tau}_c}\right)^2}{(\rho_s - \rho_f) g D_s \left(\sqrt{\bar{\tau}_o} - 0.7 \sqrt{\bar{\tau}_c}\right)} \qquad (105)$$

According to this equation, Fig. 16 shows $\bar{n}_B \bar{F}'_x$ versus $\bar{\tau}_o$ for sand, walnut grains and magnetite, for $C_M = 0.5$ and $1/\psi_c = 0.04 \pm 0.015$. For $0.01 \le (1/\psi - 1/\psi_c) \le 0.1$, the function $\bar{n}_B \bar{F}'_x / [(\rho_s - \rho_f) g D_s]$ is practically proportional to $(1/\psi - 1/\psi_c)^2$, the proportionality factor being equal to $8 = 2.55 (\rho_s/\rho_f + 0.5)$.

According to Fig. 16 at low bed-load concentrations (for $C_B \ll 1$), the average reduction in fluid shear at the bed surface, $\bar{n}_B \bar{F}'_x$, is much less than $(\bar{\tau}_o - \bar{\tau}_c)$, a functional relationship predicted by BAGNOLD (1956). For sand the reduction in fluid shear only becomes equal to $(\bar{\tau}_o - \bar{\tau}_c)$ for $(1/\psi - 1/\psi_c) = 0.12$.

For $C_B \ll 1$, the bed load will only reduce the turbulent fluid shear at a small, constantly changing part of the bed surface, and we can relate the areal average bed-load concentration to the number of particles eroded from a unit area of the bed surface due to an increase in fluid shear from $\tilde{\tau}_o$ to $(\tilde{\tau}_o + d\tilde{\tau}_o)$ as

$$n_B = \int_{\bar{\tau}_c}^{\tilde{\tau}_o} n'_E \, d\tilde{\tau}_o \qquad (106)$$

This relation is based on the assumption that we can make a clear distinction between particles of the bed load and particles of the bed. This assumption is justified because the probability that, once a particle has been eroded, it is deposited again when it strikes the bed surface, is very small ($P_D = 0.0555$). Substitution of $n_B = 1.5 c_2 (\tilde{\tau}_o - \bar{\tau}_c) / [\alpha_2 D_s^3 (\rho_s - \rho_f) g]$ as an approximation of equation (35) shows that for $0.01 < C_B \ll 1$, n'_E is almost a constant: $n'_E = 1.5 c_2 / [\alpha_2 D_s^3 (\rho_s - \rho_f) g]$.

A saltating bed-load particle can effectively reduce the turbulent fluid shear on an area of the bed surface equal to the area covered by the wake behind the particle. This area can be 10 - 20 times the projected particle area. At high bed-load concentrations, for $C_B \ge 0.1$, the bed load can thus effectively reduce the fluid shear at the entire bed surface, on an average, to

$$\tilde{\tau}_o^f \approx \tilde{\tau}_o - n_B F_x' \tag{107}$$

Figure 17 shows $\tilde{\tau}_o^f$ versus $\tilde{\tau}_o$ for sand, walnut grains and magnetite, according to equations (98), (104) and (107). This figure shows that $\tilde{\tau}_o^f$ never reaches the critical shear corresponding to the initiation of scour, $\tau_{sc} = 2.2 \, \bar{\tau}_{sc}$, which we found experimentally (see Section 7.3), while the areal bed-load concentration has a value of approximately 0.1 for $\tilde{\tau}_o = \tau_{sc}$, according to equation (104).

We stated in Section 3.2 that the bed-load must reduce the maximum turbulent fluid shear at the bed surface to τ_{sc}. From the foregoing it even appears that the bed-load reduces $\tilde{\tau}_o^f$ to a value below τ_{sc}. It also appears that BAGNOLD's assumption (1956) that $\tilde{\tau}_o^f$ must approach zero for large bed-load concentrations is justified (see Fig. 17). However, expression (105) for the average reduction in fluid shear at the bed surface cannot be correct for high bed-load concentrations because $\tilde{\tau}_o^f$ would even become strongly negative, according to that equation, for $(1/\psi - 1/\psi_c) \approx 1$ (see Fig. 16).

According to WILSON (1966), the MEYER-PETER & MÜLLER formula for bed-load transport (1948) is also valid for high transport rates. According to Table 5, expression (87) for the average particle velocity $\bar{u}_s$ is at least valid for $1/\psi \leq 0.1$, or $\bar{\Phi} \leq 0.1$. It must also be approximately valid for higher transport rates because for $u^* \gg u_c^*$ it becomes almost proportional to the shear velocity u^*, or equal to the fluid velocity at a constant distance (3.3 particle diameters) above the bed surface. Thus, we must conclude that $n_B(\tilde{\tau}_o) \approx \bar{n}_B(\bar{\tau}_o)$ will increase continuously, almost linearly, with increasing bed shear stress, also at high transport rates.

During erosion of the bed surface, with or without simultaneous deposition, the fluid part of the turbulent bed shear stress, $\tilde{\tau}_o^f$, must have a value between the limits $\bar{\tau}_c$ and τ_{sc}. The exact value of $\tilde{\tau}_o^f$ at a given moment will depend on the roughness of the bed surface at that moment. Since n_B increases continuously with increasing bed shear stress, $\tilde{\tau}_o^f$ must become practically equal to τ_{sc} during erosion of the bed surface, with or without deposition in local depressions, for $\tilde{\tau}_o > \tau_{sc}$, once the bed is so smooth due to erosion of the most protruding particles and selective deposition that it will not become any smoother by further erosion. This implies that the average fluid drag force on the saltating bed-load particles F_x' must become constant, proportional to $\alpha_3 D_s^3 (\rho_s - \rho_f) g$, for $\tilde{\tau}_o \gg \tau_{sc}$. The average particle velocity $\bar{u}_B$ will then be practically equal to the terminal velocity $\bar{u}_s$ because the average velocity reduction of the bed-load particles due to collisions with the bed surface will have to be much less than $0.85 \, \bar{u}_s$, the value we found for low transport rates.

Substitution of $\overset{\sim}{\tau}{}_o^f = \tau_{sc}$, equations (82), (83) and (101), and expression (87) for $\bar{u}_B \approx \bar{u}_s$, in equation (107) gives the following expression for F_x' at the total bed shear stress $\overset{\sim}{\tau}_o = \bar{\tau}_o \gg \tau_{sc}$

$$F_x' = \frac{\bar{\tau}_o - \tau_{sc}}{\bar{n}_B} = c_3 \alpha_3 D_s^3 (\rho_s - \rho_f) g \frac{(\bar{\tau}_o - \tau_{sc})(\sqrt{\bar{\tau}_o} - 0.7\sqrt{\bar{\tau}_{sc}})}{(\bar{\tau}_o - \bar{\tau}_c)^{3/2}} \qquad (108)$$

WILSON (1966) found that the proportionality constant in the MEYER-PETER & MÜLLER formula (84) has a best-fit value of 12 for high bed-load concentrations. Using this value and expression (87) for $\bar{u}_B \approx \bar{u}_s$, we find for factor c_3 in equation (108) a value of 0.96. For sufficiently large values of $\overset{\sim}{\tau}_o$, the average drag force on the bed-load particles F_x' must thus be approximately equal to $\alpha_3 D_s^3(\rho_s - \rho_f)g$. This can be made plausible using BAGNOLD's concept of 'dispersive grain pressure' (1954, 1956).

According to BAGNOLD (1956), the bed-load must exert an average dispersive grain pressure $\tilde{p}{}_o^s$ on the bed surface proportional to the reduction in fluid shear (equation (75a))

$$\overline{\overset{\sim}{\tau}{}_o^s} = \bar{\tau}_o - \overline{\overset{\sim}{\tau}{}_o^f} = \bar{n}_B \bar{F}_x' \qquad (109)$$

The dispersive grain pressure is related as follows to the average lift force exerted by the fluid on the bed-load particles (equation (75d))

$$\overline{\tilde{p}{}_o^s} = \bar{n}_B [\alpha_3 D_s^3 (\rho_s - \rho_f)g - \bar{F}_y'] \qquad (110)$$

The ratio

$$\frac{\overline{\overset{\sim}{\tau}{}_o^s}}{\overline{\tilde{p}{}_o^s}} = \tan \theta \qquad (111)$$

is determined by the various directions of the impact forces created by particles of the bed-load colliding with the bed and by the roughness configuration of the bed's surface. BAGNOLD (1954) measured the total shear stress and 'dispersive pressure' at the boundary of concentrated suspensions sheared in the annular space between two concentric drums with a smooth surface and found $\overline{\overset{\sim}{\tau}{}_o^s}/\overline{\tilde{p}{}_o^s} = 0.75$ in the viscous region, and $\overset{\sim}{\tau}{}_o^s/\tilde{p}{}_o^s = 0.32$ in the grain-inertia region. We found that at low rates of bed-load transport, particles colliding with the bed in water

thereby lose most of their kinetic energy and hence exert a force on the bed surface in the direction of their approach as they collide with particles of the bed. Since the angle of approach relative to the plane of the bed surface is very small (in water), the ratio $\tilde{\tau}^s_0 / \tilde{p}^s_0 > 1$. At high rates of bed-load transport, the ratio $\tilde{\tau}^s_0 / \tilde{p}^s_0$ will be smaller, but must still exceed the value BAGNOLD found for shearing along the smooth surface of two concentric drums.

Assuming that the average lift force on the bed-load particles $\overline{F}'_y$ is proportional to their submerged weight

$$\overline{F}'_y = \xi_B \alpha_3 D^3_s (\rho_s - \rho_f) g \tag{112}$$

we find the following expression for $\overline{F}'_x$, according to equations (109), (110), (111) and (112)

$$\overline{F}'_x = (1 - \xi_B) \tan \theta \, \alpha_3 D^3_s (\rho_s - \rho_f) g \tag{113}$$

$\overline{F}'_x$ will thus be equal to be submerged particle weight for $(1 - \xi_B) \tan \theta = 1$. This condition can, in principle, be well satisfied (e.g. $\tan \theta \approx 45^o$ if $\xi_B \ll 1$, thus for $\tilde{\tau}^s_0 \approx \tilde{p}^s_0$ and $\overline{F}'_y \ll \overline{F}'_x$).

8. BULK EROSION

8.1. Definition

The protective action of the bed load over the bed surface described in the preceding section can only be effective if the local instantaneous fluid-pressure gradient at the bed surface is sufficiently small. Under highly erosive flow, the instantaneous fluid-pressure gradient in the turbulent boundary layer may be such that the stability condition (20) for particles at the bed's surface cannot be fulfilled, even if the bed load reduces the fluid part $\tilde{\tau}^f_0$ of the total bed shear stress to zero. This will lead to bulk erosion. During the latter, the bed-load sediment can instantaneously absorb the total viscous-momentum transfer $\partial \tilde{\tau}^f_{xy} / \partial y$ from the surface flow to the bed surface. Accordingly, we define bulk erosion locally and instantaneously by the extreme condition that the fluid part $\tilde{\tau}^f_0$ of the total bed shear stress is reduced to zero at the instantaneous erosion boundary, while the drag and lift forces exerted by the local instantaneous fluid-pressure gradient on the particles at the instantaneous erosion boundary $y = 0$ satisfy the stability condition (76), or rather, if the local instantaneous erosion boundary has a slope in the flow direction

$$\left| \frac{(\rho_s - \rho_f)\, C\, g_x - \frac{\partial}{\partial x}\, (\tilde{p}^f - p_H)}{(\rho_s - \rho_f)\, C\, g_y + \frac{\partial}{\partial y}\, (\tilde{p}^f - p_H)} \right|_{y=0} = \tan \alpha \qquad (114)$$

The condition for bulk erosion will in general only be fulfilled locally and instantaneously if the turbulent fluid-pressure distribution above the bed changes so rapidly that large pore-pressure gradients can build up at the bed surface before the bed is eroded by shear only.

Bulk erosion can occur at high sediment-transport rates under highly turbulent flow with a relatively small time-averaged fluid pressure gradient, particularly in the case of an undulating bed where the flow contains a rapidly changing pattern of unstable stagnation points.

We can estimate the possible extent of zones of bulk erosion created in a loose granular bed by highly erosive flow. We consider a flat horizontal portion of the bed, subject to plane turbulent flow of sufficiently rapidly increasing energy for bulk erosion to occur. We define a fixed Cartesian frame [X, Y] at the threshold of sediment motion (t = 0) with the X-coordinate along the (horizontal) bed surface and the Y-coordinate normal to the bed surface and pointing upwards. The pore-pressure distribution at the instantaneous erosion boundary Y* [X], at one particular moment during bulk erosion, will then satisfy the equation

$$\left| \frac{-\frac{\partial \tilde{p}^f}{\partial X}}{\frac{\partial}{\partial Y}\, (\tilde{p} - p_H) + (\rho_s - \rho_f)\, C\, g} \right|_{Y = Y^*} = \tan (\alpha - \beta) \qquad (115)$$

where β is the downward slope of the erosion boundary

$$\frac{\partial Y^*}{\partial X} = -\tan \beta \qquad (116)$$

We can now calculate the instantaneous erosion boundary Y* [X] by solving the differential equations (115) and (116), provided we know the pore-pressure distribution in the zone of bulk erosion. For instance, in the limiting case when the suspended bed-load sediment is still in a state of 'slow' bulk motion, the filter flow satisfies Darcy's law (44) and $(p^f - p_H)$ satisfies the Laplace equation

$$\left(\frac{\partial^2}{\partial X^2} + \frac{\partial^2}{\partial Y^2} \right) (\tilde{p}^f - p_H) = 0 \qquad (117)$$

- 53 -

assuming that the solid concentration in the zone of bulk erosion changes
'slowly' as a function of time.

In general, there will be an infinite set of curves fitting the directional
field. In the case of a local instability, however, the end (in the flow direction)
of the boundary line Y* [X] must lie at the bed surface. This condition
specifies a subset of potential boundary surfaces from which the curve of
furthest deviation from the bed surface is defined as the erosion boundary.
In the next section we shall apply this method to calculate the extent of the
zone of instantaneous instability under a two-dimensional jet of rapidly
increasing energy.

8.2. Application to the problem of scour near a stagnation point in the surface flow

One of the important cases of severe scour is that which occurs near a
stagnation point of the surface flow.

A frictionless flow with a stagnation point at the origin of the fixed
co-ordinate system [X, Y], introduced in the preceding chapter, may be defined
by the following two-dimensional stream function

$$\psi^* [X, Yt] = - U(t) \frac{XY}{\sqrt{X^2 + A^2}} \qquad (y \geq 0) \qquad (118)$$

Here A characterises the stagnation area, A being the distance from the
stagnation point at which the pressure (according to Bernoulli's theorem) has
decreased to half its maximum value. The corresponding streamlines are
shown in Figure 18a. This flow maintains a fluid-pressure distribution

$$\tilde{p}^f [X, O, t] = \tfrac{1}{2} \rho_f U^2[t] \frac{A^2}{X^2 + A^2} \qquad (119)$$

at the bed surface [X, O]. The pore-pressure head in the sand bed is found
as a solution to the differential equation (117)

$$\tilde{p}^f [X, Y, t] = \tfrac{1}{2} \rho_f U^2 \frac{A (A - Y)}{X^2 + (A - Y)^2} + p_H \qquad (y \leq 0) \qquad (120)$$

Figure 18a also shows the streamlines of the corresponding flow.

Now we rapidly increase the kinetic energy of the surface flow by increasing
U [t] [equation (118)] from a value at $t = t_1$ corresponding to the threshold of
bed-load transport, to a large value at $t = t_2$; we assume that the fluid-pressure

distribution at $t = t_2$ still satisfies the differential equation (117) for $Y < 0$, and is thus given by equation (120).

The location of the boundary surface Y^* [X, t_2] of the zone of instantaneous instability in the sand bed at $t = t_2$ can be calculated numerically using the method described in Section 8.1. [solving the differential equation (116) after substitution of equations (115) and (120)]. We have calculated these potential erosion boundaries for a horizontal bed using a critical-drag angle α of 32° (equal to the maximum angle of repose of a loose medium fine sand) and for various values of U [t_2]. The results are given in Figure 18b.

Figure 18b shows that equations (115), (116) and (120) only have a solution for

$$\phi^* = \frac{\rho_f U^2}{2A (\rho_s - \rho_f) C g} \geq 1.33 \tag{121}$$

Figure 19 shows an example of such an erosive flow. A two-dimensional jet of water with a nozzle width of 2 mm was directed vertically downwards, towards an initially flat horizontal sand bed ($D_s = 1$ mm) from a distance of 44 mm. The stagnation pressure on the bed surface was $\tilde{p}^f$[0, 0] = $1.625 . 10^3$ N/m^2 (U = 1.8 m/s) and the initial width of the stagnation area was 2A = 36 mm (ϕ [A, 0] = $\frac{1}{2}$ ϕ[0,0]). The parameter ϕ^* of equation (121) had a value of 10.

Figure 20a shows the material in bulk motion, illustrating the erosive power of a flow with a large pressure gradient ($\phi^* = 10$). Figure 20b shows that the calculated zone of bulk erosion was practically eroded within 0.16 s. This corresponds approximately with the time required by the jet to reach a maximum velocity at the nozzle opening (The actual shape of the erosion boundary cannot be expected to be exactly the same as the calculated shape, because the surface flow pattern at t = 0.16 s was strongly affected by the scour pit, while this was not taken into account in our calculation.

This experiment is an example of bulk erosion under a flow with an almost steady stagnation point. However, bulk erosion can also occur locally and instantaneously under a turbulent flow with a relatively small time-averaged fluid pressure gradient, particularly in the case of an undulating bed where the flow has a rapidly changing pattern of unstable stagnation points (see Fig. 21). If the Reynolds' number of the turbulent flow is sufficiently high we may neglect the effect of internal friction and consider the fluid to be ideal. The flow near a stagnation point above a rippled bed (s_2 in Fig. 21) is thus similar to the ideal flow shown in Fig. 18a, and we may apply the condition for bulk erosion (121).

The condition for bulk erosion defined by equation (121) derived from (115), (116) and (120) is easily satisfied, locally and instantaneously, above a rippled bed. If we assume, as an example, for geometrically similar ripples, that $2A = 50 D_s$ (where D_s is the grain diameter), that $U = 12 \sqrt{\tilde{\tau}_o / \rho_f}$ (where $\tilde{\tau}_o$ is the instantaneous bed shear stress), and that $C = 0.6$, the condition for bulk erosion defined by equation (121) is satisfied for $\tilde{\tau}_o \geq 0.277 (\rho_s - \rho_f) g D_s$. This instantaneous shear can be reached at a flow intensity of only $1/\psi \geq 0.1$. It must be noted here that the seepage flow will also affect the fluid velocity distribution in the turbulent boundary layer and that this will result in high shear stresses and large particle velocities in the vicinity of the stagnation point (see eq. 65a).

We do not find scour pits in a rippled bed (Fig. 21), as we did under a two-dimensional jet (Fig. 19), because the exact location of the stagnation points s_2 changes very rapidly. We can still conclude, however, that in an area of bulk erosion above a rippled bed the bed load cannot prevent scour. An equilibrium between simultaneous erosion and deposition cannot exist and the bed is severely eroded instantaneously.

We calculated the extent of the zone bulk erosion that would be created locally and instantaneously in a loose granular bed under a two-dimensional jet, if the jet were introduced so rapidly that the zone of bulk erosion would still be in a state of 'slow' motion. We then found experimentally that the zone of bulk erosion thus calculated was completely eroded within 0.16 s, just as rapidly as the energy of the erosive flow could be increased. We concluded that in an area of bulk erosion, for instance above a rippled bed, the bed load cannot prevent scour and the bed is severely eroded instantaneously

Bulk erosion will occur where the momentum of the surface flow changes so radically that the bed load cannot protect the bed surface against scour. The change in momentum of the surface flow, and not the momentum itself, constitutes the criterion for bulk erosion.

9. CONCLUSIONS

We have arrived at a set of integral and differential 'macro'-equations that govern the momentum transfer from a Newtonian fluid to particles in a fluid-solid mixture, in particular near the surface of a loose granular bed subject to erosive flow: under the bed surface, at the bed surface, and in the saltation layer. These equations show, in combination with the results of experiments reported in the literature, that the viscous-momentum transfer from the boundary to the interior of a granular bed is absorbed entirely within a layer of two or three particle diameters only. From there on, a drag force on the solid is only exerted by a pore-pressure gradient.

SHIELDS' dimensionless expression for the critical bed shear stress at the threshold of continuous sediment motion, $1/\psi_c$, must attain a constant value for low shear Reynolds' numbers ($Re_D^* < 0.5$), as long as there is no cohesion between the particles.

Comparing the threshold drag acting at different downward slopes of the bed surface, for $\overline{C}_B = 0.001$, a critical-drag angle of 47° was found. It is concluded that, at this grain-movement condition, particles with a critical drag angle of 47° must be at the threshold of motion due to a high instantaneous bed shear stress, equal to approximately 1.74 times the mean shear.

The MEYER-PETER & MÜLLER formula for bed-load transport in horizontal flow can be gen'rlised to the case of flow over an inclied bed, at least up to downward slopes of 22° considered in the experiments.

The rate of deposition was found to be proportional to the rate of bed-load transport and the average length of individual particle steps was found to be a constant equal to 16 particle diameters for different bed materials. The probability of a bed-load particle being deposited when striking the bed surface was constant within the experimental range ($P_D = 0.0555$). This contradicts EINSTEIN's theory (1950). The bed-load particles covered a distance of 288 particle diameters, on an average, from the moment they were eroded until they were deposited again.

Close examination of the motion of saltating bed-load particles revealed that these particles are transported almost in suspension for the greater part of their trajectory. The average transport velocity of the suspended particles was equal to the average fluid velocity calculated for a turbulent flow without a bed load, at about three particle diameters above the bed surface, minus a constant. The constant was proportional to the critical shear velocity at SHIELDS' grain-movement condition. This can be explained by considering that the turbulent shear flow must exert a lift force on the suspended particles that is practically equal to their submerged weight, and by assuming that the average fluid velocity at the bed-load particle level is reduced owing to the presence of the bed-load. The longitudinal velocity of saltating bed-load particles was reduced by collisions with the bed surface, on average, at low transport rates, by 0.85 times their maximum velocity in suspension.

Combining the MEYER-PETER & MÜLLER formula for the rate of bed-load transport and the above-mentioned expression for the average transport velocity of the bed-load particles shows that the areal bed-load concentration increases linearly with increasing bed shear stress. This contradicts KALINSKE's theory (1947).

It can be concluded on a theoretical basis that the bed load must reduce the maximum turbulent fluid shear at the bed surface to a critical value, corresponding to the initiation of non-ceasing scour. The basis of this conclusion is imply that, if we make an instantaneous division between particles of the bed load (rolling and saltating) and particles of the bed (at rest by definition), separated by an imaginary 'wavy' surface $\Delta \tilde{S}[0]$, the particles of the bed must be in equilibrium and therefore, $\tilde{\tau}_o^f \leq \tau_{sc}$. At sufficiently high transport rates, $\tilde{\tau}_o^f$ must be almost equal to $\tilde{\tau}_{sc}$ during erosion, with or without simultaneous deposition.

Calculation of the average reduction in fluid shear at the bed surface due to the bed load, using empirical relations for the transfer of momentum of bed-load particles to the bed surface by intergranular collisions, and for the areal bed-load concentration, as a function of the mean bed shear stress, reveals that, at low transport rates, contrary to BAGNOLD's theory (1956), this reduction is very small. It is due to the effect of the wakes of few saltating particles on the fluid flow at the bed surface. The critical shear stress required to erode the topmost grains of the bed surface must therefore increase with increasing bed shear stress, owing to progressive smoothening of the bed surface. The increase in areal bed-load concentration per unit increase in total shear is equal to the total projected area of the particles eroded from the bed surface owing to the increase in shear. The number of particles eroded per unit area and per unit increase in total shear was found experimentally to be almost a constant at low bed-load concentrations. It was also found that the average reduction in fluid shear due to the bed load increases so rapidly with increasing bed-shear stress that at higher transport rates the remaining fluid shear will nowhere exceed the threshold drag corresponding to the initiation of non-ceasing scour measured behind a consolidated bed. If we extrapolate the experimental results to high transport rates, it is even found that the bed load must 'absorb' the total bed shear stress at high concentrations. This would be in agreement with BAGNOLD's theory (1956). However, it can be shown that the expression we found empirically for the average reduction in fluid shear at the bed surface cannot be extrapolated to such high transport rates. The expressions for the rate of bed-load transport and for the average particle velocity can be extrapolated and show that at high bed-load concentrations the average drag force on the bed-load particles must be approximately equal to their submerged weight. This can be made plausible using BAGNOLD's concept of 'dispersive grain pressure'.

It is concluded that a loose granular bed will be severely eroded instantaneously where and when the momentum of the turbulent surface flow changes radically and the bed load cannot protect the bed surface against scour. This condition, defined as the condition for bulk erosion, can occur at high sediment transport rates under highly turbulent flow, particularly in the case of an undulating bed where the flow contains a rapidly changing pattern of unstable stagnation points. This bulk erosion is due to large instantaneous fluid pressure gradients in the transition zone between the flow region and the bed. The instantaneous change in momentum of the surface flow constitutes the criterion for bulk erosion.

A method has been developed that permits determination of the extent of the zone of bulk erosion created locally and instantaneously in a loose granular bed by highly erosive flow. With this method the extent of the zone of bulk erosion is calculated that would be created locally and instantaneously under a two-dimensional jet, if the jet were introduced so rapidly that the zone of bulk erosion would still be in a state of 'slow' motion. It was found experimentally that the zone of bulk erosion thus calculated was completely eroded just as rapidly as the energy of the erosive flow could be increased (within 0.16 s). It is concluded that in an area of bulk erosion, for instance above a rippled bed, the bed load cannot prevent scour and the bed is severely eroded. The instantaneous change in momentum of the surface flow constitutes the criterion for bulk erosion.

REFERENCES

Bagnold, R.A. (1954), Experiments on gravity-free dispersion of large solid
    spheres in a Newtonian fluid under shear.
    Proc. Roy. Soc. London, Ser. A, $\underline{225}$, 49.

Bagnold, R.A. (1956), The flow of cohesionless grains in fluids.
    Proc. Roy. Soc. London, Phil. Trans., Ser. A, $\underline{249}$, No. 964.

Bagnold, R.A. (1973), The nature of saltation and of 'bed-load transport in
    water'.
    Proc. Roy. Soc. London, Ser. A, $\underline{332}$, 473.

Beavers, G.S. & Joseph, D.D. (1967), Boundary conditions at a naturally
    permeable wall.
    J. Fluid Mech., $\underline{30}$, 197.

Chepil, W.S. (1959), Equilibrium of soil grains at the threshold of movement
    by wind.
    Proc. Soil Science, Soc. of America, $\underline{23}$, 422.

Clarke, Ph.D., (1967), Trans. Instn. Chem. Engrs., $\underline{45}$, T251.

Darcy, H., (1856), Les Fontaines Publiques de la Ville de Dijon, Dalmont,
    Paris.

Deemter, J.J. van & Laan, E.T. van der (1961), Momentum and energy
    balance for dispersed two-phase flow.
    Appl. Sci. Res., A $\underline{10}$, 102.

Eilers, H. (1941), The viscosity of emulsions of a highly viscous substance
    as a function of concentration.
    Kolloïd Z., $\underline{97}$, 313.

Einstein, A. (1906), Eine neue Bestimmung der Moleküldimensionen.
    Annalen der Physik, $\underline{19}$, 289.

Einstein, A. (1911), Berichtigung zu meiner Arbeit: Eine neue Bestimmung
    der Moleküldimensionen.
    Annalen der Physik, $\underline{34}$, 591.

Einstein, H.A. (1950), The bed-load function for sediment transportation in
    open channel flows.
    U.S. Dept. Agric., Soil Conserv. Serv., T.B. No. 1026.

Fernández Luque, R. & Mandl, G. (197.), Bulk erosion.
Submitted for publication in the Journal of Hydraulic Research.

Francis, J.R.D. (1973), Experiments on the motion of solitary grains along
the bed of a water stream.
Proc. Roy. Soc. London, Ser. A, $\underline{332}$, 443.

Fröhlich, H. & Sack, R. (1946), Theory of the rheological properties of
dispersions.
Proc. Roy. Soc. A, $\underline{185}$, 415.

Grass, A.J. (1970), Initial instability of fine bed sand.
J. Hydr. Div., ASCE, $\underline{96}$, No HY 3, 619.

Heinrich, G. & Desoyer, K. (1956), Hydromechanische Grundlagen für die
Behandlung von Stationären und instationären Grundwasser-Strömungen.
Ing. Archiv, $\underline{24}$, 81.

Hinze, J.O. (1962), Momentum and mechanical energy balance equations for
a flowing homogeneous suspension with slip between the phases.
Appl. Sci. Res., A $\underline{11}$, 33.

Kalinske, A.A. (1947), Movement of sediment as bed in rivers.
Trans. Am. Geophys. Union, $\underline{28}$, 615.

Kozeny, J.S. (1927), Über kapillare Leitung der Wässer im Boden.
Ber. Wiener Akad. Abt. II a, $\underline{136}$, 271.

Mandl, G. (1963), Zur statistischen Begründung der Mechanik flüssigkeits-
gefüllter poröser Medien.
Programm der wissenschaftlichen Jahrestagung der Gesellschaft für
Angewandte Mathematik und Mechanik, Technische Hochschule, Karlsruhe.

Mandl, G. (1964), Change in skeletal volume of a fluid-filled porous body
under stress.
J. Mech. Phys. Solids, $\underline{12}$, 299.

Meyer-Peter, E. & Müller, R. (1948), Formulas for bed-load transport.
Intern. Assoc. Hydr. Res., 2d Meeting, Stockholm.

Nikuradse, J. (1933), Strömungsgesetze in rauhen Rohren.
Ver. Deut. Ing. Forschungsheft, $\underline{361}$.

Poel, C. van der (1958), On the rheology of concentrated dispersions.
Rheologica Acta (1), $\underline{2-3}$, 198.

Saffman, P.G. (1964), The lift on a small sphere in a slow shear flow.
J. Fluid Mech., 22, 385.

Saffman, P.G. (1971), On the boundary condition at the surface of a porous medium.
Studies in Appl. Math. L2, 93.

Shields, A. (1936), Anwendung der Ahnlichkeits-Mechanik und der Turbulenz-forschung auf die Geschiebebewegung.
Preussische Versuchsanstalt für Wasserbau und Schiffbau, Berlin.

Tennekes, H. (1964), Similarity laws for turbulent boundary layers with suction or injection.
PhD thesis, Technische Hogeschool Delft.

Vanoni, V.A. (1964), Measurements of critical shear stress.
Calif. Inst. Techn. Rep. No. KH-R-7.

Williams, P.B. & Kemp, P.H. (1971), Initiation of ripples on flat sediment beds.
Proc. ASCE J. Hydr. Div., 97, No HY 4, 505.

Yalin, M.S. (1963), An expression for bed-load transportation.
Proc. Am. Soc. Civil Engrs., 90, No HY 3, 221.

NOTATIONS

a	Factor in Beavers & Joseph's equation for the boundary velocity of a Poiseuille flow over a porous block
a_1	Attenuation factor for the transmission of fluid shear at the bed surface
b	Superscript for fluid/solid boundary surface inside statistical volume
A	Specific surface area of the particles per unit solid volume
A_L	Average distance covered by particles of the bed load $/D_s$
A_*	Constant in Einstein's bed-load transport equation
c_1, c_2, c_3	Proportionality factors
C	Solid concentration by volume
C_B	Areal bed-load concentration
C_D	Drag coefficient
C_L	Lift coefficient
D_s	Particle-sieve diameter
f	Subscript or superscript for fluid phase
f_i	Stress vector
F_x, F_y	'Areal-averaged' drag and lift forces exerted by the fluid on particles of the bed surface, or of the bed load
F'_x, F'_y	'Areal-averaged' drag and lift forces exerted by the flow, excluding the buoyancy force
$\tilde{F}_i$	Average force per unit bulk volume exerted by the fluid upon the particles in a fluid/solid mixture
$\tilde{F}'_i$	Average force per unit bulk volume exerted by the flow upon the particles in a fluid/solid mixture, excluding the buoyancy force
g	Acceleration due to gravity
h	Water depth
k	Ratio of terminal particle velocity over fluid velocity
k_s	Surface roughness
K	Permeability
K_v	'Shear' permeability
L	Length
n_B	Number of particles rolling and saltating over the bed surface per unit area
n_D	Number of particles deposited on the bed surface per unit area per second

n'_E	Number of particles eroded from the bed per unit area and per unit increase in fluid shear
n_i	Unit vector along the outward-drawn normal of an element dS of a smooth closed surface S around a volume V, or of an element dS^b of the fluid/solid boundary surface of the fluid volume V^f
N	Measure of ratio between inertial and viscous stresses in suspension
N_D	Dimensionless expression for the rate of particle deposition
p^f	Fluid pressure
p_H	Hydrostatic fluid pressure
$\tilde{p}^s$	Dispersive grain pressure
$\tilde{p}^s_o$	Dispersive grain pressure on the bed surface
P	Probability density
P_D	Probability of a bed-load particle being deposited as it strikes the bed
P_E	Probability of a bed-surface particle being eroded at any time
q_s	Bed-load transport rate in solid volume per unit width per second
Re_D	Particle Reynolds' number
Re^*_D	Shear Reynolds' number
R_i	Reaction force per unit bulk volume exerted by the solid on the pore fluid inside a bulk volume bounded by a smooth surface
R'_i	Reaction force per unit bulk volume exerted by the solid on the pore fluid, apart from the hydrostatic buoyancy force
s	Subscript or superscript for solid phase
S	Smooth surface (area)
$\tilde{S}$	'Wavy' surface (area)
S^b	Fluid/solid boundary surface inside bulk volume V
$\tilde{S}^b$	'Wavy' part of fluid/solid boundary along 'wavy' surface
T_o	Average shear stress exerted by the bed load on the bed surface
u_f	Longitudinal fluid velocity
u_s	Longitudinal particle velocity
$\bar{u}_B$	Average transport velocity of bed-load particles
u^*	Shear velocity
u^*_c	Critical shear velocity
U	Reference fluid velocity

u^f, u^s	Fluid/solid velocity component along x-axis
v^f, v^s	Fluid/solid velocity component along y-axis
v_i^f	Fluid velocity
v_i^s	Solid velocity
V	Volume
x_j, (x, y, z)	Coordinates of Cartesian frame
(X, Y)	Coordinates of fixed Cartesian frame
(X^*, Y^*)	Cartesian coordinates of erosion boundary
α	Critical drag angle
$\alpha_{11}, \alpha_{12}, \alpha_{21}, \alpha_{22}, \alpha_1, \alpha_2, \alpha_3$	Particle shape factors
$\alpha_1 D_s^2$	Projected particle area in a plane perpendicular to the average flow direction
$\alpha_2 D_s^2$	Projected particle area in a plane parallel to the bed surface
$\alpha_3 D_s^3$	Particle volume
β	Downward slope of the bed surface
δ	Pre-script for pseudo-micro element
δ_B	Thickness of saltation layer
δ_{ij}	Kronecker delta
Δ	Pre-script for macro-element
θ	Angle of 'friction' for the bed load
$\varkappa$	'Virtual-mass' coefficient
λ	Linear grain concentration
λ_B	Step length of saltating particles$/D_s$
μ	Fluid viscosity
μ^*	Apparent viscosity of suspension
μ^{*f}	Apparent viscosity of fluid component
ξ_0	Lift factor for the topmost grains of the bed surface
ξ_B	Lift factor for the bed load
ρ_f, ρ_s	Fluid/solid density
$\tilde{\tau}_{ij}$, $\tilde{\tau}_{ij}^f$, $\tilde{\tau}_{ij}^s$	Total/fluid/solid macro-stress tensor
$\tilde{\tau}_o$, $\tilde{\tau}_o^f$, $\tilde{\tau}_o^s$	Total/fluid/solid areal average bed shear stress
τ_c	Critical shear stress at Shields' grain-movement condition
$\bar{\tau}_c$	Mean bed shear stress at Shields' grain-movement condition
τ_{sc}	Critical shear stress at the initiation of scour
$\bar{\tau}_{sc}$	Mean bed shear stress at the initiation of scour

σ	Standard deviation
σ_{ij}^{f}, σ_{ij}^{s}	Fluid/solid stress tensor
Φ	Intensity of bed-load transport
ϕ^{*}	Dimensionless stagnation pressure
ψ	Shear intensity
ψ_{c}	Shear intensity at Shields' grain-movement condition
ψ^{*}	Stream function
$-$	Suffix for time-mean value
$-b$	Suffix for areal average along the fluid/solid boundary surface inside statistical volume
$-f$	Suffix for areal average along fluid part of smooth surface
$-s$	Suffix for areal average along solid part of smooth surface
$\sim$	Suffix for areal average along 'wavy' surface
$\sim f$	Suffix for areal average along fluid part of 'wavy' surface
$\sim s$	Suffix for areal average along solid part of 'wavy' surface
$'$	Index for turbulent fluid or solid velocity fluctuations

Table 1

BED-LOAD FUNCTIONS FOR WALNUT GRAINS ($\rho_s = 1340\,\text{kg/m}^3$, $D_s = 1.5\,\text{mm}$)

β	$\dfrac{1}{\psi}$	Re_D^*	u^* (m/s)	Φ	N_D	$\bar{u}_s$ (m/s)	
0°	0.0380	16.3	0.0137				*
	0.0550	19.7	0.0166				**
	0.0474	18.3	0.0154	0.00480	0.000039	0.0779	
	0.0550	19.7	0.0166	0.0136	0.000099	0.0907	
	0.0669	21.8	0.0183	0.0228	0.000254	0.105	
	0.0760	23.2	0.0195	0.0281	0.000255	0.119	
	0.0848	24.5	0.0206	0.0476		0.132	***
	0.0994	26.6	0.0223			0.151	****
12°	0.0300	14.6	0.0122				*
	0.0598	20.6	0.0173	0.0212	0.000128	0.0963	
	0.0659	21.7	0.0182	0.0241	0.000220	0.113	
	0.0706	22.5	0.0188	0.0284	0.000275	0.126	***
	0.0800	23.8	0.0200	0.0571		0.143	****
18°	0.0255	13.5	0.0113				*
	0.0420	17.3	0.0145	0.0121		0.0779	
	0.0531	19.4	0.0163		0.000123	0.0962	
	0.0605	20.7	0.0174	0.0256	0.000315	0.116	
	0.0714	22.5	0.0189	0.0530	0.000379	0.136	***
	0.0848	24.5	0.0206	0.0768		0.152	****
	0.1076	27.6	0.0232			0.187	
22°	0.0230	12.7	0.0107				*
	0.0297	14.6	0.0122			0.0676	
	0.0474	18.4	0.0154		0.0001025	0.0913	
	0.0647	21.4	0.0180	0.0399	0.000189	0.1075	
	0.0714	22.5	0.0189	0.0533		0.119	
	0.0760	23.2	0.0195	0.0692		0.136	***
	0.0873	24.9	0.0209			0.163	****

*   Threshold of continuous sediment motion
**   Initiation of scour
*** Initiation of ripples
**** Rapid development of ripples

Table 2

BED-LOAD FUNCTIONS FOR SAND ($\rho_s = 2640\,\text{kg/m}^3$, $D_s = 0.9\,\text{mm}$)

β	$\dfrac{1}{\psi}$	Re_D^*	u^* (m/s)	Φ	N_D	$\bar{u}_s$ (m/s)	
0°	0.0380	16.8	0.0235				*
	0.0503	19.3	0.0270				**
	0.0375	16.6	0.0233				
						0.0708	
	0.0435	17.9	0.0251	0.00319			
	0.0445	18.1	0.0254		0.0000227	0.0897	
	0.0485	18.9	0.0265	0.00716			
	0.0503	19.3	0.0270		0.0000364	0.115	
	0.0515	19.5	0.0273	0.0129			
	0.0545	20.1	0.0281		0.0000508	0.143	
	0.0642	21.8	0.0305	0.0286			***
	0.0655	22.0	0.0308			0.163	
	0.0738	23.3	0.0327			0.192	****
12°	0.0305	15.0	0.0210				*
	0.0330	15.7	0.0219		0.0000051	0.0652	
	0.0391	17.0	0.0238		0.0000194	0.0840	
	0.0408	17.4	0.0244	0.00422			
	0.0456	18.3	0.0257		0.0000662	0.104	
	0.0481	18.9	0.0264	0.0109			
	0.0496	19.1	0.0268		0.0000740	0.117	
	0.0589	20.8	0.0292	0.0216			***
	0.0609	21.2	0.0297	0.0280			****
18°	0.0270	14.1	0.0198				*
	0.0380	16.8	0.0235				**
	0.0307	15.1	0.0211		0.0000138	0.0894	
	0.0381	16.8	0.0235	0.00416			
	0.0391	17.0	0.0238		0.0000319	0.103	
	0.0462	18.5	0.0259		0.0000762	0.117	
	0.0474	18.7	0.0262	0.00971			
	0.0601	21.0	0.0295				***
	0.0634	21.6	0.0303	0.0323		0.180	****
22°	0.0240	13.3	0.0186				*
	0.0263	13.9	0.0195			0.0821	
	0.0340	15.8	0.0222		0.0000305	0.108	
	0.0381	16.8	0.0235		0.0000756	0.132	
	0.0401	17.2	0.0241	0.00647			
	0.0428	17.8	0.0249		0.0000774	0.144	
	0.0474	18.7	0.0262	0.0116			
	0.0485	18.9	0.0265			0.155	
	0.0557	20.3	0.0284	0.0299			***
	0.0655	22.0	0.0308	0.0542			****

*	Threshold of continuous sediment motion
**	Initiation of scour
***	Initiation of ripples
****	Rapid development of ripples

Table 3

BED-LOAD FUNCTIONS FOR SAND ($\rho_s = 2640\,\text{kg/m}^3$, $D_s = 1.8\,\text{mm}$)

β	$\dfrac{1}{\psi}$	Re_D^*	u^* (m/s)	Φ	N_D	$\bar{u}_s$(m/s)	
0°	0.0370	46.8	0.0327				*
	0.0506	54.6	0.0383				**
	0.0392	48.2	0.0337	0.000728			
	0.0420	49.9	0.0349	0.00297			
	0.0457	52.0	0.0364		0.0000306	0.145	
	0.0506	54.6	0.0383		0.0000579	0.186	
	0.0530	56.3	0.0394	0.00799			
	0.0539	56.3	0.0395		0.0000774	0.214	
	0.0561	57.6	0.0403	0.0185			
	0.0630	61.1	0.0427		0.000168	0.241	***
	0.0665	62.8	0.0439				****
12°	0.0290	41.4	0.0290				*
	0.0318	43.3	0.0303			0.140	
	0.0369	46.7	0.0327	0.00484		0.172	
	0.0409	49.2	0.0344	0.00858	0.0000284	0.195	
	0.0475	53.0	0.0371	0.0143			
	0.0483	53.4	0.0374		0.0000820	0.234	***
	0.0512	55.0	0.0385	0.0229			****
18°	0.0250	38.4	0.0269				*
	0.0267	39.7	0.0278			0.126	
	0.0292	41.6	0.0291	0.00153			
	0.0300	42.2	0.0295		0.0000102	0.139	
	0.0362	46.4	0.0324		0.0000684	0.170	
	0.0369	46.7	0.0327	0.00766			
	0.0423	50.0	0.0350	0.0213			
	0.0445	51.4	0.0359		0.000111	0.194	***
	0.0506	54.7	0.0383		0.000265	0.233	****
22°	0.0200	34.4	0.0241				*
	0.0214	35.5	0.0249			0.105	
	0.0237	37.4	0.0262	0.00103		0.125	
	0.0272	40.1	0.0281				
	0.0294	41.6	0.0292	0.00731		0.150	
	0.0338	44.7	0.0313				
	0.0369	46.8	0.0327			0.181	
	0.0432	50.5	0.0354			0.212	***
	0.0490	53.9	0.0377			0.233	****

*	Threshold of continuous sediment motion
**	Initiation of scour
***	Initiation of ripples
****	Rapid development of ripples

Table 4

BED-LOAD FUNCTIONS FOR GRAVEL ($\rho_s = 2640\,\text{kg/m}^3$, $D_s = 3.3\,\text{mm}$)

β	$\dfrac{1}{\psi}$	Re_D^*	u^* (m/s)	Φ	N_D	$\bar{u}_s$ (m/s)	
0°	0.0455	129	0.0492				*
	0.0580	145	0.0555				**
	0.0480	132	0.0505	0.000704			
	0.0505	136	0.0518			0.171	
	0.0616	150	0.0572	0.00681	0.000092	0.210	
	0.0692	159	0.0606		0.000161	0.249	***
	0.0747	165	0.0630			0.304	****
12°	0.0365	115.3	0.0440				*
	0.0501	135	0.0516	0.0124	0.0000508		
	0.0572	144	0.0551		0.000142		***
	0.0722	162	0.0619		0.000153		****
18°	0.0305	113	0.0431				*
	0.0301	105	0.0400			0.114	
	0.0339	111	0.0424	0.00144	0.0000108	0.151	
	0.0400	121	0.0461	0.00532		0.187	
	0.0488	133	0.0502	0.0141			
	0.0501	135	0.0516			0.220	***
	0.0557	142	0.0544			0.265	****
22°	0.0270	99.2	0.0379				*
	0.0276	100	0.0383			0.149	
	0.0355	114	0.0434	0.00517	0.0000203	0.180	
	0.0371	116	0.0444		0.0000397	0.208	
	0.0450	128	0.0489			0.237	***
	0.0572	144	0.0551				****

*   Threshold of continuous sediment motion
**   Initiation of scour
***   Initiation of ripples
****   Rapid development of ripples

Table 5

BED-LOAD FUNCTIONS FOR MAGNETITE ($\rho_s = 4580 \text{ kg/m}^3$, $D_s = 1.8 \text{ mm}$)

β	$\dfrac{1}{\psi}$	Re_D^*	u^* (m/s)	Φ	N_D	$\bar{u}_s$ (m/s)	
0°	0.0420	73.6	0.0515				*
	0.0514	81.4	0.0570				**
	0.0475	78.2	0.0548	0.00174	0.0000223	0.198	
	0.0514	81.4	0.0570	0.00636	0.0000548	0.240	
	0.0622	89.6	0.0627	0.0144	0.0001045	0.282	
	0.0650	91.6	0.0641	0.0181		0.298	***
	0.0729	97.0	0.0679				****
12°	0.0340	66.2	0.0464				*
	0.0327	65.1	0.0455			0.147	
	0.0448	76.0	0.0532	0.00458	0.0000298		
	0.0491	79.6	0.0557	0.0102	0.0000596	0.243	
	0.0514	81.4	0.0570	0.0215	0.000118	0.267	
	0.0560	85.0	0.0595	0.0408		0.295	***
	0.0579	86.4	0.0605				****
18°	0.0270	59.0	0.0414				*
	0.0310	63.2	0.0443			0.175	
	0.0391	71.0	0.0497	0.00880	0.0000699	0.240	
	0.0436	75.0	0.0525	0.0128	0.0000955	0.272	
	0.0486	77.8	0.0554	0.0232	0.000189	0.294	
	0.0503	80.5	0.0564				***
	0.0549	84.1	0.0589				****
22°	0.0220	53.3	0.0372				*
	0.0283	60.4	0.0422	0.00253	0.0000292		
	0.0346	66.9	0.0468	0.0111	0.0000695		
	0.0386	70.5	0.0494	0.0146	0.000133		
	0.0468	77.7	0.0543	0.0349	0.000182		***
	0.0554	84.6	0.0592				****

*   Threshold of continuous sediment motion
**   Initiation of scour
***   Initiation of ripples
****   Rapid development of ripples

Table 6

Average transport velocity $\bar{u}_B$ of saltating bed-load particles measured by projecting a sequence of individual frames of a motion picture taken at 45 frame/s, versus average particle velocity $\bar{u}_s$ measured visually by projecting the motion picture at 16 frame/s and following small groups of particles moving simultaneously on the screen.

$$\rho_s = 2640 \text{ kg/m}^3, \ D_s = 1.8 \text{ mm}$$

$$1/\psi_c = 0.0370, \ u_c^* = 0.0327 \text{ m/s}$$

$1/\psi$	u^* m/s	$\bar{u}_s$ m/s	$\bar{u}_B$ m/s	$\bar{u}_B/\bar{u}_s$	Number of counted time intervals of 0.0222 s
0.0457	0.0364	0.145	0.107	0.74	489
0.0506	0.0383	0.186	0.149	0.80	657
0.0539	0.0395	0.214	0.171	0.80	1197
0.0630	0.0427	0.241	0.193	0.80	241
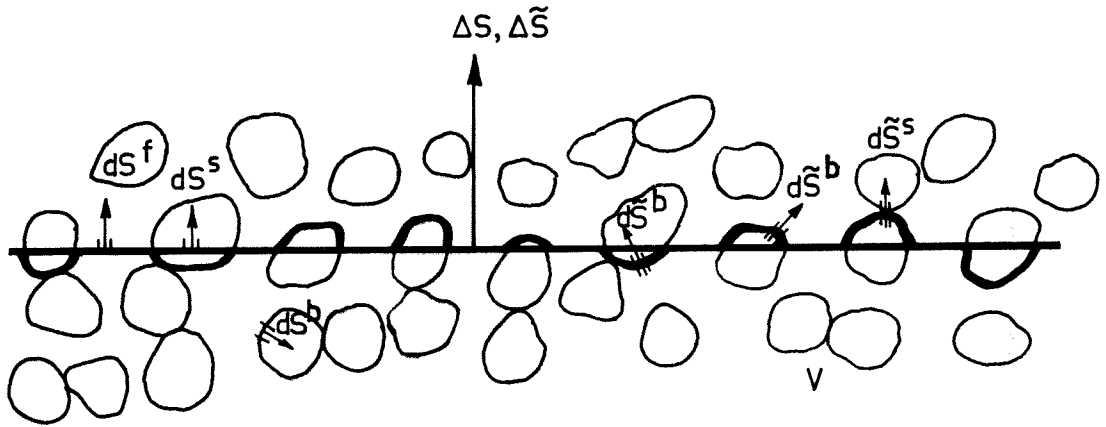
FIG.1

SMOOTH, FLAT, MACROSCOPIC SURFACE ELEMENT ΔS IN A
FLUID CONTAINING SOLID PARTICLES INTERSECTING THE FLUID
AND THE SOLID AT RANDOM, AND 'WAVY' MACROSCOPIC
SURFACE ELEMENT $\Delta \tilde{S}$, FLUCTUATING TO A MINIMUM ABOUT ΔS
AND THEREBY INTERSECTING THE SOLID AT INTERGRANULAR
CONTACTS ONLY.

$$\Delta S = \Delta S^f + \Delta S^s; \quad \Delta \tilde{S} = \Delta \tilde{S}^f + \Delta \tilde{S}^s; \quad \Delta \tilde{S}^f = \Delta S^f + \Delta \tilde{S}^b$$
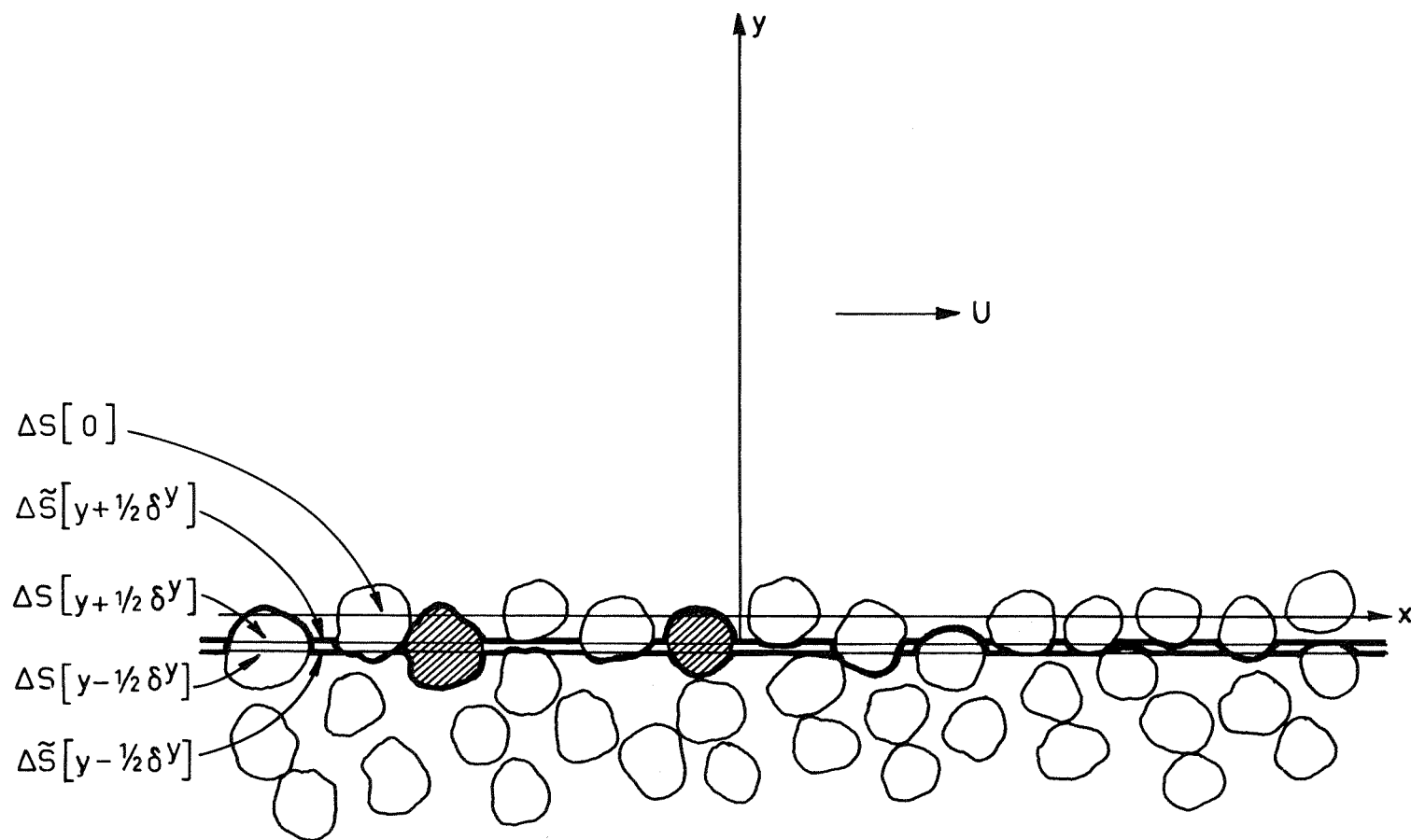
FIG. 2

CROSS-SECTION OF A SMOOTH SAND BED AND
PARTICLES BOUNDED BY TWO 'WAVY' SURFACES,
$\Delta\tilde{S}\left[y-\tfrac{1}{2}\delta^{y}\right]$ AND $\Delta\tilde{S}\left[y+\tfrac{1}{2}\delta^{y}\right]$
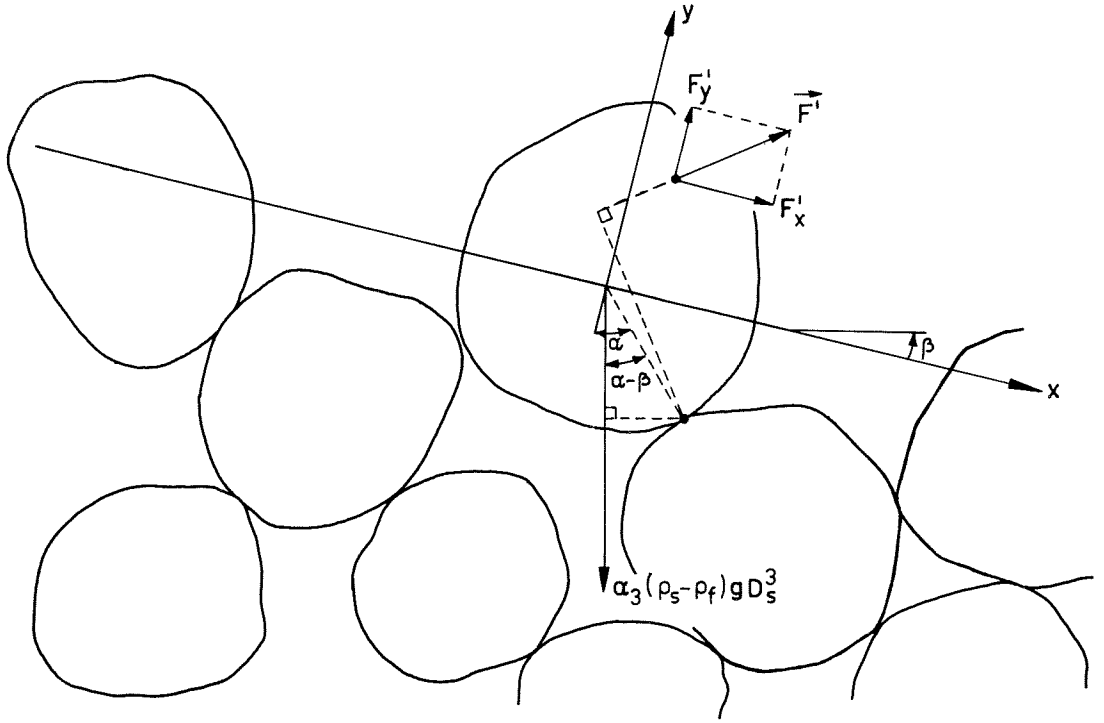
FIG. 3

OVERRIDING MOMENT EXERTED ON PARTICLE OF SUBMERGED WEIGHT $\alpha_3(\rho_s-\rho_f)gD_s^3$, SUBJECTED TO DRAG FORCE $F_x' \sim D_s^2\,\bar{\tau}_0^f$ AND LIFT FORCE $F_y' \sim F_x'$, BY A SHEAR FLOW AT THE SURFACE OF AN INCLINED BED.

$$\frac{1}{\psi_c} = \frac{\bar{\tau}_0}{(\rho_s-\rho_f)gD_s} = \left(\frac{1}{\psi_c}\right)_{\beta=0} \frac{\sin(\alpha-\beta)}{\sin\alpha}$$
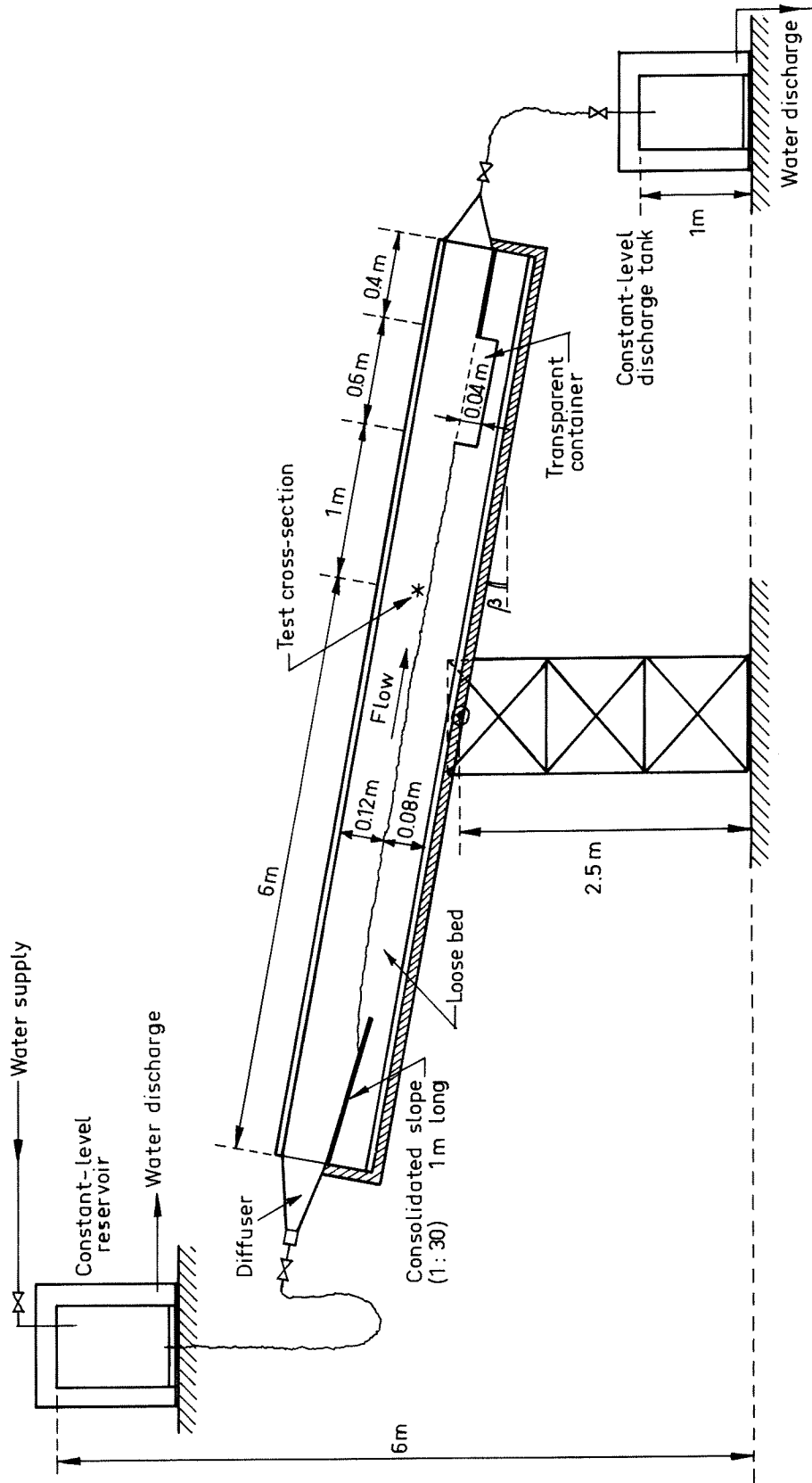
FIG.4a

CLOSED FLOW CHANNEL
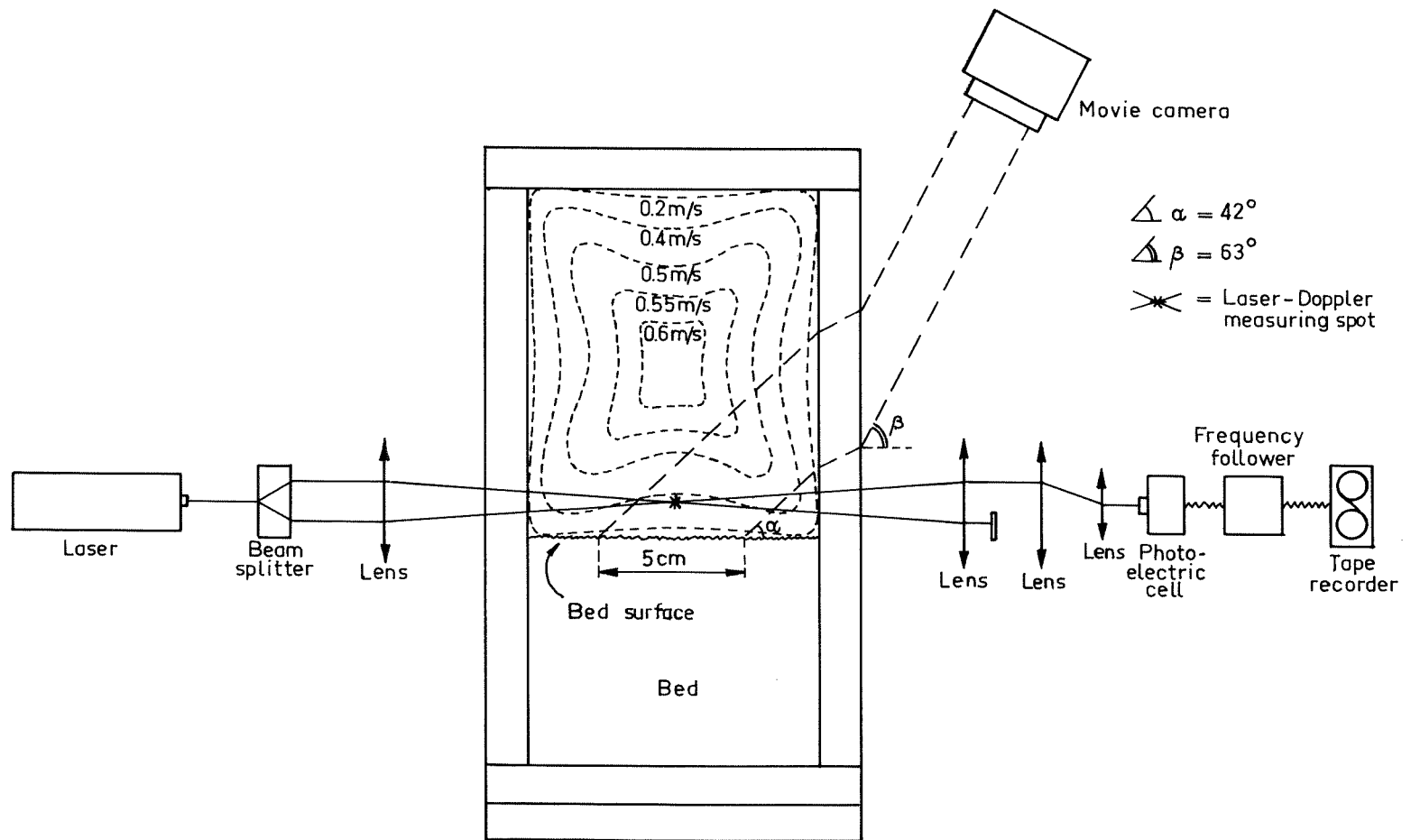
FIG. 4b

CROSS-SECTION OF FLOW CHANNEL WITH CONTOUR PLOT OF AVERAGE FLOW-VELOCITY
DISTRIBUTION AND SET-UP OF LASER-DOPPLER VELOCITY METER AND MOVIE CAMERA.
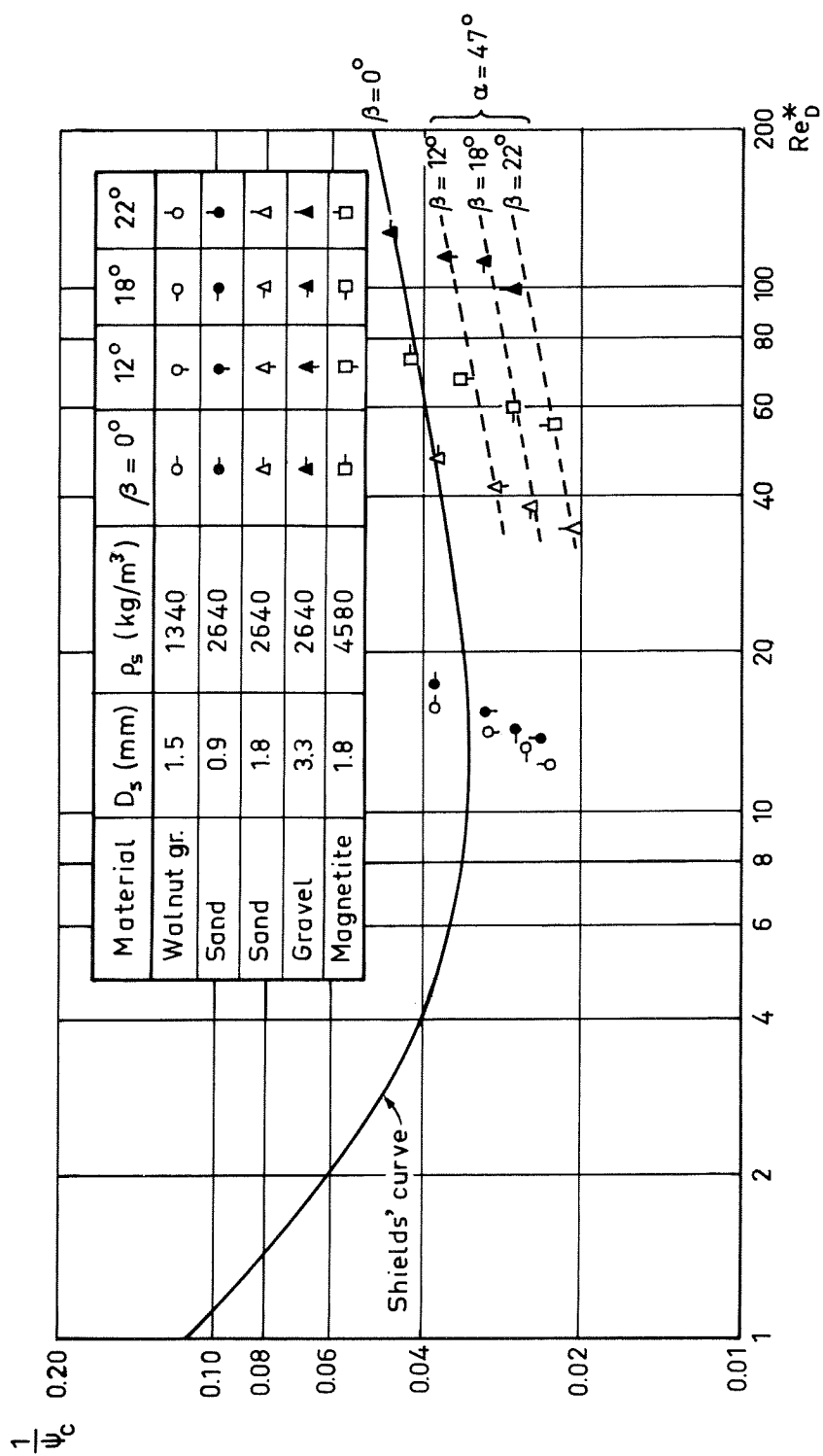
FIG. 5

MEAN BED SHEAR STRESS AT THE THRESHOLD OF CONTINUOUS SEDIMENT MOTION ($\bar{\tau}_c$) VERSUS SHEAR REYNOLDS' NUMBER (Re_D^*).

$$\frac{1}{\psi_c} = \bar{\tau}_c \left[(\rho_s - \rho_f)\, g D_s \right]^{-1} \; ; \quad Re_D^* = \frac{D_s}{\mu} \left[\rho_f \bar{\tau}_o \right]^{1/2}$$

6a. MAGNETITE (D_s =1.8mm)
Total sample size 246

y = 4.5 mm
h = 80 mm
$\bar{u}$ = 0.44 m/s
σ = 0.19 $\bar{u}$
u_{max} = 1.64 $\bar{u}$
u_{min} = 0.49 $\bar{u}$
R_e = 9.5×10^4
$1/\psi$ = 0.0275
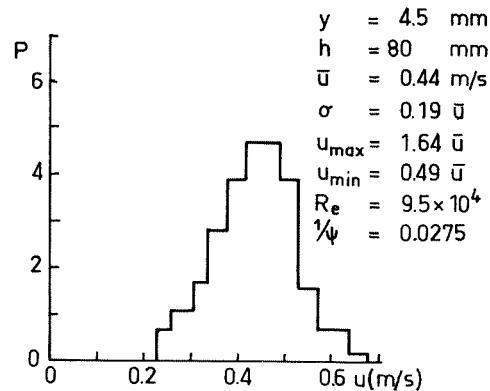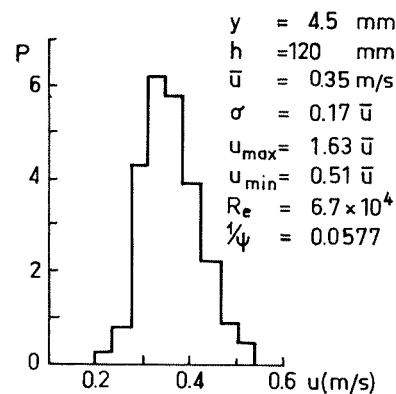
6b. SAND (D_s =0.9mm)
Total sample size 246

y = 4.5 mm
h = 120 mm
$\bar{u}$ = 0.35 m/s
σ = 0.17 $\bar{u}$
u_{max} = 1.63 $\bar{u}$
u_{min} = 0.51 $\bar{u}$
R_e = 6.7×10^4
$1/\psi$ = 0.0577

6c. MAGNETITE (D_s =1.8mm)
Total sample size 246

y = 9 mm
h = 80 mm
$\bar{u}$ = 0.66m/s
σ = 0.18 $\bar{u}$
u_{max} = 1.60 $\bar{u}$
u_{min} = 0.50 $\bar{u}$
R_e = 9.75×10^4
$1/\psi$ = 0.0455
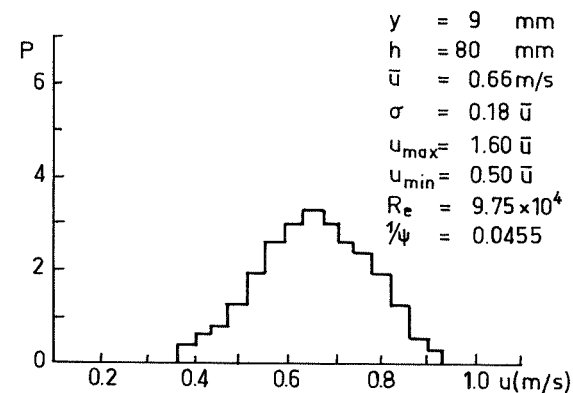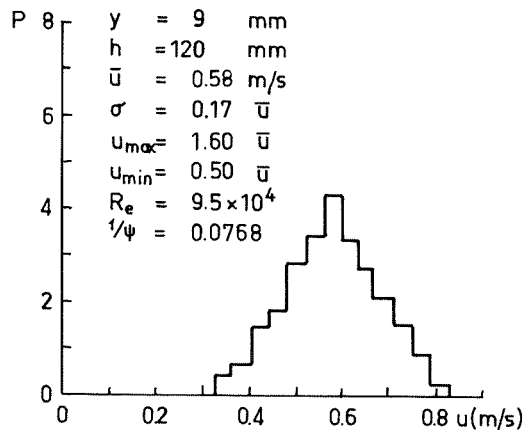
6d. SAND (D_s =1.8mm)
Total sample size 244

y = 9 mm
h = 120 mm
$\bar{u}$ = 0.58 m/s
σ = 0.17 $\bar{u}$
u_{max} = 1.60 $\bar{u}$
u_{min} = 0.50 $\bar{u}$
R_e = 9.5×10^4
$1/\psi$ = 0.0768
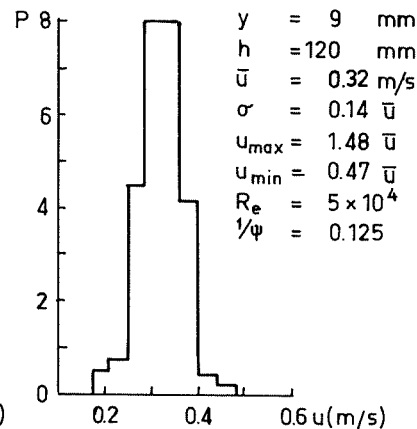
6e. WALNUT GRAINS (D_s =1.5mm)
Total sample size 244

y = 9 mm
h = 120 mm
$\bar{u}$ = 0.32 m/s
σ = 0.14 $\bar{u}$
u_{max} = 1.48 $\bar{u}$
u_{min} = 0.47 $\bar{u}$
R_e = 5×10^4
$1/\psi$ = 0.125
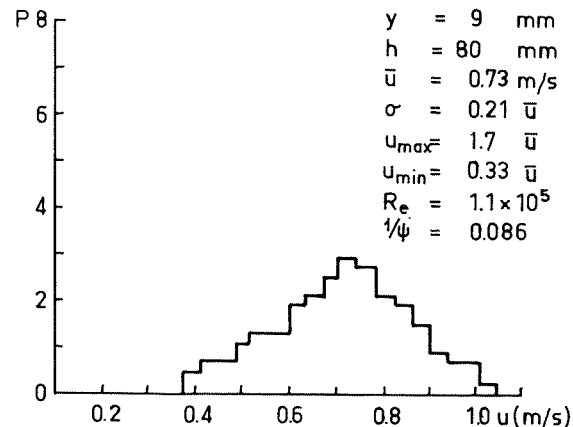
6f. GRAVEL (D_s =3.3mm)
Total sample size 246

y = 9 mm
h = 80 mm
$\bar{u}$ = 0.73 m/s
σ = 0.21 $\bar{u}$
u_{max} = 1.7 $\bar{u}$
u_{min} = 0.33 $\bar{u}$
R_e = 1.1×10^5
$1/\psi$ = 0.086

FIG. 6

DISTRIBUTION FUNCTIONS P(u) DERIVED BY SAMPLING TURBULENT FLUID-VELOCITY FLUCTUATIONS MEASURED DURING BED-LOAD TRANSPORT WITH LASER-DOPPLER VELOCITY METER

Material		D_s [mm]	ρ_s [kg/m³]	$\overline{\tau}_0$ [N/m²]	$\sigma/\overline{\tau}_0$	$\widetilde{\tau}_{0,max}/\overline{\tau}_0$
Sand	●	0.9	2640	0.80	0.36	2.57
Magnetite	□	1.8	4580	2.52	0.37	2.58
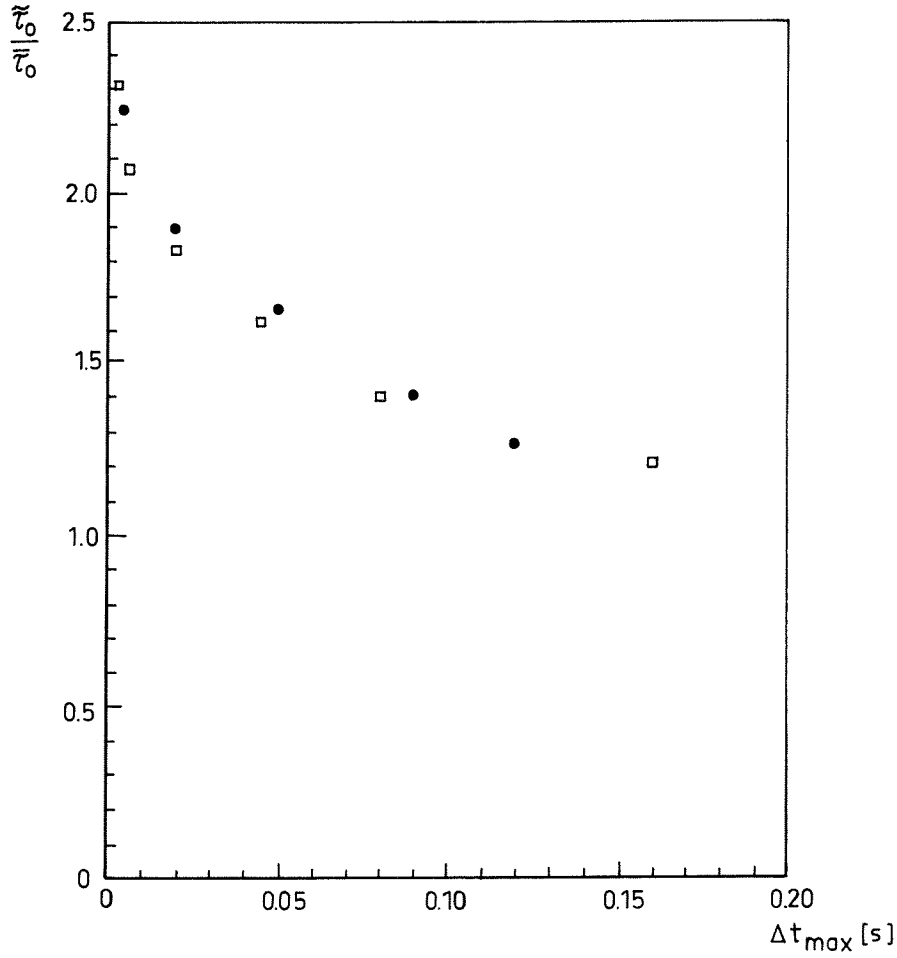
FIG. 7

MAXIMUM TIME INTERVAL Δt_{max} [s] DURING WHICH THE INSTANTANEOUS SHEAR STRESS $\widetilde{\tau}_0$ EXCEEDS A GIVEN VALUE WITHOUT INTERRUPTION (measured for a total period of 10 s)

Material	D_s (mm)	ρ_s (kg/m³)	$\beta = 0°$
Walnut gr.	1.5	1340	○
Sand	0.9	2640	●
Sand	1.8	2640	△
Gravel	3.3	2640	▲
Magnetite	1.8	4580	□

Shields' curve

Re^*_D
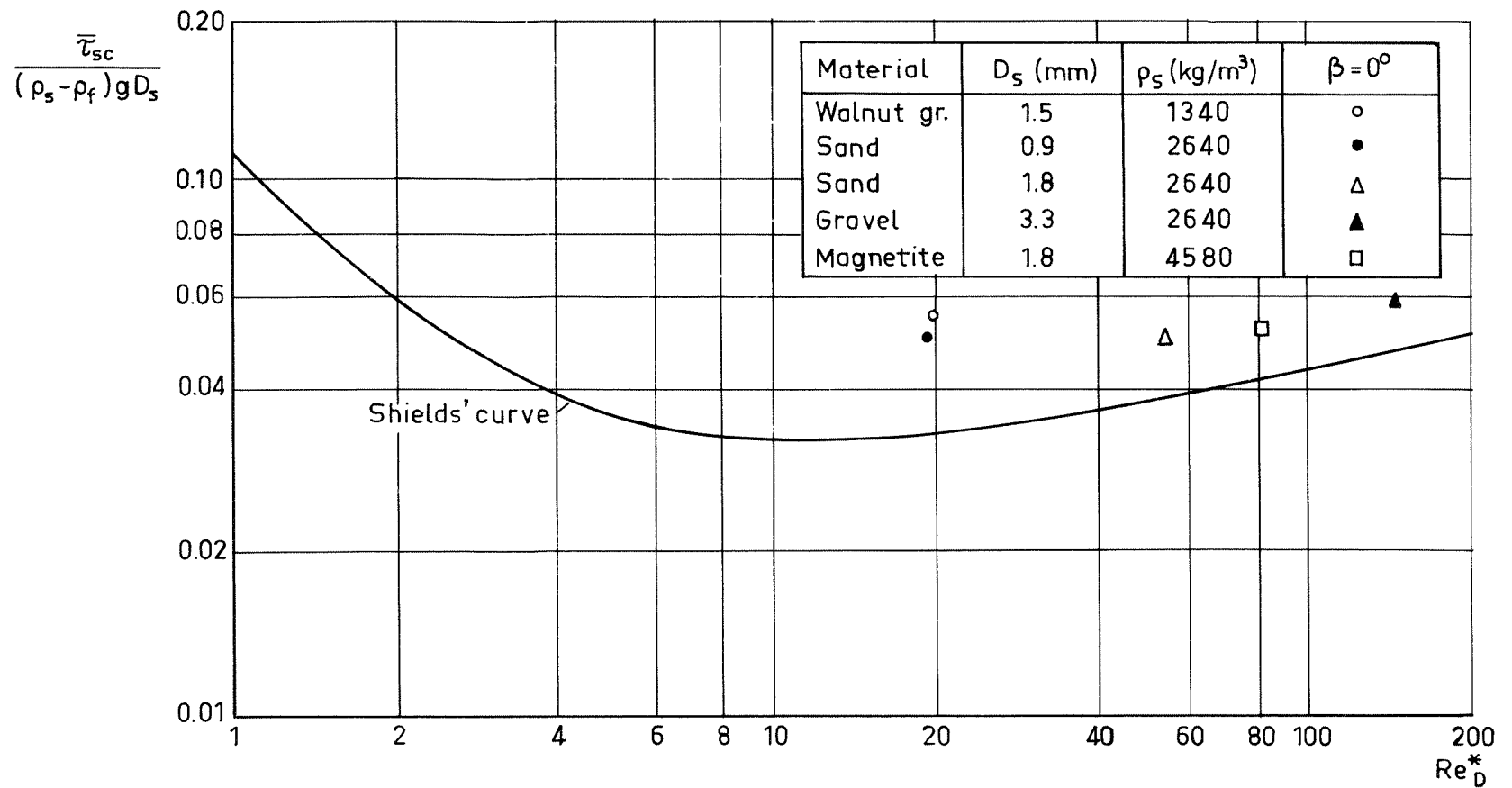
FIG. 8

MEAN BED SHEAR STRESS AT THE INITIATION OF SCOUR ($\overline{\tau}_{sc}$)
VERSUS THE SHEAR REYNOLDS' NUMBER (Re^*_D)

$$\frac{1}{\psi_{sc}} = \overline{\tau}_{sc} \left[(\rho_s - \rho_f) g D_s \right]^{-1} ; \quad Re^*_D = \frac{D_s}{\mu} \left[\rho_f \overline{\tau}_o \right]^{\frac{1}{2}}$$

Material	D_s (mm)	ρ_s (kg/m³)	β 0°	12°	18°	22°
Walnut gr.	1.5	1340	⊖	⊕	⊖	⊙
Sand	0.9	2640	●	●	●	●
Sand	1.8	2640	△	△	△	△
Gravel	3.3	2640	▲	▲	▲	▲
Magnetite	1.8	4580	⊡	⊡	⊡	⊡

FIG. 9

AVERAGE RATE OF BED-LOAD TRANSPORT IN
SOLID VOLUME PER UNIT CHANNEL WIDTH AND
UNIT TIME, $\bar{q}_s$, VERSUS MEAN BED SHEAR STRESS

$$\bar{\tau}_o = (\rho_s - \rho_f) g D_s / \psi.$$

$$\Phi = \bar{q}_s \left[\left(\frac{\rho_s}{\rho_f} - 1 \right) g D_s^3 \right]^{-\frac{1}{2}}$$

Material	D_s (mm)	ρ_s (kg/m³)	$\beta = 0°$	12°	18°	22°
Walnut gr.	1.5	1340	○-	○	-○	○
Sand	0.9	2640	●-	●	-●	●
Sand	1.8	2640	△-	△	-△	△
Gravel	3.3	2640	▲-	▲	-▲	▲
Magnetite	1.8	4580	▣-	▣	-▣	▣

FIG. 10

AVERAGE NUMBER OF PARTICLES DEPOSITED
ON THE BED SURFACE PER UNIT AREA AND UNIT
TIME, $\bar{n}_D$, VERSUS MEAN BED SHEAR STRESS

$$\bar{\tau}_0 = (\rho_s - \rho_f) g D_s / \psi$$

$$N_D = \bar{n}_D D_s^3 \left[\left(\frac{\rho_s}{\rho_f} - 1 \right) g D_s \right]^{-\frac{1}{2}}$$

Material	D (mm)	ρ (kg/m³)	β=0, 12,18 and 22°
Walnut gr.	1.5	1340	o
Sand	0.9	2640	●
Sand	1.8	2640	△
Gravel	3.3	2640	▲
Magnetite	1.8	4580	☐
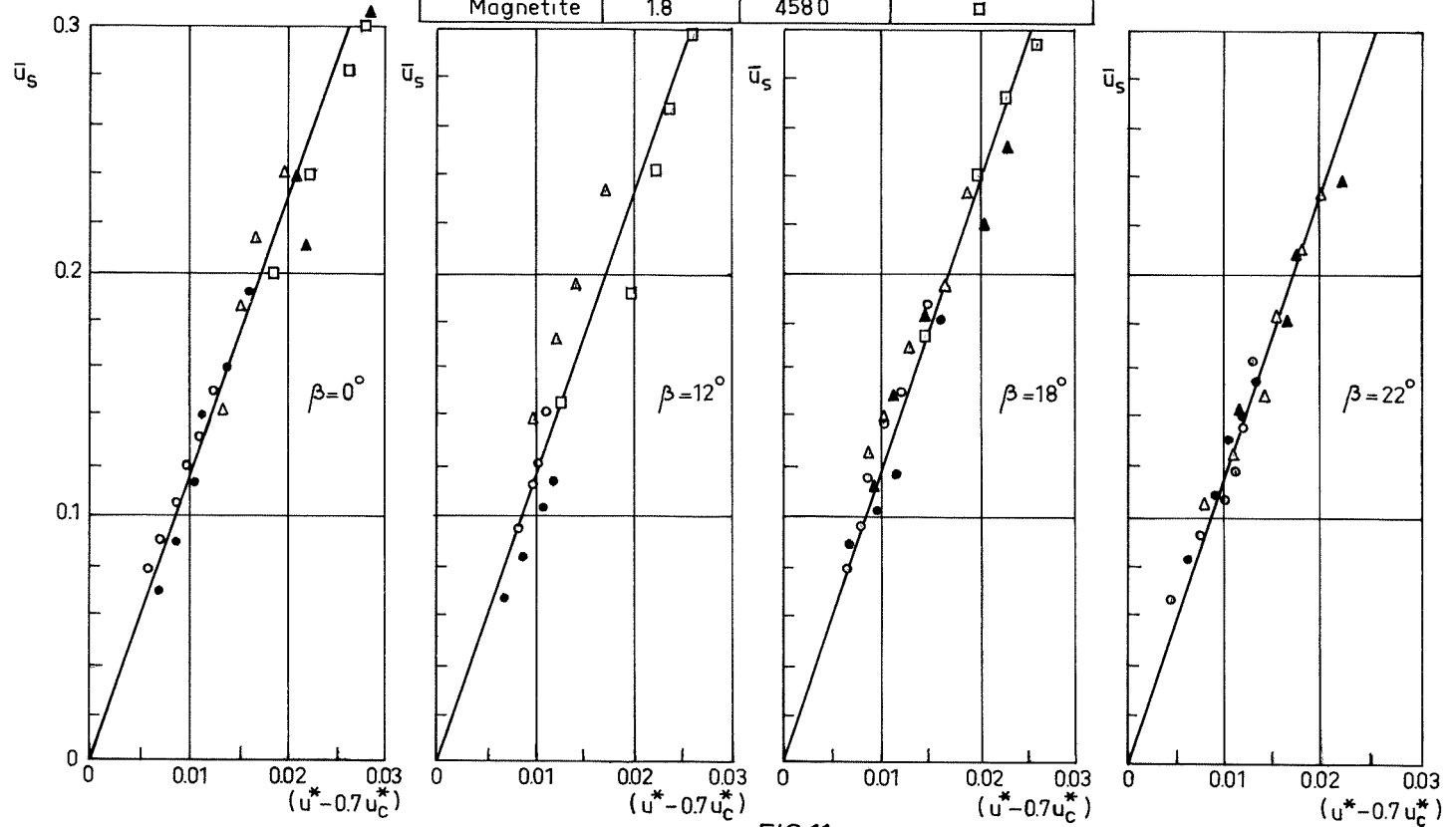
FIG. 11

AVERAGE PARTICLE VELOCITY $\bar{u}_s$ [m/s] MEASURED VISUALLY, AS A FUNCTION OF
SHEAR VELOCITY u^* [m/s] $=(\bar{\tau}_o/\rho_f)^{1/2}$.
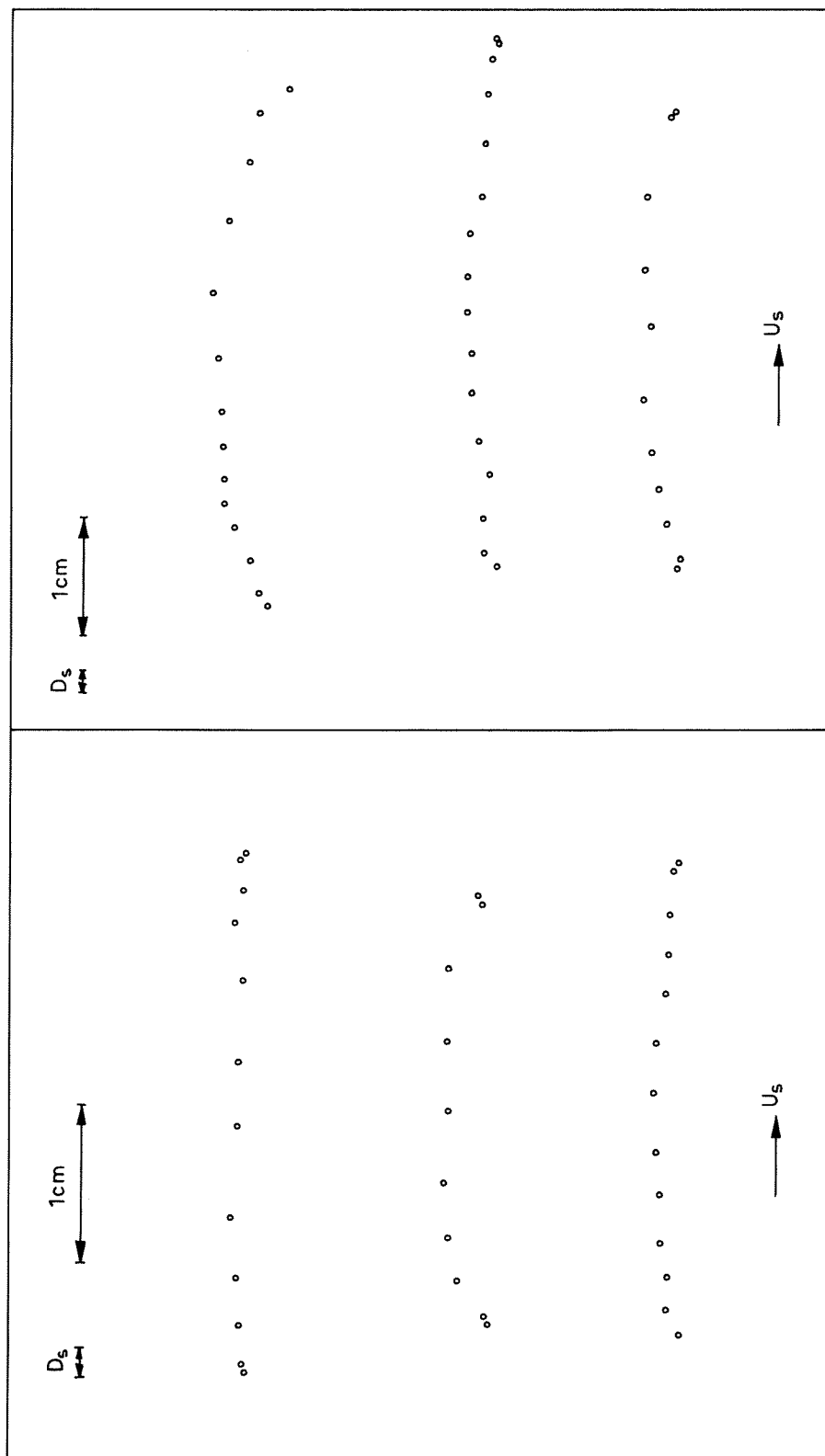
FIG. 12

POSITION OF SALTATING SAND PARTICLES OBSERVED AT 0.022S INTERVALS

$\rho_s = 2640 \, \text{kg/m}^3$, $D_s = 1.8 \, \text{mm}$ $\bar{\lambda}_B = 16$, $1/\psi_c = 0.037$, $u_c^* = 0.0327 \, \text{m/s}$.

$1/\psi = 0.0506$, $\bar{u}_s = 0.186 \, \text{m/s}$, $\bar{u}_B = 0.149 \, \text{m/s}$

$1/\psi = 0.0539$, $\bar{u}_s = 0.214 \, \text{m/s}$, $\bar{u}_B = 0.171 \, \text{m/s}$
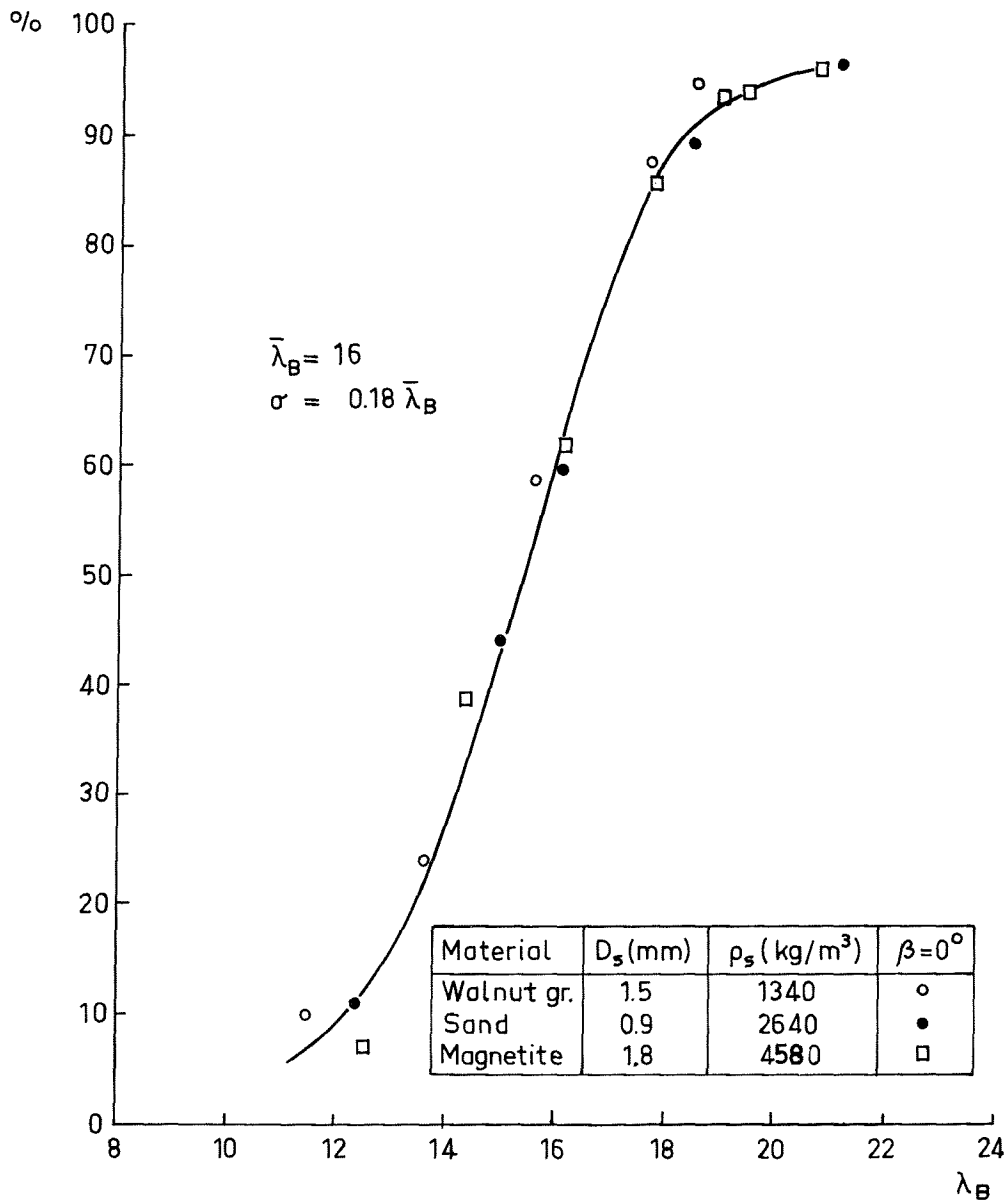
FIG. 13

CUMULATIVE FREQUENCY CURVE OF THE LENGTH $\lambda_B \cdot D_S$ OF
INDIVIDUAL STEPS PERFORMED BY SALTATING PARTICLES
OF THE BED LOAD AT VARIOUS FLOW RATES.

FIG.a. MAGNETITE (D_S = 1.8 mm)

$$y = 4.5 \text{ mm}$$
$$h = 80 \text{ mm}$$
$$\bar{\tau}_o = 1.74 \text{ N/m}^2$$
$$\sigma = 0.37 \ \bar{\tau}_o$$
$$\tilde{\tau}_{o,max} = 2.58 \ \bar{\tau}_o$$
$$\tilde{\tau}_{o,min} = 0.24 \ \bar{\tau}_o$$
$$Re_D^* = 59.6$$
$$1/\psi = 0.0275$$

FIG.b. SAND (D_S = 0.9 mm)

$$y = 4.5 \text{ mm}$$
$$h = 120 \text{ mm}$$
$$\bar{\tau}_o = 0.83 \text{ N/m}^2$$
$$\sigma = 0.36 \ \bar{\tau}_o$$
$$\tilde{\tau}_{o,max} = 2.57 \ \bar{\tau}_o$$
$$\tilde{\tau}_{o,min} = 0.25 \ \bar{\tau}_o$$
$$Re_D^* = 20.6$$
$$1/\psi = 0.0577$$
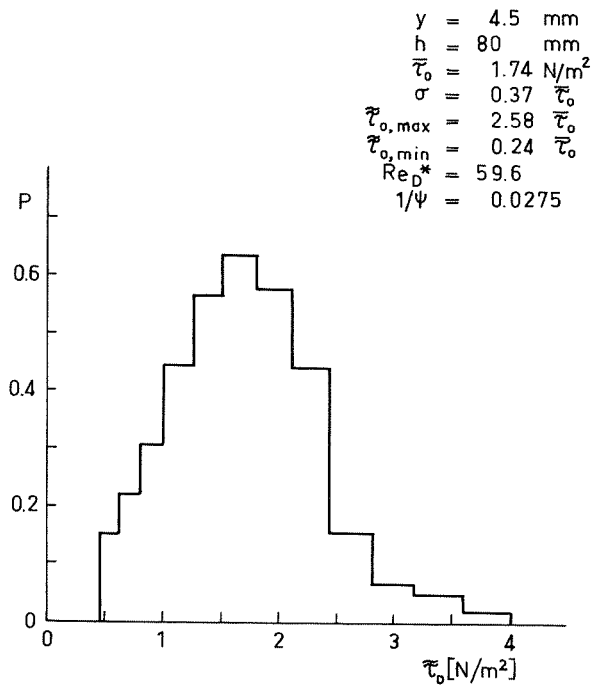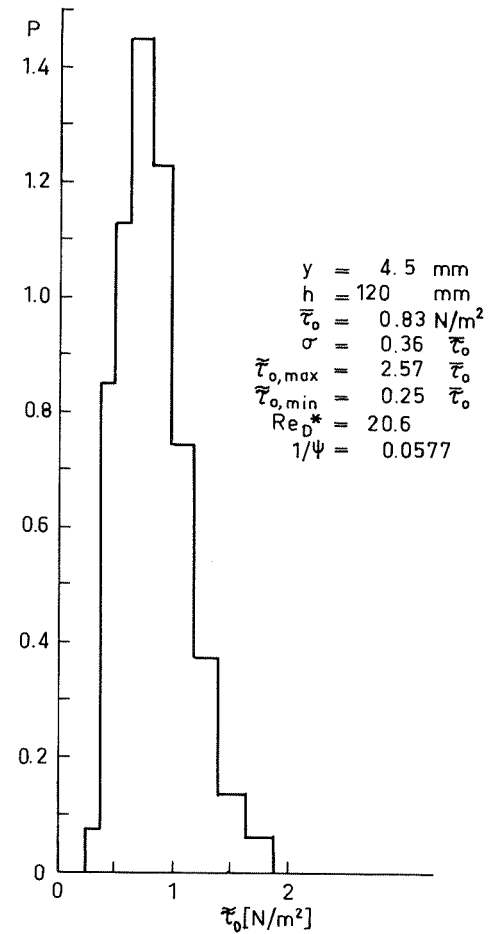
FIG. 14

ESTIMATED PROBABILITY DENSITY $P(\tilde{\tau}_o)$ OF THE TURBULENT BED SHEAR STRESS
FOR MAGNETITE (D_S = 1.8 mm) AND SAND (D_S = 0.9 mm)
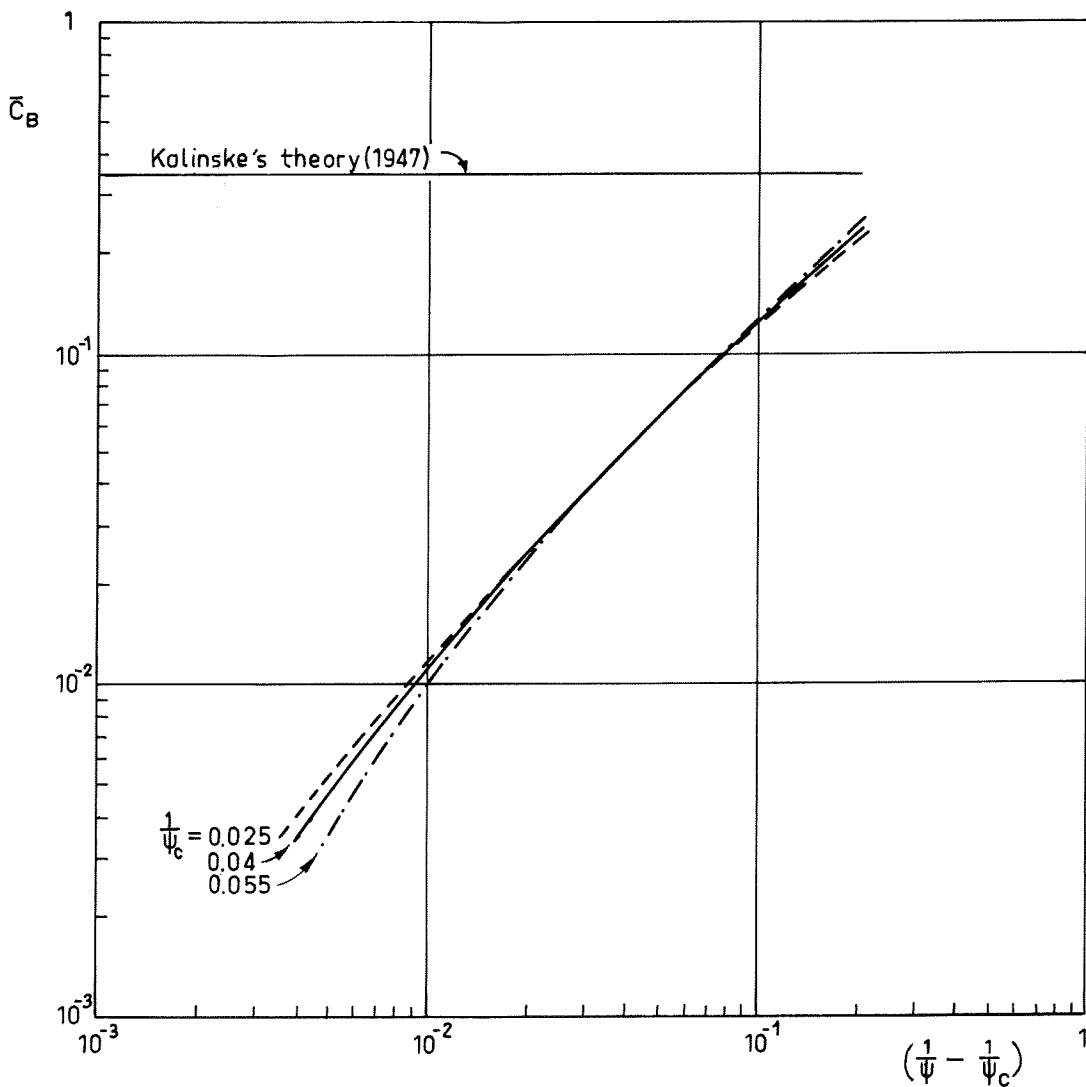
FIG. 15

AVERAGE BED-LOAD CONCENTRATION $\bar{C}_B = \alpha_3 D_s^2 \bar{n}_B$ VERSUS MEAN
BED SHEAR STRESS $\bar{\tau}_0 = (\rho_s - \rho_f)gD_s / \Psi$ FOR SAND ($c_2 = 0.914$)

$$\bar{C}_B = c_2 \frac{\left(\frac{1}{\Psi} - \frac{1}{\Psi_c}\right)^{3/2}}{\left(\sqrt{\frac{1}{\Psi}} - 0.7\sqrt{\frac{1}{\Psi_c}}\right)}$$
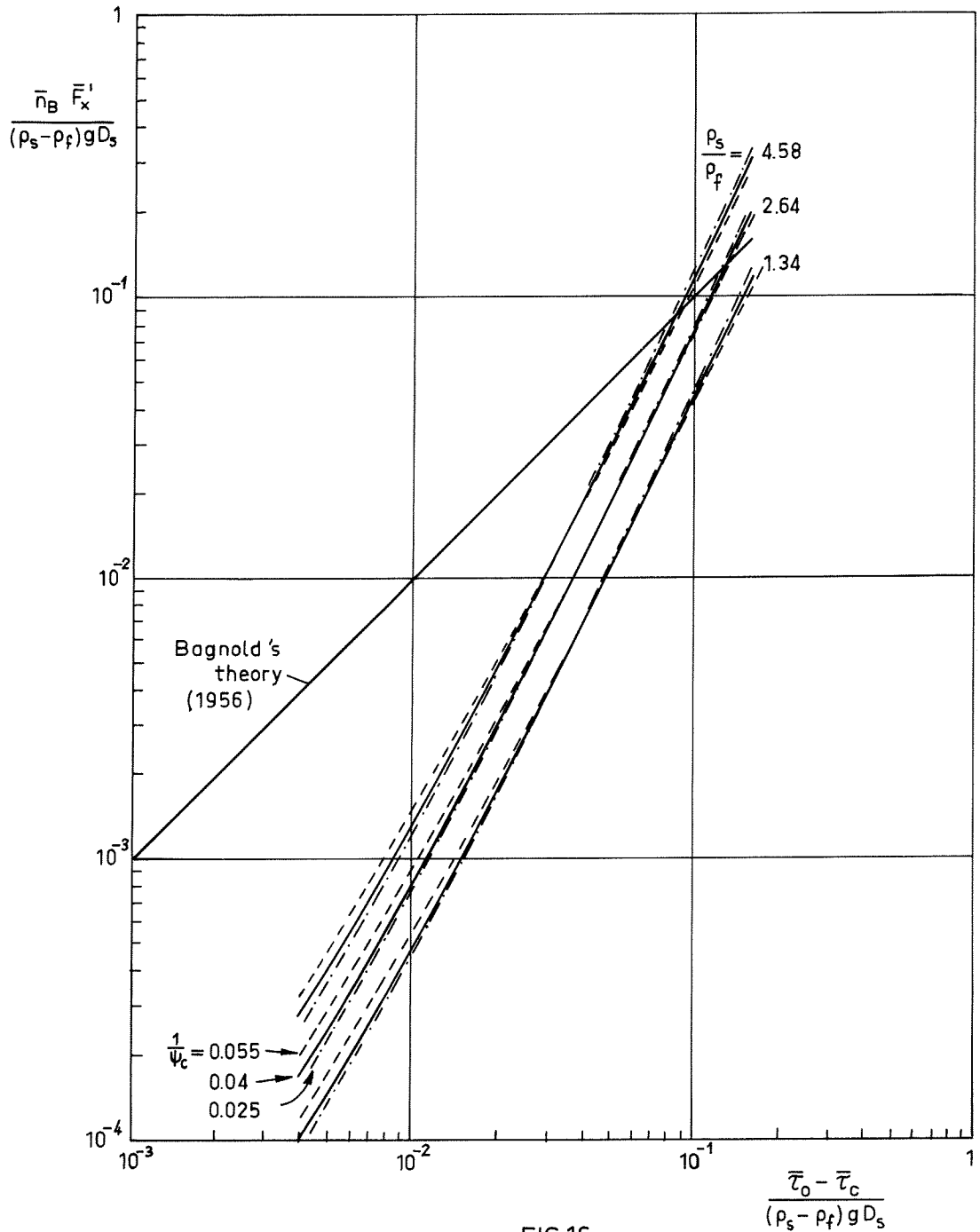
FIG. 16

AVERAGE REDUCTION IN FLUID SHEAR AT THE BED SURFACE DUE
TO THE BED-LOAD, $\bar{n}_B\,\bar{F}_x'$, AS A FUNCTION OF TEMPORAL MEAN BED
SHEAR STRESS $\bar{\tau}_0$.

$$\bar{n}_B\,\bar{F}_x' = 3.48\left(\frac{\rho_s}{\rho_f}+0.5\right)\frac{(\bar{\tau}_0-\bar{\tau}_c)^{3/2}\,(1.02\sqrt{\bar{\tau}_0}-0.7\sqrt{\bar{\tau}_c})^2}{(\rho_s-\rho_f)\,g\,D_s\ \ (\sqrt{\bar{\tau}_0}-0.7\sqrt{\bar{\tau}_c})}$$
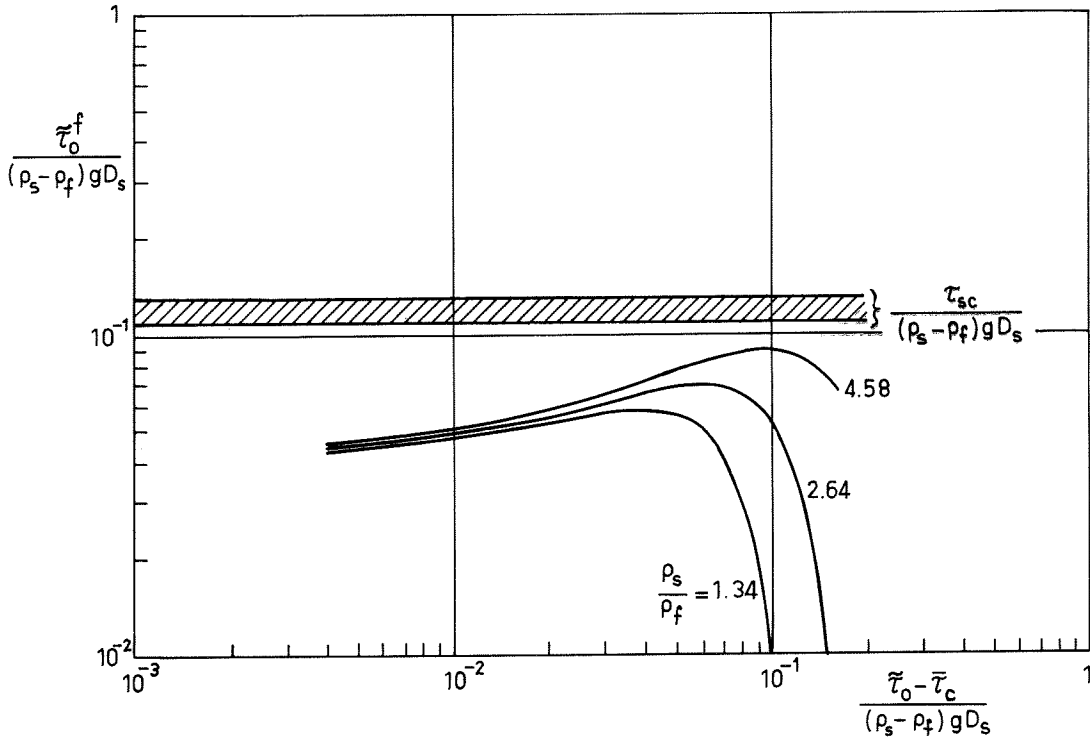
FIG.17

AREAL-AVERAGE FLUID SHEAR STRESS AT THE BED SURFACE,
$\tilde{\tau}_o^f$, VERSUS INSTANTANEOUS BED SHEAR STRESS $\tilde{\tau}_o$,
for $\bar{\tau}_c = 0.04\,(\rho_s - \rho_f)\,gD_s$.

$$\tilde{\tau}_o^{\,f} = \tilde{\tau}_o - 3.48 \left(\frac{\rho_s}{\rho_f} + 0.5\right) \frac{(\tilde{\tau}_o - \bar{\tau}_c)^{3/2}\,(1.02\,\sqrt{\tilde{\tau}_o} - 0.7\sqrt{\bar{\tau}_c})^2}{(\rho_s - \rho_f)\,gD_s\,(\sqrt{\tilde{\tau}_o} - 0.7\sqrt{\bar{\tau}_c})}$$
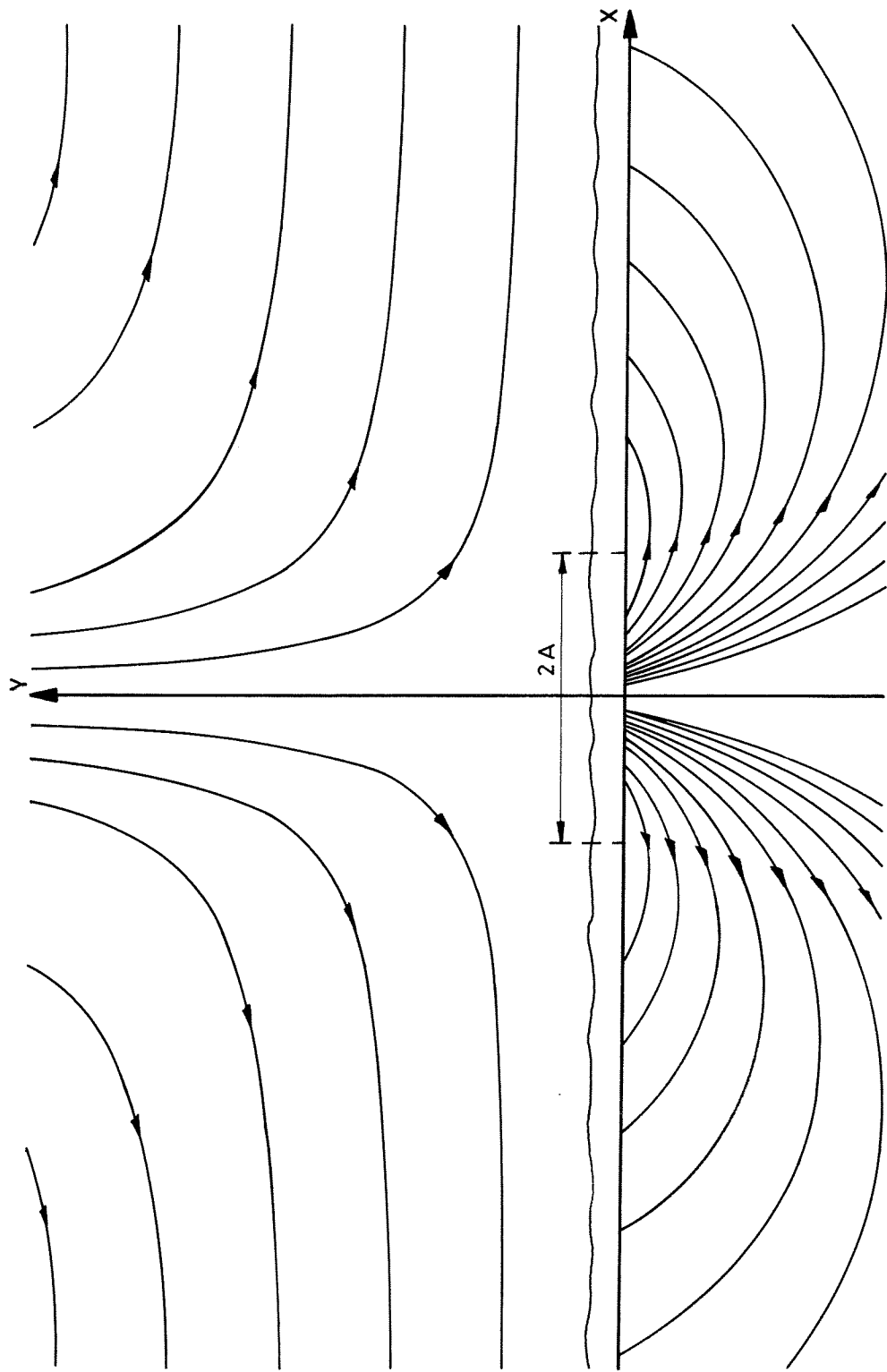
FIG. 18a

STREAMLINE PATTERN OF AN EROSIVE FLOW ABOVE AND BELOW THE SURFACE OF A POROUS BED

$$\phi^* = \frac{\rho_f U^2}{2A(\rho_s - \rho_f)Cg}$$

$\bar{p}^f(X,0)$

ϕ^*
16.7

6.7

2.9

1.35

1.35

2.9

6.7

16.7

2A

Y

X

Y*(X)
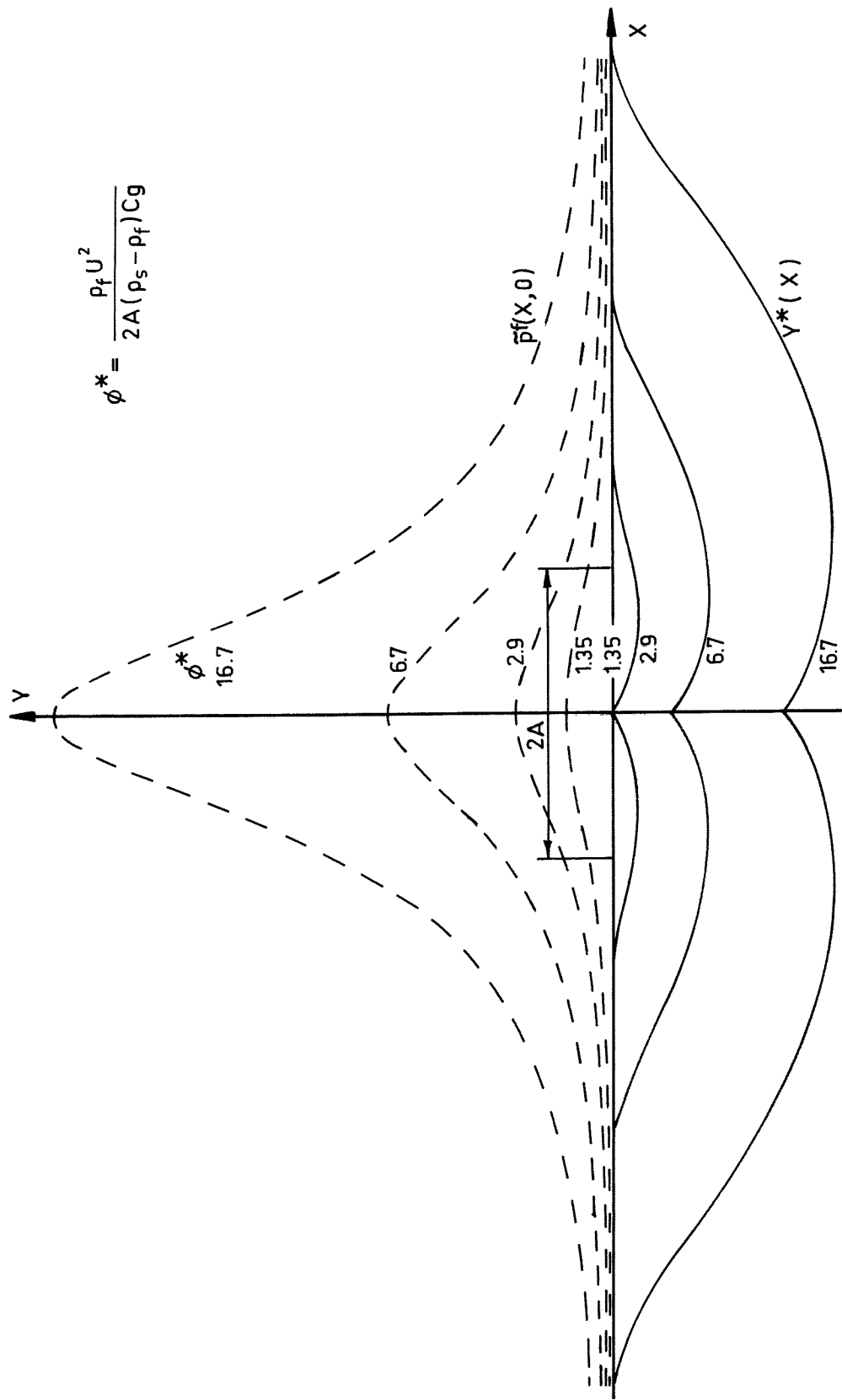
FIG. 18b

PRESSURE DISTRIBUTIONS $\bar{p}^f(X,0)$ ALONG THE BED SURFACE AND EROSION BOUNDARIES Y*(X)
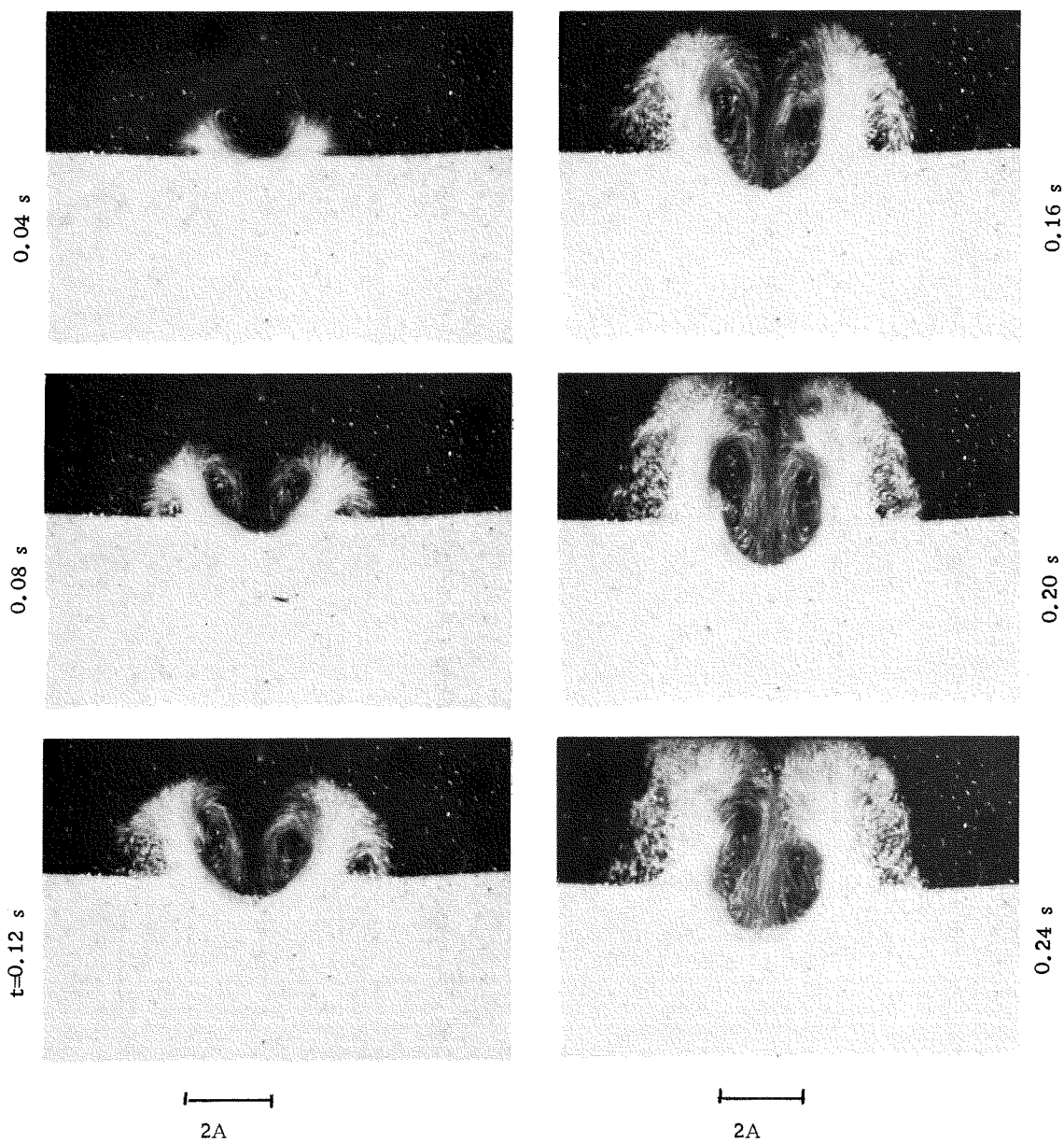
FIG. 19

Erosion of a sand bed by a two-dimensional jet.
Stagnation pressure $\widetilde{p}\,(0,0) = 1.625 \cdot 10^3\ \mathrm{N/m}^2$.
Initial width of stagnation area $2A = 36$ mm.
Photographs taken at 0.04 s intervals.

2 A
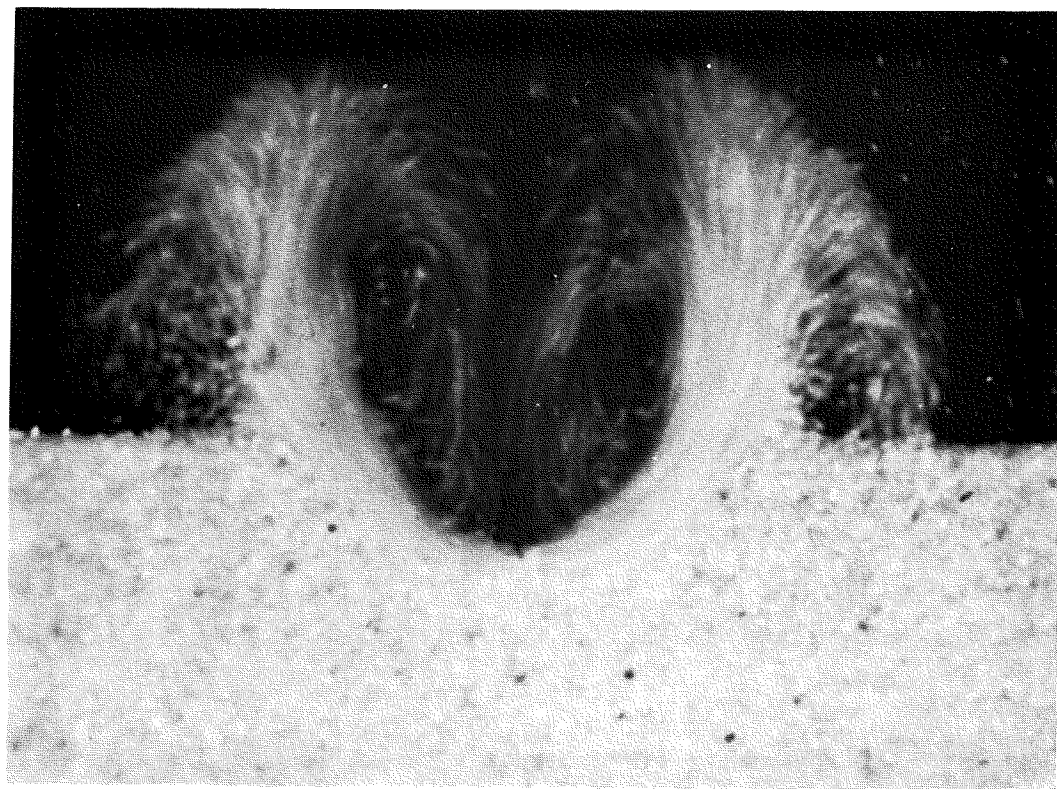
FIG.20a. EROSION OF A SAND BED BY A TWO - DIMENSIONAL JET
PHOTOGRAPH TAKEN AFTER 0.16 s

Calculated
erosion boundary

Actual erosion boundary

2A
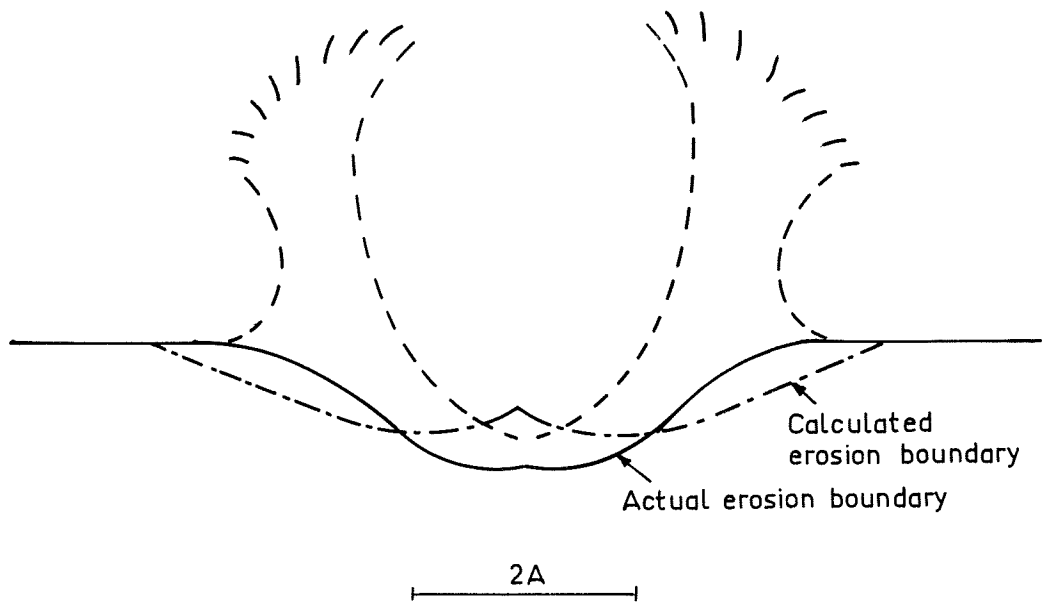
FIG. 20 b

EROSION OF A SAND BED BY A TWO-DIMENSIONAL JET. COMPARISON OF
CALCULATED WITH ACTUAL EROSION BOUNDARY OBSERVED AT $t = 0.16\,s$
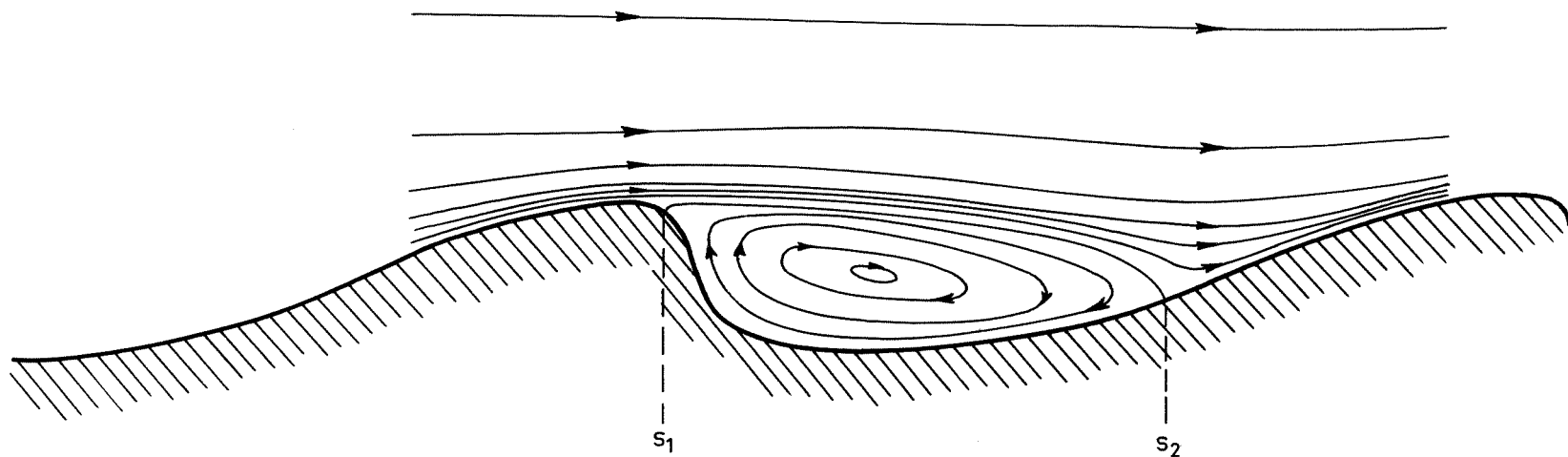
FIG. 21

STREAMLINE PATTERN AND STAGNATION POINTS OF THE FLOW
ABOVE AN UNDULATING BED

SUMMARY

In this thesis first a general derivation is given of the 'macro'-equations
of mass- and linear-momentum balance that govern the momentum transfer
from a Newtonian fluid to rigid particles in a fluid-solid mixture. In particular,
attention is paid to a) the attenuation of viscous-momentum transfer from the
boundary to the interior of a granular bed subject to a surface flow, b) the drag
and lift forces exerted by a turbulent shear flow on particles of the bed surface,
and, c) the balance of forces acting on a bed load under uniform-flow conditions.

It is shown that filter flow driven by shearing along the boundary of a
granular sediment bed exerts a drag force on a layer of only two or three
particle diameters within the bed. A drag force on the bulk mass of sediment
is only exerted by a pore-pressure gradient.

Stability conditions are formulated for a loose granular bed subject to
erosive flow, at SHIELDS' grain-movement condition and during bed-load
transport. 'Macro'-stresses acting along 'wavy' surfaces parallel to the bed
are defined for that purpose, and an attenuation factor is introduced for the
transmission of turbulent fluid shear from the surface towards the interior of
the bed.

It is shown that SHIELDS' dimensionless expression for the critical bed
shear stress at the threshold of continuous sediment motion, $1/\psi_c$, must reach
a constant value for low-shear Reynolds' numbers ($Re_D^* < 0.5$), as long as
there is no cohesion between the particles.

It is concluded that the bed load, consisting of particles rolling and
saltating over the bed, must reduce the maximum turbulent fluid shear at the
bed surface, at sufficiently high bed shear stress, to the critical threshold
drag that would lead to the initiation of non-ceasing scour.

Results are presented of a series of experiments in which were measured:
the mean critical bed shear stress at SHIELDS' grain-movement condition and
at the initiation of non-ceasing scour, the rate of bed-load transport, the
average particle velocity, the rate of deposition, and the average length of
individual steps of saltating bed-load particles, in water, as a function of the
time-mean bed shear stress.   These experiments were performed in a
closed rectangular flow channel at different slopes of the bed surface and using
five different bed materials (two sands, gravel, magnetite and walnut grains).

Comparing the threshold drag acting at different downward slopes of the
bed surface (0°, 12°, 18° and 22°), a surprisingly large critical-drag angle
of 47° was found. The initiation of non-ceasing scour of a loose granular bed
was studied experimentally behind a consolidated bed of the same material as

the loose bed. The corresponding instantaneous threshold drag was about three times larger than the threshold drag acting at SHIELDS'. grain-movement condition. Ripples started to develop at even larger values of the instantaneous bed-shear stress.

The rate of bed-load transport measured as a function of the mean bed-shear stress satisfies a generalised MEYER-PETER & MULLER formula (1948), also at various downward slopes of the bed surface, as investigated up to 22°. The rate of particle deposition was found to be proportional to the rate of bed-load transport, and the average length of individual particle steps was found to be a constant. This implies that the probability of a bed-load particle being deposited when striking the bed surface is independent of the flow rate within the experimental range. This result contradicts EINSTEIN's theory of bed-load transport (1950).

Close examination of the motion of saltating bed-load particles revealed that these particles are transported almost in suspension for the greater part of their trajectory. The average transport velocity of the suspended particles was found to be equal to the average fluid velocity calculated for a turbulent flow without a bed load, at about three particle diameters above the bed surface, minus a constant. The constant was proportional to the critical shear velocity at SHIELDS' grain-movement condition. This can be explained by considering that the turbulent shear flow must exert a lift force on the suspended particles that is practically equal to their submerged weight, and by assuming that the average fluid velocity at the bed-load particle level is reduced owing to the presence of the bed load.

Combining the MEYER-PETER & MULLER formula for the rate of bed-load transport and the above-mentioned expression for the average transport velocity of the bed-load particles shows that the areal bed-load concentration increases linearly with increasing bed-shear stress. This contradicts KALINSKE's theory (1947).

Calculation of the average reduction in fluid shear at the bed surface due to the bed load, using empirical relations for the transfer of momentum of bed-load particles to the bed surface by intergranular collisions and for the areal bed-load concentration, reveals that at low transport rates this reduction is very small. The critical shear stress required to erode the topmost grains of the bed surface must therefore increase with increasing bed shear stress. The number of particles eroded per unit area and per unit increase in total shear was found experimentally to be almost a constant at low bed-load concentrations. It was also found that the average reduction in fluid shear due to the bed load increases so rapidly with increasing bed-shear stress that at

higher transport rates the remaining fluid shear will nowhere exceed the threshold drag corresponding to the initiation of non-ceasing scour measured behind a consolidated bed.

It is concluded, on a theoretical basis, that at high transport rates, during erosion, with or without simultaneous deposition, the turbulent fluid shear at the bed surface must be approximately equal to the critical threshold drag at the initiation of non-ceasing scour. It is found on this basis, by extrapolating empirical expressions for the rate of bed-load transport and for the average transport velocity of bed-load particles, that at high bed-load concentrations the average drag force on the bed-load particles must be approximately equal to their submerged weight. This can be made plausible using BAGNOLD's concept of 'dispersive grain pressure' (1954, 1956).

It is concluded that a loose granular bed will be severely eroded instantaneously where and when the momentum of the turbulent surface flow changes radically and the bed-load cannot protect the bed surface against scour. This condition, defined as the condition for bulk erosion, can occur at high sediment-transport rates under highly turbulent flow, particularly in the case of an undulating bed where the flow contains a rapidly changing pattern of unstable stagnation points. This bulk erosion is due to large instantaneous fluid-pressure gradients in the transition zone between the flow region and the bed. The instantaneous change of momentum of the surface flow constitutes the criterion for bulk erosion.

A method has been developed that permits determination of the extent of the zone of bulk erosion created locally and instantaneously in a loose granular bed by highly erosive flow. The method is applied to a specific example, verified experimentally, in which local stagnation of the main flow creates a zone of bulk erosion in the bed via the associated pressure field.

SAMENVATTING

   In dit proefschrift worden eerst macroscopische massa- en impuls-
balansvergelijkingen afgeleid die de overdracht van lineaire impuls
beheersen vanuit een newtonse vloeistof naar vaste deeltjes in die vloeistof.
In het bijzonder wordt aandacht geschonken aan

a) de demping van viskeuze impulsoverdracht vanaf het oppervlak naar het
   binnenste van een korrelbed onder oppervlaktestroming,

b) de sleepkracht en de liftkracht die een turbulente stroming op deeltjes aan
   het oppervlak uitoefenen,

c) het krachtenevenwicht op over de bodem getransporteerde deeltjes onder
   uniforme stromingscondities.

   Aangetoond wordt dat filterstroming gedreven door een schuifspanning aan
het oppervlak van een korrelbed een sleepkracht uitoefent op een laag van
slechts twee of drie korreldiameters onder het oppervlak. Een sleepkracht op
de bulkmassa onder het oppervlak kan alleen worden uitgeoefend door middel
van een poriëndrukgradiënt.

   Stabiliteitsvoorwaarden worden vervolgens afgeleid voor een los korrelbed
onderworpen aan een erosieve stroming, onder SHIELDS' conditie voor het
begin van bodemtransport, en gedurende continu bodemtransport. 'Macro'-
spanningen langs een 'golvend' oppervlak evenwijdig aan het bed worden daartoe
gedefiniëerd, en een dempingsfactor wordt geïntroduceerd om de overdracht
van turbulente schuifspanning vanuit de vloeistof naar de korrels van het
bedoppervlak te beschrijven.

   Er wordt aangetoond dat SHIELDS' dimensieloze uitdrukking voor de
kritische bodemschuifspanning $(1/\psi_c)$ aan het begin van continu bodemtransport
een constante waarde moet bereiken voor lage schuifspannings-Reynolds'-
getallen $(Re_D^* < 0.5)$, zolang er geen cohesie is tussen de korrels.

   De conclusie wordt getrokken dat de 'bed load', bestaande uit korrels die
rollend en 'springend' (saltating) over het bedoppervlak worden getransporteerd,
de maximale turbulente vloeistofschuifspanning aan het bedoppervlak moet
beperken bij voldoend hoge totale bodemschuifspanning tot een kritische schuif-
spanning die continue uitschuring van het bed zou veroorzaken.

Resultaten worden gegeven van een serie experimenten, waarbij werden
gemeten: de tijd-gemiddelde kritische bodemschuifspanning bij SHIELDS' conditie
voor het begin van bodemtransport, en bij het begin van continue uitschuring,
de intensiteit van het bodemtransport, de gemiddelde korrelsnelheid, de snelheid
van afzetting, en de gemiddelde lengte van de stappen die 'springende' korrels
boven het bed maken, als functie van de gemiddelde bodemschuifspanning.
Deze experimenten werden in een gesloten rechthoekige stroomgoot uitgevoerd,
en wel in water, bij verschillende hellingen van het bedoppervlak en gebruik
makend van vijf verschillende materialen (twee zandsoorten, grind, magnetiet
en walnootkorrels).

Door de kritische bodemschuifspanning bij het begin van continu bodem-
transport te meten bij verschillende neerwaartse hellingen van het bedoppervlak
(0°, 12°, 18° en 22°), werd een verrassend grote kritische sleephoek van 47°
gevonden. Het begin van continue uitschuring van een los korrelbed werd
experimenteel bepaald achter een geconsolideerd bed van hetzelfde materiaal
als het losse bed. De corresponderende kritische schuifspanning was ongeveer
drie keer zo hoog als de bodemschuifspanning bij SHIELDS' conditie voor het
begin van bodemtransport. Ribbels ontstonden pas bij een nog grotere bodem-
schuifspanning.

De intensiteit van het bodemtransport, gemeten als functie van de
gemiddelde bodemschuifspanning, voldoet aan een gegeneraliseerde MEYER-
PETER & MÜLLER formule (1948), ook bij verschillende neerwaartse hellingen
van het bed, in ieder geval tot de maximale hoek van 22° bij de proeven.
De snelheid van afzetting bleek evenredig te zijn aan de intensiteit van het
bodemtransport en de gemiddelde staplengte van 'springende' korrels bleek
constant te zijn. Dit houdt in dat de waarschijnlijkheid dat een korrel van de
'bed load' wordt afgezet bij een botsing met het bed onafhankelijk is van de
stroomsnelheid, althans binnen ons meetgebied. Dit resultaat is in tegenspraak
met de theorie van EINSTEIN (1950).

Een nauwgezette studie van de beweging van 'springende' korrels toonde
aan dat deze korrels praktisch in suspensie worden getransporteerd voor het
grootste deel van hun traject. De gemiddelde transportsnelheid van de gesus-
pendeerde deeltjes bleek gelijk te zijn aan de gemiddelde stroomsnelheid,
berekend voor een turbulente stroming zonder korreltransport, op ongeveer
drie korreldiameters afstand van het bed, minus een constante. De constante
was evenredig met de kritische schuifspanningssnelheid bij SHIELDS' conditie
voor het begin van bodemtransport. Dit kan worden verklaard door in aan-
merking te nemen dat de turbulente stroming een liftkracht op de gesuspendeerde

deeltjes uitoefent die praktisch gelijk is aan hun ondergedompeld gewicht, en door aan te nemen dat de gemiddelde vloeistofsnelheid op het niveau van de getransporteerde korrels gereduceerd is door de aanwezigheid van de 'bed load'.

Een combinatie van de MEYER-PETER & MÜLLER formule voor de intensiteit van het bodemtransport en de hierboven genoemde uitdrukking voor de gemiddelde transportsnelheid van de 'bed load' toont aan dat de oppervlakte-concentratie van de 'bed load' lineair toeneemt met toenemende bodemschuif-spanning. Dit is in tegenspraak met de theorie van KALINSKE (1947).

Een berekening van de gemiddelde reductie van de vloeistofschuifspanning aan het bedoppervlak ten gevolge van de 'bed load', gebruik makend van empirische formules voor de impulsoverdracht van korrels van de 'bed load' aan het bedoppervlak bij intergranulaire botsingen, en voor de oppervlakte-concentratie van de 'bed load', toont aan dat deze reductie bij lage transport-intensiteit erg klein is. De kritische schuifspanning die vereist is om de bovenste laag korrels van het bedoppervlak te eroderen, neemt dus toe bij toenemende bodemschuifspanning. Het aantal korrels dat per eenheid van bedoppervlak en per eenheid van toename van de totale bodemschuifspanning wordt geërodeerd, bleek experimenteel praktisch constant te zijn bij lage transportintensiteit. Het bleek ook dat de gemiddelde reductie van de vloeistof-schuifspanning aan het bedoppervlak ten gevolge van de 'bed load' zo snel toeneemt met toenemende bodemschuifspanning, dat bij hogere transport-intensiteiten de resterende vloeistofschuifspanning de kritische schuifspanning die continue uitschuring van het bed zou veroorzaken, niet zal overschrijden.

Op theoretische basis wordt geconcludeerd dat bij hoge transportintensiteit, gedurende erosie, met of zonder gelijktijdige afzetting, de turbulente vloeistof-schuifspanning aan het bedoppervlak ongeveer gelijk moet zijn aan de kritische schuifspanning die continue uitschuring van het bed zou veroorzaken. Op die basis wordt gevonden, door empirische uitdrukkingen voor de intensiteit van het bodemtransport en voor de gemiddelde transportsnelheid van de 'bed load' te extrapoleren, dat bij hoge concentraties de gemiddelde sleepkracht op de korrels van de 'bed load' ongeveer gelijk moet zijn aan hun eigen gewicht. Dit kan plausibel worden gemaakt door gebruik te maken van BAGNOLD's uitdrukking voor de 'dispersieve korreldruk' aan het bedoppervlak (1954,1956).

De conclusie wordt getrokken dat een los korrelbed sterk en ogenblikkelijk zal worden geërodeerd, op plaatsen waar de impuls van de turbulente stroming aan het oppervlak radicaal verandert en de 'bed load' het bed niet tegen uit-schuring kan beschermen. Deze conditie, gedefinieërd als de voorwaarde voor bulkerosie, kan zich bij hoge transportintensiteiten voordoen, onder een sterk

turbulente stroming, in het bijzonder bij een geribbeld bed waar de oppervlakte-
stroming een snel veranderend stromingspatroon met instabiele stuwpunten bevat.
Deze bulkerosie is een gevolg van grote vloeistofdrukgradiënten die instantaan
in de overgangszone tussen de oppervlaktestroming en het bed optreden. De
instantane verandering van impuls van de oppervlaktestroming is een maat
voor bulkerosie.

Een methode wordt getoond om de penetratiediepte van een zone van
bulkerosie te bepalen die lokaal en instantaan in een los korrelbed onstaat
door een sterk erosieve stroming. Deze methode wordt toegepast om een
specifiek geval door te rekenen, waarbij een lokale stagnatie van de opper-
vlaktestroming een zone van bulkerosie in het bed opwekt via het daarme
samenhangende poriëndrukveld. De uitkomst wordt experimenteel geverifiëerd.

ACKNOWLEDGEMENTS

CURRICULUM VITAE

R. Fernández Luque was born in Murcia, Spain, in September 1937.
In 1946 he moved to the Netherlands. In 1956 he passed the final examination
of the HBS-B department of the Amsterdams Lyceum. In the same year he
became a student of Mining Engineering at the Delft University of Technology,
where he passed the preliminary examination (Propadeutisch Examen) in 1957.
He then switched to the study of physics at the University of Amsterdam.
He chose Experimental Physics as main subject and worked in the field of
Nuclear Magnetic Resonance at the van der Waals Laboratory (Director Prof.
Dr. N.J. Trappeniers). At the same time he studied Oceanography and
Meteorology at the Free University at Amsterdam (Prof. Dr. P. Groen). After
taking his university degree in February 1965, he joined Koninklijke/Shell
Exploratie en Produktie Laboratorium (KSEPL) in Rijswijk, the Netherlands,
where he was active as a research physicist in the fields of sediment transport
and off-shore engineering. In 1969 he was transferred to Houston (Texas),
where he worked in the field of off-shore civil engineering at Bellaire Research
Centre (Shell Dev. Co.) for a period of one year. After his return to KSEPL
he continued his investigation of sediment transport and the stability of sea
beds, and then joined Production-Engineering Research Department, where he
is now working in the field of rock mechanics. He is currently also engaged
on sediment transport problems in exploration research.